Investigating Medulloblastoma metabolism for better diagnosis and treatment

By

Haydn Munford

A thesis submitted to the University of Birmingham for the degree of DOCTOR OF PHILOSOPHY

Institute of metabolism and systems research

College of Medical and Dental Sciences

University of Birmingham

2019

UNIVERSITY OF BIRMINGHAM

Abstract

Cancer cells are able to reprogram their metabolism in order to supply biosynthetic and bioenergetic demands of rapid proliferation. Glutamine is required by most cancers in significant quantities, as it serves as a major anabolic carbon and nitrogen source for synthesis of macromolecules, a source of high energy electrons for ATP production and the regulation of ROS homeostasis via glutamate through the synthesis of glutathione. The metabolism of glutamine in Medulloblastoma (MB) - the most common high grade childhood tumour – is largely unknown.

Using publically available databases of MB gene expression, we observed that genes associated with glutamine metabolism were prognostic in MB patients. Furthermore, employing a combination of analytical approaches to study metabolism, we show the importance of glutamine catabolism in MB cell lines. Finally, we investigated the effect of pharmacological manipulation of glutamine metabolism and observed that inhibition of glutaminase 1 (GLS1) – the enzyme responsible for glutamate biosynthesis - can increase cisplatin and irradiation cytotoxicity. Taken together our data suggests that understanding glutamine metabolic pathways may generate prognostic bio-markers of survival and may serve to improve current therapies.

Acknowledgements

My genuine thanks go to Georgie Moseley and the Help Harry Help Others charity for funding my PhD. The colours used in my result figures are dedicated to you.

I wish to thank my supervisors Dr Daniel Tennant and Professor Andrew Peet for their extensive knowledge and support throughout my PhD. I would also like to acknowledge the current and past members of the Tennant group. I thank Katherine Eales, Katarina Kluckova and Christina Escribano (I know you miss me really) for their amazing support throughout my PhD. In particular I would like to thank previous lab members Robert Murren and Kate Hollinshead for their support and friendship. I would like to also thank Connar Westgate for always providing support and friendship. Special thanks go to Alpesh Thakker for his invaluable help with running the GC-MS samples throughout my PhD. I additionally thank my collaborators Prof. Steve Clifford (University of Newcastle, UK) and Dr. Jurre Kamphorst (University of Glasgow, UK), for their input.

I am extremely grateful to my family and girlfriend, for without whom I would not have been able to do any of this. Your love and support is unyielding.

Finally, I would like to thank the many others not mentioned by name.

Contents

List of figures

List of tables

List of abbreviations

2HG	2-hydroxyglutarate
2-ME	2-Mercaptoethanol
3PG	3-phosphoglycerate
3PHP	3-phosphohydroxypyruvate
αKG	α-ketoglutarate
αKGDH	α-ketoglutarate dehydrogenase
A.U.	Arbitrary units
AcCoA	Acetyl coenzyme A
ACTB	Beta actin
AKT	Serine/threonine protein kinase B
Ala	Alanine
ALDH18A1	Pyyroline-5-carboxylate synthetase
AMP	Adenosine monophosphate
Asn	Asparagine
Asp	Aspartate
BBB	Blood brain barrier
BCAA	Branched chain amino acids
BPTES	Bis-2-(5-phenylacetamido-1,3,4-thiadiazol-2-yl)ethyl sulphide
CAIX	Carbonic anhydrase 9
CB	Control cerebellum
Cit	Citrate
CoA	Coenzyme A
COX	Cytochrome c oxidase
DMEM	Dulbecco's modified Eagles Medium
DMEM/F12	Dulbecco's modified Eagles Medium Hams/F12
ECM	Extracellular matrix
EMT	Epithelial-mesenchymal transition
ETC	Electron transport chain
F6P	Fructose 6-phosphate
FAD+	Flavin adenine dinucleotide
FBS	Foetal bovine serum
FDG-PET	18F-deoxyglucose-positron emission tomography
FITC	Fluorescein
FPKM	Fragments per kilobase of transcript per million reads
FSC	Forward scatter
Fum	Fumarate
G3P	Glycerol 3-phosphate
G6P	Glucose 6-phosphate
GAPDH	Glyceraldehyde 3-phosphate dehydrogenase

GC-MS	Gas chromatography mass spectrometry
GDH	Glutamate dehydrogenase
Glc	Glucose
Gln	Glutamine
GLS1	Glutaminase 1
GLS2	Glutaminase 2
GLUD	Glutamate dehydrogenase
GLUT or SLC2A	Glucose transporter family; solute carrier 2
Gly	Glycine
GOT1	Cytosolic aspartate aminotransferase
GOT2	Mitochondrial aspartate aminotransferase
Grp3	Group 3 Medulloblastoma
Grp4	Group 4 Medulloblastoma
GSH	Reduced glutathione
GSSG	Oxidised glutathione
H_2O_2	Hydrogen peroxide
HIF	Hypoxia-inducible factor
HK	Hexokinase
HRP	Horseradish peroxidase
IDH	Isocitrate dehydrogenase
IMP	Inosine monophosphate
Iso	Isocitrate
KD	Knockdown
KO	Knock-out
Lac	Lactate
LAT1; SLC7A5	L-type amino acid transporter 1; solute carrier 7
LDHA/B	Lactate dehydrogenase A/B
Mal	Malate
MCT	Monocarboxylate transporter
MDH	Malate dehydrogenase
ME	Malic enzyme
MB	Medulloblastoma
MID	Mass isotopologue/istopopmer distribution
MRS	Magnetic resonance spectroscopy
MYC	v-myc avian myelocytomatosis viral oncogene homolog
NAD+	Oxidised nicotinamide adenine dinucleotide
NADH	Reduced nicotinamide adenine dinucleotide
NADP+	Oxidised nicotinamide adenine dinucleotide phosphate
NADPH	Reduced nicotinamide adenine dinucleotide phosphate
NEAA	Non-essential amino acids
NMR	Nuclear Magnetic Resonance
OAA	Oxaloacetate

P5CDH	Pyrroline 5-carboxylate dehydrogenase
P5CS	Pyrroline 5-carboxylate synthetase
PARP	Poly ADP ribose polymerase
PBS	Phosphate buffered solution
PBST	1x PBS with 0.05% Tween-20
PC	Pyruvate carboxylase
PDH	Pyruvate dehydrogenase
PDK1	Pyruvate dehydrogenase kinase 1
PFK	Phosphofructokinase
PHDs	HIF prolyl hydroxylases
PHGDH	Phosphoglycerate dehydrogenase
PI	Propidium Iodide
PI3K	Phosphoinositol 3-kinase
PK	Pyruvate kinase
PPP	Pentose phosphate pathway
Pro	Proline
PRODH	Proline dehydrogenase
PSAT	Phosphoserine aminotransferase
PSPH	Phoshoserine phosphatase
PTCH1	Protein patched homolog 1
PTEN	Phosphatase tumour suppressor
pVHL	Von Hippel-Lindau
PYCR	Pyrroline 5-carboxylase reductase
Pyr	Pyruvate
RNAi	RNA interference
ROS	Reactive oxygen species
RT qPCR	Quantitative real time polymerase chain reaction
SDS-PAGE	Sodium dodecyl sulphate polyacrylamide gel electrophoresis
SHH	Sonic hedgehog
SHMT1/2	Serine hydroxymethyltransferase 1/2
siRNA	Short interfering RNA
SLC25A12	Aspartate-glutamate antiporter
SLC25A13	Aspartate-glutamate antiporter
SMO	Smoothened
SRB	Sulfohodamine B
SSP	Serine synthesis pathway
Suc	Succinate
SUFU	Suppressor of fused homolog
TCA	Tricarboxylic acid cycle or Trichloroacetic acid solution
THF	Tetrahydrofolate
TIGAR	TP53-induced glycolysis and apoptosis regulator
TMSP	(3-trimethylsilyl)propionic-(2,2,3,3-d4)-acid sodium salt

WHO	World Health Organisation
WNT	Wingless/Integrated signalling pathway
WT	Wild-type

Chapter 1

Introduction

1.1 Introduction

In 2016 Cancer research UK estimated that 5,187 deaths resulted from brain tumours in the UK, with a >10 year survival rate of little as 14% (CRUK, 2016). Furthermore, in this same year, the World Health Organisation (WHO) reported that brain and central nervous system tumours accounted for 8.8 million deaths worldwide (Louis *et al.*, 2016). Despite the significant research into these tumours, advancements in their treatment remain poor, with a clear need for novel effective therapies. One such approach with a hope to improve the diagnosis and treatment comes from the exploration of the tumour metabolome, which may be able to reveal phenotypic differences in relation to biological function.

1.2 Introduction to Medulloblastoma

Medulloblastoma (MB) is a rapid growing tumour of the cerebellum or medulla/brain stem. MBs are the most common malignant brain tumour observed in children, with extensive clinical and biological heterogeneity (Cavalli *et al.*, 2017). The cell of origin for a number of different cancer types, including MB, is somewhat controversial. In MB, this is an ongoing debate, in which granule neurone precursors were speculated as being the cells of origin, due to the morphology and location of the arising tumours (Yang *et al.*, 2008). However, stem cell markers have also been shown as being expressed on MB cells (Hemmati *et al.*, 2003), raising the argument that these tumours may arise from neural stem cells (NSCs). With the classification of MB into different subgroups (see below), it has been speculated that both cell types may equally be precursors, but result in a different subgroup of tumour (Robinson *et al.*, 2012). Much of the controversy regarding MB cell of origin was due to difficulties in studying the initial phases of the neoplastic process (Huang *et al.*, 2016). The

establishment of genetically engineered mouse (GEM) models led to an increased understanding of MB cellular origins, where it is now accepted that Shh-driven MBs are derived from the external germinal layer (EGL) (Schüller *et al.*, 2008), Wnt MBs from the dorsal brainstem progenitors (Gibson *et al.*, 2010) and Group 3 MBs from cerebellar stem cells (Fan and Eberhart, 2008), (Pei *et al.*, 2012). Despite our increased knowledge of the neoplastic events leading to MB, the cell of origins in Group 4 MB remains elusive (Huang *et al.*, 2016).

1.3 The Who classification system for Medulloblastomas

Over the past century, brain tumours have typically been classified based on their histological presentation (WHO 2007). However, the 2016 WHO classification of CNS tumours included molecular parameters alongside histology to characterise these tumours (Louis *et al.*, 2016). Specifically, the WHO classification of MBs adheres to the widely accepted 4 genetic subgroups: WNT activated, SHH-activated, group 3 and group 4 (Taylor *et al.*, 2012). While the histological variants of MB (desmoplastic/nodular, extensive nodular, large cell and anaplastic) remain more relevant for clinical purposes (i.e. diagnosis, prognosis and treatment), clinical trials are starting to use genetic subgroup for stratification Both the genetic and histological groups are associated with different prognoses and treatment regimens, where it is expected that pathologists should integrate their diagnosis with the histological phenotype and molecular group together.

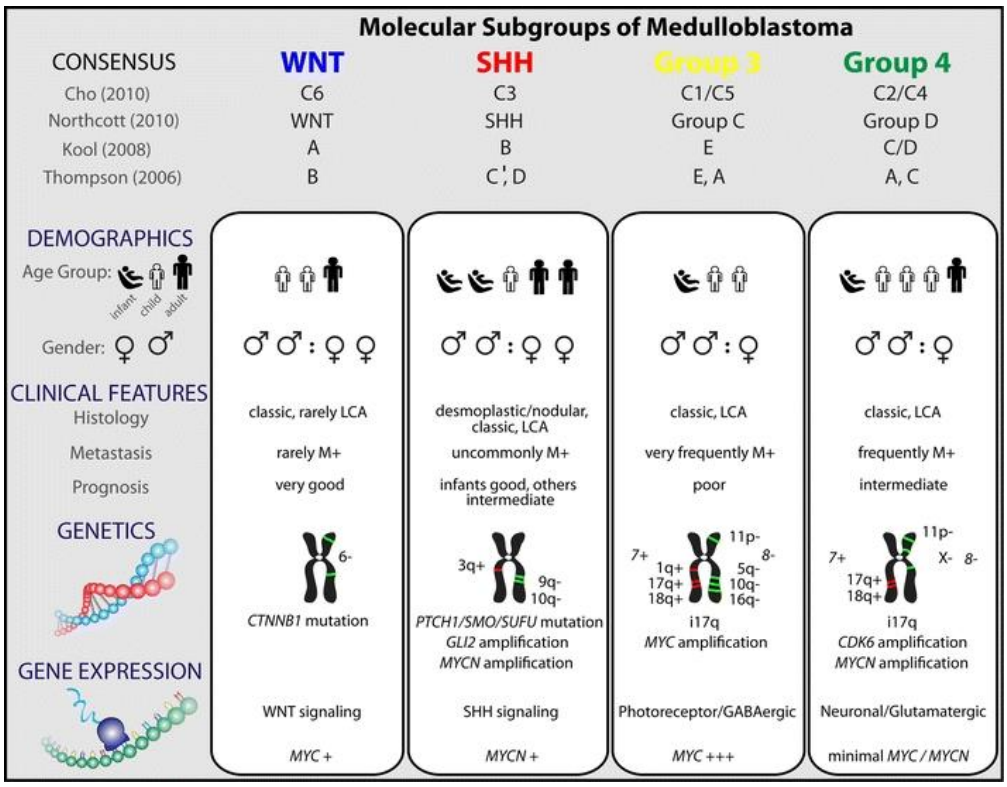

***Figure 1.1* Historic 4 subgroups of Medulloblastoma.** Taken from Taylor *et al*, 2012.

1.3.1 WNT

The WNT subgroup of MB has a peak incidence of around 10-12 years (Kool *et al.*, 2008), and accounts for around 11% of MB tumours, making it the rarest subgroup. Despite this, Wnt tumours are the best studied of the subgroups, in part, due to its better clinical prognosis, with overall survivals reaching 90% (DeSouza *et al.*, 2014). These tumours typically present as classic histology variants, although some large cell/anaplastic tumours are from this subgroup. Interestingly, this appears not to affect their more favourable prognosis compared to other subgroups (Louis *et al.*, 2016).

Mutations of the β-catenin encoding gene *CTNNB1* are commonly observed in patients with WNT subgroup MB (Northcott et al*., 2012),* which leads to a disrupted Wingless *(Wnt)* system, a family of growth factor receptors involved in embryogenesis (Kool *et al.*, 2008). In addition, germline mutations in *APC* (inhibitor of the Wnt pathway), which predispose

individuals to Turcot syndrome, also brings a heightened risk of MB. Less frequent mutations that are observed in sporadic MB, include APC and AXIN1/2, all of which are crucial parts of the Wnt pathway. This therefore highlights the strong aetiological role for the canonical Wnt pathway activation in the formation of these tumours (Jenkins et al., 2016). Activation of Wnt signalling leads to accumulation of β-catenin in the nucleus, which binds to TCF-4/lef-1 and has a role in cell proliferation (Niehrs and Acebron, 2012), cell to cell adhesion (Niehrs, 2012) and in the breakdown of the extracellular matrix (Baryawno *et al.*, 2010).

1.3.2 SHH

Another subgroup of MB attributed to altered signalling is the SHH subgroup, which account for around 28% of MBs, and have an intermediate prognosis. As the name suggests, these tumours are understood to be driven through oncogenic signalling through the sonic hedgehog pathway (DeSouza *et al.*, 2014). Similarly to the WNT subgroup, *SHH* tumours can arise due to a germline mutation - in some cases mutations in *PTCH*, which lead to Gorlin syndrome, or mutations in *SUFU*, also predispose to MB (Smith *et al.*, 2015). Sporadic *SHH* MBs are frequently associated with mutations in these same genes, but also of *SMO* (G protein-coupled receptor involved in *shh* signalling), in addition to genetic amplifications of *GLI1* and *GLI2* transcription factors (Bayly et al, 2012). The sonic hedgehog (*Shh*) pathway induces proliferation in neuronal precursor cells in the developing cerebellum and is therefore vital in regular cerebellar development (Álvarez-Buylla and Ihrie, 2014). More specifically, *shh* encourages development of the external germinal layer (EGL) within the upper rhombic lip (the origin of *SHH* tumours), directed by the Shh ligand which is usually secreted by Purkinje neurons (Ramsbottom and Pownall, 2016). All mutations associated

with this subgroup result in *Shh* signalling pathway over-activation. The binding of Shh ligand to its receptor PTCH1 overcomes SMO inhibition, allowing for the release of Gli transcription factors, which are normally bound to inhibitory protein complexes, typically SUFU (S. *et al.*, 2016). Consequentially, this activation further results in an increased expression of Snail protein, and disruption of E-cadherin to decrease cell–cell adhesion (Li *et al.*, 2007). Hedgehog activation has also been shown to strongly regulate angiogenesis and metastasis via Rho kinase-dependant mechanisms (Renault *et al.*, 2010).

Due to the progress made in molecular understanding of MB, it would be inappropriate to class SHH tumours as a single entity. The presence of TP53 mutations can dictate whether a SHH tumour has a moderate or a poor survival, with TP53 mutations leading to a high-risk subtype (Kool *et al.*, 2014), (Schwalbe *et al.*, 2017) and are responsible for a large proportion of treatment failures in SHH MBs (Ramaswamy *et al.*, 2016).

1.3.3 Group 3 (Grp3)

Grp3 MBs are typically referred to as the C-MYC amplified subgroup and make up about 28% of all cases, a similar prevalence seen in SHH tumours (Cavalli *et al.*, 2017) . These tumours have the worst prognosis across all of the subgroups and frequently metastasise (Robinson *et al.*, 2012). Grp3 tumours are rarely observed in adults while their prevalence in infants and children is high, where they typically present histologically as classic or large cell/anaplastic (Taylor *et al.*, 2012). It has been suggested that OTX2, a transcription factor that is strictly regulated during development and has been shown to upregulate the transcription of MYC, may be implicated in Grp3 MB aetiology (Bunt *et al.*, 2011).

1.3.4 Group 4 (Grp4)

Due to the unclear molecular pathogenesis of this subgroup, it is simply referred to as Grp4 subtype, although there is an association with isochromosome 17q. Grp4 MBs are the most frequently occurring subtype, occurring in 34% of all cases, and usually occur in children, with a peak incidence at 10 years old (Taylor *et al.*, 2012). Despite isochromosome 17q being observed in 26% of group 3 tumours, it is drastically more associated with Grp4 MB, being present in 66% of tumours (Desouza et al, 2014). Another noteworthy cytogenetic change within group 4 tumours is a common loss (80%) of Chromosome X in affected females (*Northcott et al, 2012)*. These tumours present histologically as classic, though less often can present as large cell/anaplastic and despite common observations of metastatic disease, these tumours have an intermediate prognosis (Packer and Vezina, 2008)

1.3.5. Beyond the conventional 4 groups of MB

The inclusion of molecular phenotypes in the classification of MB has been a natural consequence of the recent increase in genetic research in MB tumours. More recently, genetic stratification into seven groups has been suggested (Figure 1.2). Schwalbe *et al*, stratified MB into seven molecular subgroups, of which the WNT subgroup was unaffected and each of the other recognised subgroups were split in two distinct groups. The SHH subgroup was divided into age-related subgroups corresponding to infant (<4-3 years) and childhood patients (≥4-3 years), while Grp3 and Grp4 MB were divided into low and high risk subgroups (Schwalbe *et al.*, 2017).

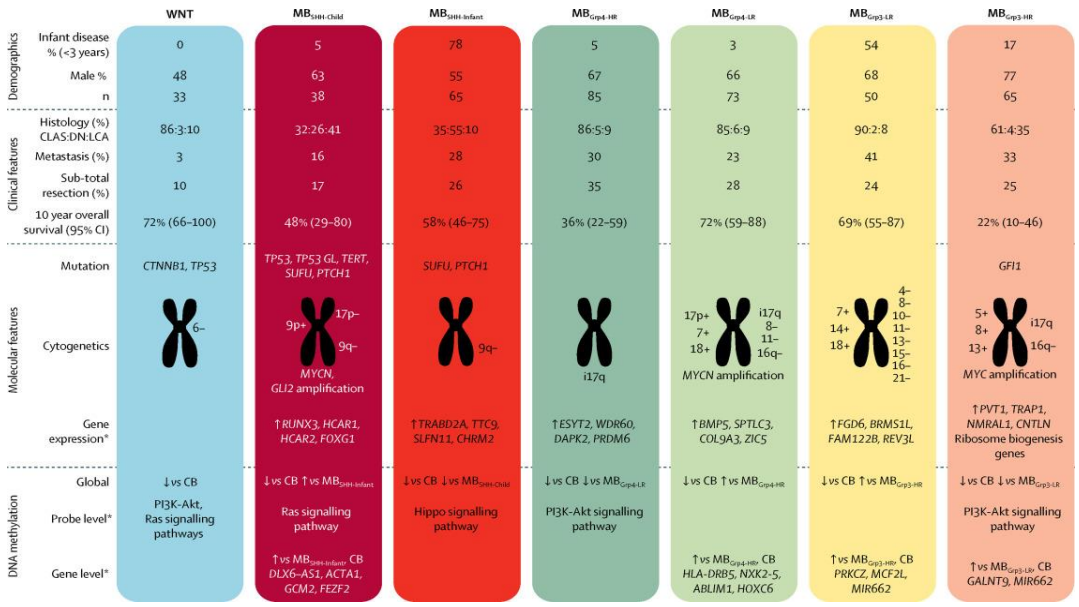

Figure 1.2 Summary of the seven primary childhood Medulloblastoma subgroups. Image taken from Schwalbe et al., 2017.

However, in the same year Cavalli *et al* proposed 12 MB subtypes, in which the WNT tumours were split into two groups (Figure 1.3). Although the two WNT subtypes (WNT α and WNT β) were found to have similar prognoses. WNT α was found to affect mainly children and demonstrate monosomy 6, while WNT β occurred in older patients and were frequently diploid for chromosome 6. Interestingly, monosomy 6 had previously been defined as a defining feature of WNT MB (Zhao *et al.*, 2016). However the more recent study suggested that WNT β patients could be misdiagnosed if this criterion were used alone (Cavalli *et al.*, 2017).

The same group identified four distinct groups of SHH MB; α, β, γ, and δ. The variant with the worst prognosis was found to be SHH α, affecting children between the ages of 3-16 years and were typically enriched for GLI2 and MYCN amplifications. Somatic copy-number aberrations (CNAs) such as YAP1 amplifications, 9q, 10q and 17q loss were also observed in

this group. Furthermore, the SHH α group were highly enriched for *TP53* mutations, where the *TP53* mutation profile was only prognostic in the SHH α variant tumours. Furthermore, it was observed that infant SHH tumours were generally associated with SHH β and SHH γ with contrasting clinical consequences; SHH β tumours frequently metastasised and had a poorer overall survival compared to the SHH γ group, while SHH δ were associated with tumours in adults, contained activating mutations in the *TERT* promoter and were more likely to have a better prognosis (Cavalli *et al.*, 2017).

Grp3 MB were also subdivided into three variants; α, β, and γ. The most surprising finding from this study was the observation that Grp 3γ have a poor prognosis independently of *MYC* amplification, identifying for the first time a group of high-risk Grp3 tumours, irrespective of *MYC* status (Cavalli *et al.*, 2017).

Grp 4 remained the most prevalent MB subgroup in this study, although was also split into 3 variants (again, α, β, and γ). However, their frequency was found to be >40% of all MB compared to the previous finding of 34% (Louis *et al.*, 2016). Grp 4α were observed to be enhanced for *MYCN* amplifications. Grp 4α and 4γ generally had 8p loss and 7q gain, while Grp 4β harboured *SNCAIP* (Synphilin-1) duplications and almost universal isochromosome 17q. It had been previously proposed that Grp4 MBs were GFI1 and GFL1B activated (Northcott *et al.*, 2014)- this report observed GFI activation only in Grp3 β.

The genetic information regarding tumour classification is providing important steps forward in our understanding the tumourigenic processes in MB. However, it is not always clear how this can lead to novel biology-driven treatments to better treat MB tumours.

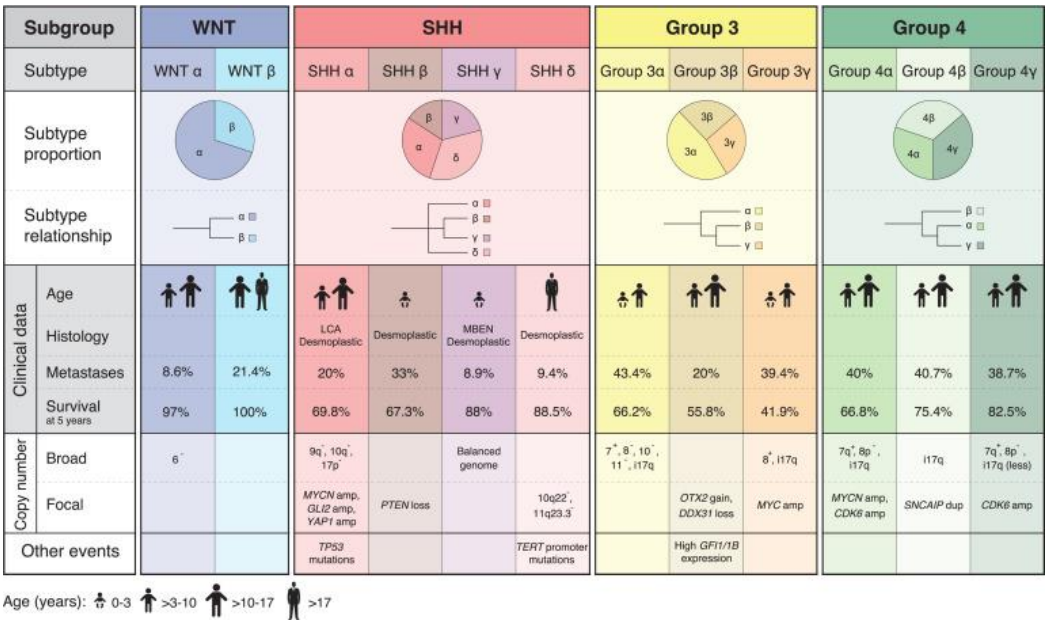

Figure 1.3 Graphical Summary of the 12 Medulloblastoma Subtypes. Figure taken from Cavalli et al., 2017.

1.4 Clinical diagnosis

The median interval from the onset of symptoms to eventual diagnosis in MB is around 8 weeks, but can range from days to years (Gerber *et al.*, 2012). Symptoms present as hydrocephalus and/or cerebellar dysfunction, comprising of increasing head circumference and vomiting in infants and cranial nerve palsy, ataxia, vomiting and headaches in older individuals (Gerber *et al.*, 2014). Magnetic resonance imaging (MRI) is an invaluable tool in the diagnosis of MB, where tumours are visualised in the cerebellum, with regular fourth ventricle compression. Tumours typically obstruct draining of the cerebral spinal fluid (CSF), resulting in expansion of the lateral and third ventricles. Spinal MRI also contributes towards the diagnosis of metastatic MB.

1.5 Management of Medulloblastoma

Recent developments in multimodal therapy such as chemotherapy, radiotherapy and surgery have shown promise, yet recurrence occurs in roughly 40% of these children, and approximately 30% succumb to their disease (Fossati, Ricardi and Orecchia, 2009). Furthermore, MB survivors have a considerably reduced quality of life due to treatment-related side effects (Gerber *et al.*, 2014). Whenever possible, surgery is favoured across all four subtypes, where maximal tumour resection is the foremost goal. Subsequent to surgery, older patients tend to receive varying doses (dependent on risk stratification) of multimodal chemotherapy in combination with craniospinal radiation. Stratification of patients into separate risk groups has been vital in controlling the de-escalation of treatment intensities, the purpose of which is to increase quality of life both directly after treatment and for those who are cured (Gerber *et al.*, 2014).

1.5.1. Molecular targeting of MB tumours

Our increased understanding of the molecular alterations between MB subgroups has catalysed the development of targeted therapies, with the hope that these will reduce treatment associated side-effects in patients. Despite this, limited drugs targeted towards the Wnt pathway have been established in MB, which may be a result of their already excellent cure rate (Baryawno *et al.*, 2010). Canthradin has previously been shown to inhibit phosphatase 2A (PP2A), which is needed in the stabilisation of β-catenin and functions downstream of the Wnt ligand, offering a potential target in WNT tumours (Polakis, 2012).

Targeting SHH tumours on the other hand, has received considerably more attention. The vast majority of inhibitors developed have been targeted towards SMO, a vital component of the sonic pathway (Kieran, 2014), where a number of inhibitors have been assessed in clinical trials. However, despite initial responses, patients often relapse after treatment with SMO inhibitors, with secondary mutations in SMO likely driving resistance mechanisms (Yauch *et al.*, 2009). The GLI family of transcription factors have presented as potential targets in patients with resistance to SMO inhibitors, though only arsenic trioxide (ATO) has progressed to clinical trials, despite other agents showing encouraging results in pre-clinical settings (Lin *et al.*, 2016).

In comparison to WNT and SHH MBs, the molecular targeting of Grp3 and Group4 MB has proven more difficult in recent years, possibly due to the scarce nature of recurrent mutations in these subgroups (DeSouza *et al.*, 2014). Despite this, epigenetic manipulation has been a growing area of interest in these tumours, with chromatin modification genes shown to be involved in a number of patients. It was recently observed that class 1 and 2 HDAC inhibition prompted significant responses in MYC amplified MB cell lines (Ecker *et al.*, 2015), although several trials have failed to reproduce these *in vitro* results in solid tumours (Vansteenkiste *et al.*, 2008; Rathkopf *et al.*, 2013), nor in MB patients. Some encouraging data regarding the targeting of metastatic Group3 tumours- in which high expression of PRUNE1 is observed, have been published (Ferrucci *et al.*, 2018). Through use of a small molecule, AA7.1 (a pyrimido-pyrimidine derivative), they observed increased PRUNE1 degradation resulting in a disrupted PRUNE1/TGF-β/OTX2/PTEN axis. They further demonstrated that in orthotropic xenograft mice, AA7.1 strongly impairs tumour growth and metastatic dissemination (Ferrucci *et al.*, 2018).

Recent studies from Schwallebe and Cavalli have transformed our understanding of the genetic underpinning of MB, how this can inform subgrouping and permit the development and use of novel targeted therapies. The results are thus far encouraging for the management of MB, although primary and secondary drug resistance present significant clinical challenges and highlights the potential need for high quality second and third line therapies. Therefore, it is no surprise that many novel therapies are now targeting alternative mechanisms in cancer biology, including cancer metabolism.

1.6 Introduction to cancer metabolism

Metabolic alterations in tumours have been observed for nearly a century; one of the earliest seminal observations being that of aerobic glycolysis by Otto Warburg in the 1920's (Warburg, 1925). However, cancer metabolism has received renewed attention over the past decade and is now considered a hallmark of cancer (Hanahan and Weinberg, 2011). This interest has been catalysed by innovation in analytical platforms such as mass spectrometry and nuclear magnetic resonance (NMR) spectroscopy, allowing for the expansion of our understanding of tumour-associated alterations in metabolism. Cancer cells, unlike the majority of normal, differentiated cells, typically consume glucose at higher rates, producing increased amounts of lactate - a phenotype originally described by Otto Warburg as aerobic glycolysis, and more commonly referred to as the Warburg effect (Hanahan and Weinberg, 2011). Warburg proposed that the increased consumption of glucose was a direct consequence of compromised oxidative mitochondrial metabolism, and suggested that this was a common and unique component of all cancers (Warburg 1956). It

was later confirmed that this was not a feature unique to only cancer cells (Hedeskov, 1968), and that not all tumours exhibited defects in oxidative metabolism (Wang, Marquardt and Foker, 1976; Brand, 1985). The transformed metabolism observed in tumours supports many of the other hallmarks outlined by Hanahan and Weinberg, including unrestrained growth. In order to support this increased rate of cell division, most tumours alter their metabolism in three main ways; enhanced generation of energy in the form of ATP, anabolic precursors capable of fulfilling macromolecule synthesis and anti-oxidants to counteract increased oxidising effects brought about by both the tumour microenvironment and anti-tumour therapy. Two of the most significantly-utilised nutrients to support increased metabolism in tumours are glucose and glutamine.

1.6.1 Glucose metabolism

The enhanced rate of glycolysis observed in most tumours increases the production of ATP in the cytosol. Compared to the other process for ATP generation – oxidative phosphorylation – glycolytic ATP production is less efficient in terms of nutrient use, as it produces 2 moles of ATP per mole of glucose, compared to 38 moles of ATP per mole glucose by oxidative phosphorylation. However, the significant uptake and metabolism of glucose through glycolysis observed in tumours can compensate for this difference (Gillies, Robey and Gatenby, 2008; Bryant *et al.*, 2014). This also conveys an added advantage to a tumour, as glycolysis can be sustained in the absence of oxygen (Pavlova and Thompson, 2016). The increased uptake of glucose by tumours can be harnessed clinically for diagnosis and staging, by assessing the uptake of radioactive fluorine-labelled glucose (^{18}F-fluorodeoxyglucose) uptake by positron emission tomography (PET)-based imaging (Almuhaideb, Papathanasiou and Bomanji, 2011).

As result of increased glucose uptake, there is also an accumulation of glycolytic intermediates needed for macromolecule biosynthesis. This additional carbon can be diverted into several pathways stemming from glycolysis, where it is utilised in the synthesis of lipids, proteins and nucleotides. An example of this is the flux of carbon through phosphoglycerate dehydrogenase (PHGDH) for *de novo* serine production (Locasale and Cantley, 2011). In addition to ATP production and macromolecule biosynthesis, glucose can also support the production of reducing equivalents in cancer cells, where increased flux into the pentose phosphate pathway allows for NADPH generation (Ward and Thompson, 2012). Furthermore, one of the major consequences of the Warburg Effect is the enhanced regeneration of NAD+ from NADH through the reduction of pyruvate to lactate (Heiden, Cantley and Thompson, 2009), which sustains the high rates of glycolysis (Le *et al.*, 2010) and reduces the requirement of NADH oxidation by the tumour mitochondria. Pyruvate is a major metabolic hub, which as well as being reduced to lactate can be transaminated to form alanine for protein synthesis, or oxidised in the mitochondria by pyruvate dehydrogenase (PDH) to form acetyl coenzyme A (CoA), which then condenses with oxaloacetate to produce citrate in the first step of the tricarboxylic acid (TCA) cycle (Hay, 2016).

1.6.2 Glutamine metabolism

As mentioned in the above section cancer cells require a plethora of additional nutrients in order to maintain their enhanced proliferation and survival in a sub-optimal environment. Although not technically an essential amino acid, glutamine is required by most cancers in significant quantities (Wise and Thompson, 2010), as it serves as a major anabolic carbon and nitrogen source for synthesis of macromolecules, a source of high energy electrons for

ATP production and the regulation of ROS homeostasis via glutamate through the synthesis of glutathione. Cells import glutamine through neutral amino acid transporters, such as the alanine/serine/cysteine/threonine transporter 2 (ASCT2; SLC1A5 (Carr *et al.*, 2010). Alongside the fates above, glutamine may also be exported from the cell through certain antiporters, such as the L-type amino acid transporter (LAT1 or SLC7A5), in exchange for leucine or other branched chain amino acids (BCAAs), which has been shown to be an important compensatory mechanism in leukaemic cells after glycolytic inhibition (Polet *et al.*, 2016). Furthermore, cytosolic glutamine can be used in the synthesis of glutamate, where the amide group can either be removed by glutamine phosphoribosyl pyrophosphate amidotransferase (GPAT) for nucleotide biosynthesis (Metzler, Gfeller and Guinet, 2016), glutamine fructose-6-phosphate amidotransferase 1 (GFAT1) for hexosamine biosynthesis (Oikari *et al.*, 2016), or primarily by glutaminase (GLS).

1.6.3 Glutamate metabolism

Glutamate has diverse roles within the cell, where it can be utilised as an amino acid, or donate its amine group in the biosynthesis of other non-essential amino acids (NEAAs) and nucleotides. NEAAs synthesis is directed through a group of diverse transaminases, which catalyse the transfer of the amine group of glutamate to α-ketoacids; examples being OAA, 3PG and pyruvate, while in the process producing aspartate, serine, and alanine, respectively (Yang *et al.*, 2018). These NEAAs can then be used in several ways, where aspartate is a precursor for asparagine as well as all nucleotides, and serine is a precursor for glycine (as well as a major donor of 1C units for nucleotide synthesis). Independent of transaminase activity, glutamate is also involved in the synthesis of the NEAA proline, which occurs in a two-step enzyme-catalysed reduction (Wu *et al.*, 2011; Coloff *et al.*, 2016).

Recent studies have increased our understanding of how cancer cells utilise glutamine for intermediary carbon metabolism. A large part is of this metabolism is through the deamination of glutamate to form α-ketoglutarate (αKG), which is either produced through transaminase enzymes, or by glutamate dehydrogenase (GDH) - an enzyme whose activity results in the NAD(P)+ dependent release of the amine group as ammonia. Glutamate-derived αKG is able to supplement TCA cycle metabolism and sustain energy production in proliferating cancer cells (Weinberg *et al.*, 2010). Evidence from several cell types highlights the importance of αKG directed anaplerosis (Forbes et al., 2006; Villar et al., 2015; Yang, Venneti and Nagrath, 2017). Moreover, this αKG may also be used to fuel lipid synthesis, which under certain conditions can occur independently of oxidative TCA cycle metabolism. Reductive carboxylation (RC) of αKG allows for the synthesis of citrate and resulting *de novo* lipogenesis through IDH1 and 2, and ACO 1 and 2, in an NADPH-dependant manner. RC was first defined in a brown adipocyte cell line (Yoo *et al.*, 2008) and is now known to be enhanced under hypoxic conditions (Metallo *et al.*, 2012). Moreover, glutamine-derived malate can be used to synthesise pyruvate, through the activity of malic enzyme (ME) (Dey *et al.*, 2017; Murai *et al.*, 2017). This process results in NADPH production, supporting cellular redox and reductive reactions (DeBerardinis *et al.*, 2007). Mitogen stimulation has also been shown to stimulate similar effects in lymphocytes (Brand, 1985) and the use of ^{13}C-labelled glutamine identified glutaminolysis as an anaplerotic process in gliomas (DeBerardinis et al., 2007), although this has since been refined (Tardito et al., 2015).

In addition, glutamate maintains the pool of intracellular glutathione (GSH) - a tripeptide produced from cysteine, glutamate and glycine. The production of GSH from these amino acids requires a two-step, ATP dependant reaction: the first of which involves the rate-limiting enzyme glutamate cysteine ligase (GCL), which converts glutamate and cysteine to

gamma-glutamylcysteine. The second step is then catalysed by glutathione synthetase (Harris *et al.*, 2015).

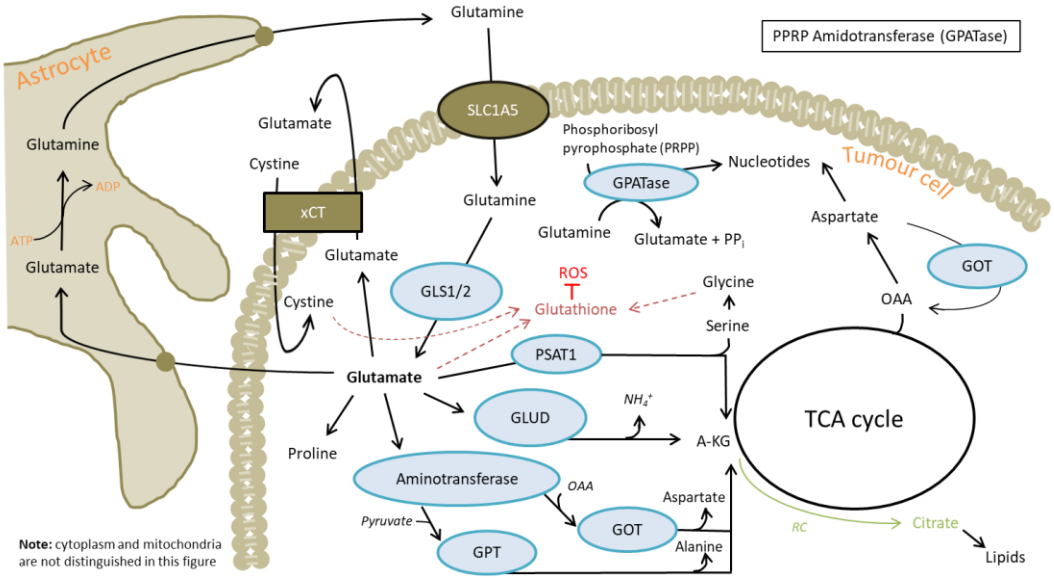

Figure 1.4 An overview of glutamine/glutamate metabolism.

1.6.3.1 Glutamate as a neurotransmitter

Glutamate is the major excitatory neurotransmitter in the central nervous system (CNS), its activity under normal circumstances being governed by numerous transporters, along with ionotropic and metabotropic receptors (Miladinovic, Nashed and Singh, 2015). More recently however, glutamatergic dysregulation has been implicated in gliomas (de Groot and Sontheimer, 2011; Robert and Sontheimer, 2014). Glioma cells have been previously shown to export cytotoxic concentrations of glutamate *in vitro* (Ye and Sontheimer, 1999), which helps promote the growth of malignant gliomas via glutamate receptor signalling (Takano *et al.*, 2001), and may result in neuronal cell death, allowing for the expansion of tumour into the necrotic void (Sontheimer, 2008). The release of glutamate by many tumour types, including gliomas, breast, melanoma and prostate cancers, is largely mediated via system

x_c^- transport (x^{CT}; SLC7A11) (Sharma, Seidlitz and Singh, 2010; de Groot and Sontheimer, 2011). Increased x^{CT} activity conveys additional benefit to cancer cells via cystine uptake and support of GSH synthesis.

In addition to its role as an excitatory neurotransmitter, glutamate is also a substrate for the synthesis of the inhibitory neurotransmitter Gamma-aminobutyric acid (GABA). The synthesis of GABA from glutamate is catalysed by the enzyme glutamate decarboxylase (GAD) (Bak, Schousboe and Waagepetersen, 2006). The role of GABA in the context of cancers has been relatively unexplored, and the few studies into its role are conflicting. It has been reported that pancreatic cancers with GABA-A receptor overexpression demonstrated amplified growth through GABA signalling (Takehara *et al.*, 2007). However, an opposing role in colon carcinoma cells has also been described (Miao *et al.*, 2010). Furthermore, the pattern of GABA receptor gene expression is predictive of prognosis in non-small cell lung cancer, where a low expression of $GABR_{A3}$ with a high expression of $GABBR_2$ predicts a better outcome in these patients (Zhang *et al.*, 2013). There is clearly more research required on the biological effects of GABA production in tumours.

1.6.2.1 Glutaminase

The amidohydrolase enzyme glutaminase (GLS) is a crucial component of glutamine metabolism, where it catalyses the hydrolysis of the γ-amino group of glutamine to form glutamate and ammonia (Yuneva et al, 2007). The resulting ammonia can be utilised to produce carbamoyl phosphate, or may simply diffuse from the cell. The GLS family comprise of two isozymes which are encoded on separate genes located on different chromosomes: the Kidney (K-type) GLS gene, which is situated within chromosome 2 and encodes two variants KGA and GAC (Figure 1.4 A), and the liver (L-type) GLS2 gene, which is positioned on

chromosome 12 and encodes for an additional two isozymes, LGA and GAB (Figure 1.4 B). GLS1 has been shown as being highly expressed in tumour cells, where it aids proliferation and oncogenic transformation. GLS2, however, is commonly down regulated in tumours and is often described as tumour suppressive, although, it is important to note that this does not apply to all tumour types (Xiang et al, 2013).

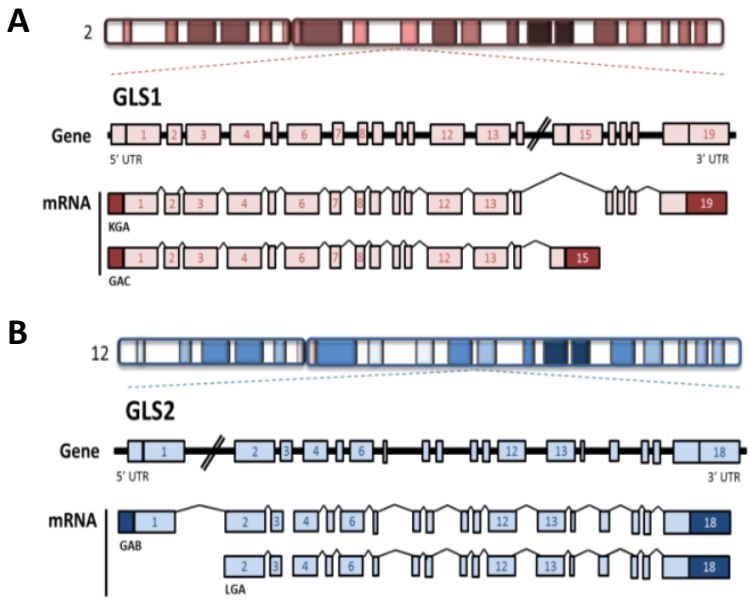

Figure 1.5 Genomic structure of GLS1 and GLS2 genes and mRNA transcripts. Introns are depicted as solid black lines and exons as numbered red (GLS1) or blue (GLS2) boxes. mRNA reveals differences between splice variants, KGA and GAC for GLS1 and GAB and LGA for GLS2.

In MB, the same is likely to apply, given the oncogenes and tumour suppressors associated with this tumour. C-MYC expression has a strong, indirect effect on GLS1 expression through the repression of microRNA-23A and microRNA23-B, which act to inhibit GLS1 expression. Furthermore, it has also been reported that GLS2 is a p53 target gene, and is regulated through three p53 consensus DNA-binding elements within the promotor region. This was

confirmed in both tumour and non-tumour cells, where the degree of its regulation altered depending on cell type and levels of stress (Suzuki et al, 2010).

It seems key to elucidate the opposing roles of these proteins and to investigate why different GLS isoforms have evolved. The weight of data suggests that GLS1 expression positively correlates with heightened proliferation, while GLS2 expression appears to be associated with non-proliferating cells (Campos-Sandoval *et al.*, 2015). In view of that, it is no surprise that increased GLS1 expression has been observed in several cancers, including lung, breast, brain, B cell lymphomas and cervical (Szeliga and Obara-Michlewska, 2009). However, GLS1 exists as two splice variants and it is also important to elucidate whether their expression or relative activity differs in cancer. KGA and GAB are typically referred to as mitochondrial glutaminases, however, this nomenclature appears inaccurate as increasing number of studies have shown differential expression in the cytosolic fractions of cells (Cassago *et al.*, 2012; Campos-Sandoval *et al.*, 2015). The nomenclature also generates confusion within the literature, with some studies referring to GLS1 as KGA, encompassing GAC along with it, therefore disregarding these as two separate variants. Few studies have examined the phenotypic differences between KGA and GAC, although, the identification of differential intracellular localisation highlights the need for increased investigations. One important aspect to consider will be the compartmentalisation of glutamate and the role this may play in different metabolic pathways.

Unlike GLS1, GLS2 is commonly silenced in gliomas through promoter methylation (Szeliga and Obara-Michlewska, 2009). In fact, overexpression of GLS2 in glioblastoma cell lines was shown to elicit a reversion of their tumourigenic phenotype (Szeliga *et al.*, 2014). The visualisation of GLS2 in the nucleus (Olalla *et al.*, 2002) has fuelled much debate about its

role in transcriptional reprogramming- indeed it is possible that the overexpression of GLS2 may have reduced the malignant phenotype in a glioma cell line through direct alteration of the transcriptome (Suzuki et al, 2010). However, there is currently a paucity of data regarding this putative nuclear role of GLS2. As mentioned previously, GLS2 expression is commonly lost in gliomas, despite high expression in healthy brain. In agreement with this observation, GLS2 is also greatly reduced in other brain tumours, as well as hepatocellular carcinomas, which highlights the clinical implications of this protein and its potential role in tumour suppression. However, the behaviour of GLS2 in cancer is more complicated than previously assumed, as there are some types of cancer where increased GLS2 expression is observed, conferring resistance to current therapies (Hu *et al.*, 2010). Furthermore, GLS2 expression increases in response to oxidative stress or DNA damage in a p53-dependent manner, which may be protective through enhancement of mitochondrial respiration and therefore, ATP production, and decrease of ROS levels through the increase in cellular concentrations of glutathione (Rufián et al, 2015).

Although, it has previously been suggested that the differing regulation of GLS and GLS2 may account for their opposing roles in human biology, it is possible that these roles may be determined by their structure. GLS2 appears to have greater potential than GLS1 for regulation through interactions with other proteins or indeed metabolites, as it contains a number of consensus motifs and domains within its structure. It has been found that the GAB isoform contains a consensus sequence essential for interaction with PDZ proteins; specifically glutaminase-interacting protein (GIP) and α1-syntrophin (Olalla *et al.*, 2002).Little is known, however, about potential protein: protein interactions of GLS. GLS isozymes are therefore thought to differ in their kinetics, regulation and evidence suggests that they may have alternative roles in immunological responses. Their differences in

activity are largely related to the dependence on inorganic phosphate as an activator; GLS2 has little dependency, while GLS1 is more dependent for its activity. The relative affinity for glutamine has also been established with GLS1 exhibiting a higher affinity. A novel characteristic of GLS1 isozymes have also been revealed, where glutamate has been found to have an inhibitory effect (De la Rosa et al, 2009). Surprisingly, the GAB variant of GLS2 exhibits kinetics reflecting both GLS1 and GLS2 characteristics; GAB displays both low dependence on inorganic phosphate for its activity, but was surprisingly inhibited by glutamate (Szeliga et al, 2013). This emphasises the plethora of effectors that may modulate the activity of GLS isozymes and may go some way to explain how cancer cells can selectively express GLS isoforms that support different phenotypes - whether 'go' or 'grow'.

1.6.3 The role of genetics on cancer metabolism

Mutations in tumour suppressors and oncogenes are the basis of cancer. Recent work, however, has revealed a tightly regulated network between oncogenic mutations and resulting metabolic phenotypes. For instance, p53 is a potent regulator of metabolism, where it is able to elicit effects at several points of both glycolysis and oxidative phosphorylation. Alterations in the flux through glycolysis is achieved through activation of p53-induced glycolysis and apoptosis regulator (TIGAR), which inhibits PFK-1 activity diverting glucose 6-phosphate into the pentose phosphate pathway (PPP) (Bensaad *et al.*, 2006), while increased oxidative phosphorylation is mediated through p53-induced cytochrome c oxidase assembly factor SCO2 (Matoba *et al.*, 2006). As introduced earlier (section 1.6.2.1*),* p53 induces GLS2 expression, increasing glutamate and αKG levels and enhances the rate of the TCA cycle (Hu *et al.*, 2010). These metabolic changes through p53-dependant target gene expressions may provide a mechanism of reducing tumorigenesis, by

resisting 'Warburg metabolism'. However, they may also support tumourigenesis after initial oncogenic stimulus through increased resistance to oxidative stress and enhanced anabolism. The MYC proto-oncogene is frequently activated in human cancers and can also regulate genes involved in cellular metabolism, such glutamine metabolism (Wise *et al.*, 2008), mitochondrial biogenesis (Morrish *et al.*, 2010) and lipid synthesis (Eberlin *et al.*, 2014). Furthermore, tumourigenic mutations seldom arise in isolation and the combination of mutations in a given cancer cell can alter its metabolic network. Comprehending the mechanisms by which specific mutations alter cellular metabolism is important to understand the metabolic dependencies and/or deficiencies in specific tumours, which may be exploited therapeutically. Many of the mutations in tumours result in similar changes in metabolism, thus, metabolic targeting rather molecular targeting may be more successful in a range of tumours. An example of this was demonstrated In the case of Kirsten rat sarcoma viral oncogene homolog (KRAS) mutations in pancreatic ductal adenocarcinoma (PDAC) (Biankin *et al.*, 2012), which despite occurring in around 95% of tumours, has no effective targeted treatments (Kamisawa *et al.*, 2016). Several studies have highlighted oncogenic KRAS as a major player in regulating tumour metabolism, where is has been shown to stimulate glucose uptake (Yun *et al.*, 2009), alter glutamine metabolism (Son et al. 2013), induce autophagy and macropinocytosis (Mann *et al.*, 2016).

1.7 Metabolism in Medulloblastoma

Metabolism in cells undergoing neural development appears to share several of the traits also observed in cancer, including an increase in aerobic glycolysis (Warburg effect) and increased lipogenesis (Bhatia *et al.*, 2011). This is not surprising seeing as neurogenesis, similarly to cancer, requires rapid proliferation. These metabolic phenotypes observed in

neural progenitors are preserved or reinstated in MB, which arises from progenitor-derived brain cells.

During the first 12 months of life, cerebellar granule neuron progenitors (CGNPs) proliferate in a germline matrix along the external granule layer (EGL) of the cerebellum. This proliferation is prompted by the introduction of sonic hedgehog (shh) signalling, which is halted upon completed cerebellar development, but may continue when shh signalling is aberrantly controlled, thus predisposing to MB (Noguchi et al, 2015). In addition to proliferation, shh signalling alters CGNPs metabolic phenotype by increasing aerobic glycolysis and lipogenesis, with a concurrent decrease in fatty acid oxidation. To achieve this, shh transcriptionally regulates proteins needed for lipid synthesis, such as acetyl-CoA carboxylase 1 (ACC1) and fatty acid synthase (FASN), medium chain acyl-CoA dehydrogenase (MCAD) and also acyl-CoA oxidase 1 (ACOX1) (Foster et al, 2012). This transcriptional regulation is largely controlled through shh-dependent stimulation of E2F1 through Retinoblastoma protein (RB) modulation. A *shh*-driven MB transgenic mouse model, which recapitulates the lipid deposition observed in patient tumours, was used to investigate whether, *ex vivo*, this could be observed in CGNPs. When explanted CGNPs were cultured in shh-rich media, the same transcriptionally altered phenotype as outlines above was observed, confirming the signalling mechanism responsible for this phenotype. Furthermore, role of the Rb-E2F axis in MB phenotype, downstream of shh, was also noted: after knocking down of E2F1 a reduction in *shh*-mediated expression of FASN and MCAD was recorded in these CGNP cells (Bhatia *et al.*, 2011). As further evidence, palmitate oxidation was monitored in the shh-MB tumour model- the decreased oxidation was rescued upon E2F1 knockdown. Therefore, Shh resulted in synthetic lipid metabolism in CGNPs rather than being catabolic, and this switch was facilitated by E2F1 and negatively

controlled by Rb. This metabolic phenotype is upheld in MB-bearing mice where it has been shown that therapeutic inhibition of FASN or the Rb-E2F axis slowed tumour progression and lengthened the overall survival in these mice (Bhatia *et al.*, 2012).

The similarities between energy metabolism during neurogenesis and MB can be found within the Peroxisome Proliferator-Activated Receptor-γ (PPARγ) signalling axis. In particular, a study showed that E2F1 is able to activate PPARγ, which in turn leads to the upregulation of several glycolytic enzymes, such as Pyruvate kinase M2 (PkM2), Hexokinase 2 (HK2), and GLUT4 (Bhatia *et al.*, 2012). In the same study, it was also demonstrated that the blockade of PPARγ significantly inhibited tumour cell growth, thereby prolonging mouse survival, similarly to that observed with FASN and Rb-E2F inhibition.

It is therefore understood that MB is a heterogeneous collection of tumours; with potentially 12 subgroups (previously seen in section 1.3.5). However, much of the described metabolic regulation and effectors have been focused on SHH signalling, despite this subgroup only constituting around a third of all cases of MB. This raises the question of whether the metabolic phenotypes described in CGPNs and SHH MB bear resemblance to the other subgroups, given their suggested different cell type of origin. However, given that many of the metabolic phenotypes observed in CGPNs, including that of high glycolytic flux, are common to most if not all progenitor/stem cells, it is likely that all neural progenitors that are the origins of MB share similar metabolic networks (Ito and Suda, 2014). Despite cerebellar proliferation being dependent on SHH signalling, HK1 is not expressed in any progenitor regions within the postnatal brain, implying a shift to HK2 can be initiated by various growth factors (Gershon et al, 2013). In relation to this, PKM2 integrates the signalling pathways from several growth factors in order to decrease PK activity. Therefore,

CGPN activation of aerobic glycolysis in response to SHH signalling could be a generic reaction of these cells to individual growth factors that drive their proliferation.

As well as SHH signalling, there are increasing data indicating that WNT/β-catenin signalling is able to regulate metabolism in tumour cells. It was established in ovarian cancer that a significant number of genes controlling metabolism- in particular glutamine and fatty acid metabolism- were found to be transcriptional targets of β-catenin. Recent studies have uncovered the role of the canonical WNT pathway in cancer cell metabolism (Wetering et al, 2002). For example, in hepatocarcinoma, WNT signalling was found to increase aerobic glycolysis by suppressing mitochondrial respiration through the reduction of cytochrome c oxidase. It has been well documented that WNT signalling transcriptionally increases C-MYC (Calvisi *et al.*, 2001) In fact N-MYC and its homologue C-MYC are vital in the regulation of progenitor cell function in neural tissue, where N-MYC is commonly activated in all subtypes of MB and C-Myc plays a significant role in Grp3 MB (Roussel and Robinson, 2013). Interruption of the MYC-MAX complex in CGNPs prevented the shh-dependent initiation of aerobic glycolysis and proliferation. This evidence strongly supports the notion that MYC may be a common metabolic conversion point between subgroups, that may act downstream of multiple mitogenic signalling pathways.

Importantly, SHH and WNT pathway stimulation are able to drive MB progression by activating downstream oncogenes, such as N-MYC. Understanding the mechanisms that regulate the metabolism of cerebellar progenitors during development may thus lead to novel, metabolic approaches to anti-cancer therapy.

1.8 Methods used to investigate cancer metabolism

1.8.1 Metabolomics

Although genomics provide a plethora of information regarding cell genotype, it does not reveal the phenotypical nature of cancers. Instead, it provides insights into the phenotype which is 'likely' to occur. Metabolomics describes the field of study dedicated to the exploration of the metabolome within a biological system allowing for a more in depth understanding of cellular functions in cancer, allowing us to measure biological 'end points'. Technologies dedicated to the study of metabolomics are typically founded on sensitive spectroscopic and spectrometric approaches, such as chromatography, mass spectrometry (MS) and nuclear magnetic resonance (NMR) spectroscopy.

Metabolic profiles are becoming increasingly seen as a way of stratifying tumours. For brain tumours particularly it is beneficial as it can be conducted through non-invasive imaging. A retrospective study analysed patients with MB using ^{1}H magnetic resonance spectroscopy (MRS) and identified that glutamate was a marker of survival across all MB subgroups (Wilson *et al.*, 2014).

1.8.2 Stable isotope tracing

Unless 'essential' within a system, metabolites can be produced by several interconnecting pathways. One example of this is the synthesis of glutamate, which can be synthesised or utilised by 200 known reactions, spanning 55 metabolic pathways (Fan et al. 2012). This makes it difficult to distinguish which pathway is responsible for eliciting changes observed in glutamate concentrations, and therefore, highlights the importance of being able to determine the origin or 'destination' of any given metabolite. This can be achieved with isotopic label incorporation methods, which rely on the use of naturally-occurring

metabolites, enriched in one or more heavy isotopes (Antoniewicz, 2013). The most popular isotope used today is ^{13}C, owing to the significant proportion of metabolites containing carbon backbones, and the fact that it has a non-integer spin and a detectably different mass compared to ^{12}C, allowing it to be measured using spectroscopic and spectrometric techniques. Other viable tracers include ^{15}N and ^{18}O, which are gaining popularity. To perform these analysis, isotopically enriched tracer metabolites, such as glutamine are fed to cells, resulting in metabolites downstream to be enriched with the isotope of choice. The differing amounts and ways in which subsequent metabolites can be labelled with stable isotope reveals information regarding the pathway used.

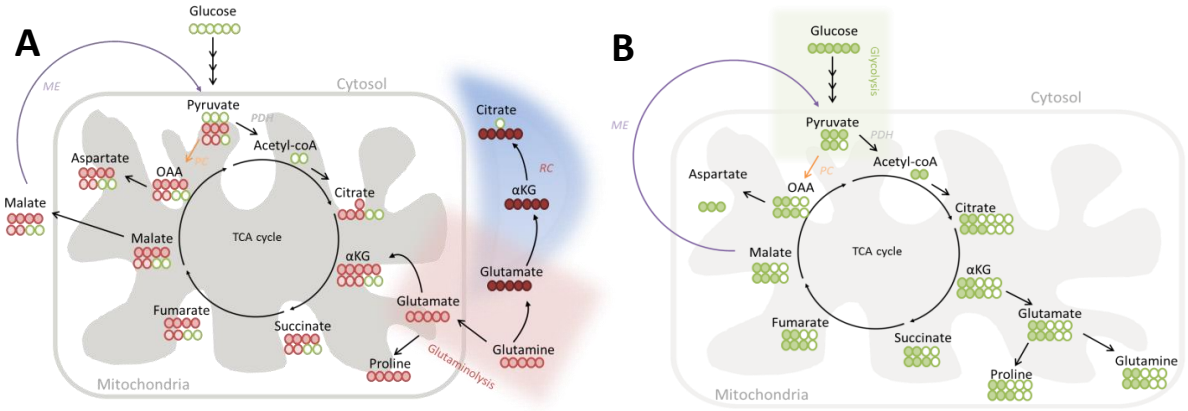

Figure 1.6 Isotope labelling. A) example of ^{13}C-U-glutamine isotopic labelling. B) Example of 13C-U-glucose labelling. Different labels can be used to identify various metabolic pathways.

1.8 Manipulating metabolism in the treatment of cancer

Since Otto Warburg's observation of increased lactate production in aerobic conditions in cancer cells (Warburg, 1925), significant studies, including clinical trials, have examined the effectiveness of blocking this metabolic pathway to reduce tumour growth, or as a means of

sensitising tumours to existing treatment. Such effects have been directed towards reducing tumours glucose uptake, where Ritonavir (inhibitor of GLUT4) blocks glucose uptake in multiple myeloma cells leading to the induction of apoptosis. Ritonavir was also shown to decrease the viability of primary myeloma cells and increase sensitivity to doxorubicin (McBrayer *et al.*, 2012). Efforts have also been directed towards disrupting tumour glycolysis. 2-deoxyglucose (2-DG) is a glucose analogue shown to increase killing of breast cancer cells when combined with irradiation or chemotherapeutic treatments (Aghaee, Islamian and Baradaran, 2012). However, an early phase clinical trial with intravenous infusions of 2-DG in pancreatic tumour patients were discontinued due to adverse side effects (Landau *et al.*, 1958). A significant problem with these therapies lies in the non-specific nature of targeting glycolysis, highlighting the need for more specific metabolic pathway targeting approaches.

1.8.1 Targeting glutamine metabolism.

It has been shown that many types of cancer cells are sensitive to glutamine starvation, including cells derived from small cell lung carcinoma, glioblastoma multiforme and acute myelogenous leukaemia (Wu, Arimura and Yunis, 1978). Glutamine analogues including 6-diazo-5-oxo-L-norleucine (L-DON), azaserine, and acivicin have also been investigated with varying degrees of success. Preclinical testing of each of these agents displayed significant cytotoxicity's in specific tumour types, both in cell lines and in mouse xenograft models (Ahluwalia *et al.*, 1990). However, owing to severe toxicities observed in clinical trials, the use of glutamine analogues is restricted. Other efforts have been directed towards suppressing glutamine uptake in tumour cells with a study demonstrating how the targeting

of SLC1A5 with small molecule inhibitors, L-γ-glutamyl-p-nitroanilide and benzylserine suppresses the growth of non-small cell lung tumours in vivo (Hassanein *et al.*, 2015).

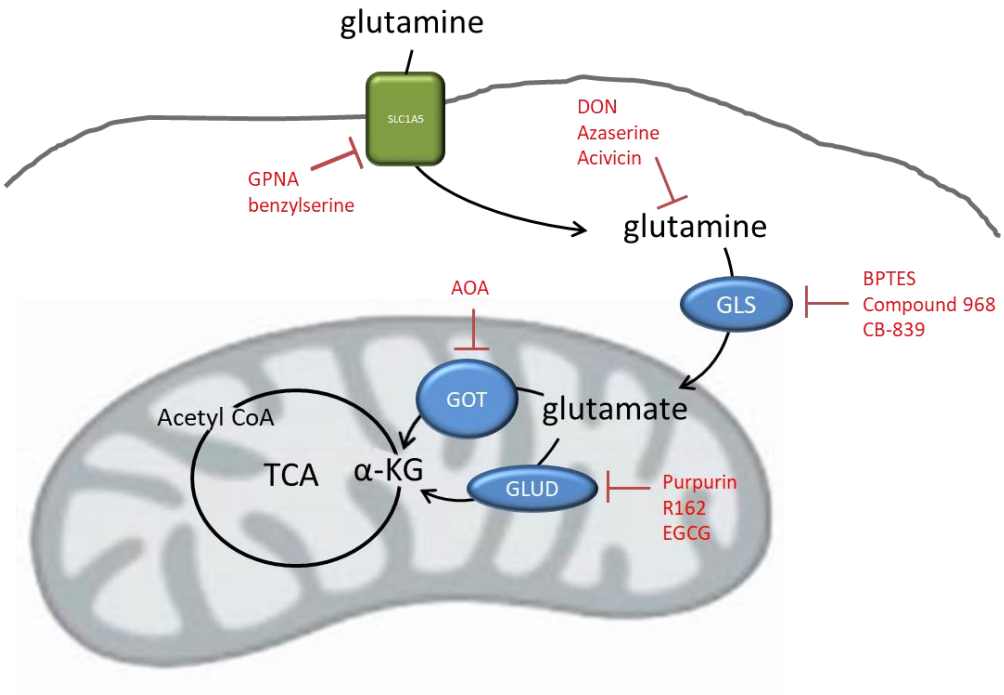

Figure 1.7 Druggable targets in glutaminolysis. Enzymes are shown in blue, transporter in green. Inhibitors of these are shown in red.

Due to the importance of glutamine in cancer, substantial efforts have been made to inhibit its uptake and resulting metabolism. Reduction of GLS expression through siRNA has been shown to reduce ATP while raising intracellular ROS levels in breast cancer, highlighting it as a potential target in certain tumours. Furthermore, GLS can be therapeutically targeted with small molecule inhibitors such as compound 968 (Wang *et al.*, 2010), CB-839 (Gross *et al.*, 2014) or the most widely studied GLS inhibitor bis-2-[5–phenylacetamido-1, 2, 4-thiadiazol-2-yl] ethyl sulfide (BPTES) (Shukla *et al.*, 2012). The use of these inhibitors in the treatment of cancers is summarised in table 1.1

Table 1.1 Inhibitors of GLS1 and their use in the clinic

BPTES	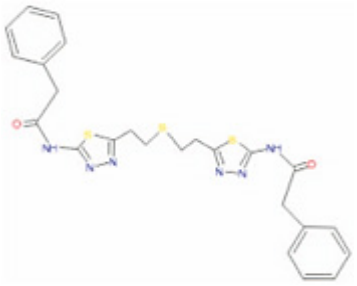	BPTES specifically inhibits glutaminase and suppress tumour growth in several preclinical animal models including hepatocellular carcinoma (Xiang *et al.*, 2015), renal cell carcinomas(Shroff *et al.*, 2015) and lymphoma (Le *et al.*, 2012)
CB-839	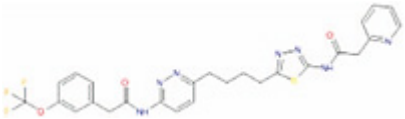	Triple negative breast cancer (Gross *et al.*, 2014)
Compound 968	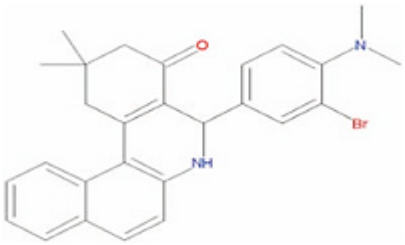	Compound 968 has been shown to suppress oncogenic transformation induced by Rho GTPases in fibroblasts. C968 also shows synergistic action in combination with mTOR inhibitor in glioblastoma (Tanaka *et al.*, 2015)

The binding of BPTES to GLS, elucidated through investigations of the crystal structure, is through an allosteric pocket at the dimer interface, which results in the stabilisation of the tetrameric, inactive form of GLS (Thangavelu *et al.*, 2012). Several studies have shown the effectiveness of BPTES on inhibiting proliferation of tumour cells, including renal cell carcinoma (Shroff *et al.*, 2015), hepatocellular carcinoma (Xiang *et al.*, 2015) and in B-cell lymphoma (Le *et al.*, 2012). Interestingly, pyruvate carboxylase (PC) expression has been shown to determine BPTES efficacy, with higher PC reducing the sensitivity of lung cancer cells to BPTES (Ulanet *et al.*, 2014), suggesting a potential benefit of duel targeting of GLS and PC simultaneously. CB-839 is a relatively new derivative of BPTES and is currently in phase 1 clinical trials to treat triple negative breast cancer (Gross *et al.*, 2014). However, few

other studies have made meaningful progress as of yet. The mode of action of compound 968 is different to that of BPTES; this inhibitor preferentially binds to the monomeric ,inactive form of GLS, and as a result prevents the dimerization required for GLS activation (Stalnecker *et al.*, 2015). Therefore, compound 968 is unable to inhibit GLS when the enzyme is already in an active conformation. The effectiveness of compound 968 has been demonstrated in breast cancer, where inhibition prevented Rho GTPase dependant oncogenic transformation and exhibited synergistic activity in glioblastoma when combined with mTOR inhibitors (Tanaka *et al.*, 2015). Importantly, compound 968 appears to demonstrate a reasonable potential therapeutic window, as concentrations that are inhibitory in cancer cells, often show minimal effects upon non-transformed cells (Wang *et al.*, 2010). In part, these results can be accounted for the fact that non-transformed cells are able to bypass the need for glutaminase, and typically use glucose for oxidative phosphorylation. However, as highlighted above, glutamine-derived glutamate has a significant physiological role in the brain, through its neurotransmitter activity, which leads to side-effects of this treatment. Despite encouraging *in vitro* results using compound 968, use in pre-clinical animal models has been challenging, due to its hydrophobic nature (Katt and Cerione, 2014).

It is interesting to see that different allosteric mechanisms observed between BPTES and compound 968 results in differential effects in the treatment of tumours. The inhibition differences caused by these compounds on KGA and GAC have not been elucidated yet and may be needed to shed light on possible differences observed clinically.

Unlike GLS1, the therapeutic targeting of GLS2 has been relatively neglected, until more recently, due to a lack of specific inhibitory compounds. Lee and colleagues, however, have

identified Alkyl benzoquinones as novel inhibitors of GLS2, the use of which leads to mTORC1 inhibition and results in reduced tumorigenesis (Lee *et al.*, 2014). It will be interesting to see the use of these inhibitors in future studies.

As a metabolite interlinked with glutamine, proline has received more interest in recent times with disruption of this metabolism proving a potential target in the treatment of cancers (Phang *et al.*, 2015). The importance of proline is also highlighted by the fact that MYC induces its biosynthesis from glutamine (Liu *et al.*, 2012), which was later elucidated to be a direct cause of MYC-induced upregulation of Δ1-pyrroline-5-carboxylate (P5C) synthase (P5CS), and P5C reductase-1 (PYCR1) (Liu *et al.*, 2015). Inhibition of this proline metabolism reduced the growth of a number of tumour cell lines, which was thought to be a result of reduced pyridine nucleotide synthesis (Liu *et al.*, 2015).

1.9 Summary

Our molecular understanding of MB tumours has been advanced dramatically over the past few years, with invaluable studies from Schwallebe and Cavalli, revealing new MB subgroups, each with different prognoses. Despite this, no real success has been made in the way of molecular targeting of these tumours, where we know from past attempts that primary and secondary drug resistance present significant clinical challenges. In the clinic, patients still receive the same treatment regimens, albeit at different intensities, and it is clear other attempts must be made to treat these tumours. Glutamate is a predictive marker of survival in MB, irrespective of subgroups. This, along with Niklison-Chirou's study last year, highlights the potential importance of glutamine metabolism in these tumours and the potential for the clinical targeting of this metabolism.

1.10 Thesis aims

This thesis aims to investigate the importance of glutamine metabolism in MB, with added emphasis on understanding the impact of increasing glutamate concentrations. We intend to identify key glutamine - derived metabolic pathways utilised in MB cell line, with the aim of targeting these pathways to increase currently used cytotoxic treatments.

Chapter 2

General methods & materials

2.1 Cell Lines

All cell lines used were derived from SHH-MB patients. ONS-76 (TP53 WT) cells were purchased from the Japanese cell line bank (JCLB), DAOY (TP53 mutant) cells were purchased from the American Type Culture Collection (ATCC), and the UW228.3 cells were kindly gifted by Professor Steve Clifford (University of Newcastle). All cell lines were cultured in DMEM HAMS/F12 (Sigma-Aldrich, D5796) supplemented with 10% FBS (Hyclone Thermo Scientific, SV30180.03). Cell lines were maintained using standard procedures in a 37^{o}C humidified incubator, 5% CO_2 and regularly tested and excluded for Mycoplasma contamination using EZ-PCR Mycoplasma Test Kit, (Geneflow, K1-0210).

2.2 MB patient mRNA expression & survival cohorts

2.2.1. GEO: GDS4471

Clinical and mRNA expression data, from MB patients, was extracted from an online NCBI Geo repository (accession number: GDS4471). This Expression profiling array, included 76 samples, each belonging to the separate MB subgroups; WNT (n=8), SHH (n=11), G3 (n=16) and G4 (n=39). Two of the patients did not fit into one of these subgroups and thus, were excluded from this dataset.

2.2.2. GEO: GSE42658

We analysed mRNA-sequence data collected from 9 MB patient samples and 4 CB samples, using the NCBI Geo repository accession number: GSE42658. Subgrouping information for the 9 MB patients were not attained. A non-parametric t-test with a Mann Whitney post-test was performed on the data obtained, using GraphPad Prism. *p<0.05, **p<0.01, ***p<0.001, ****p<0.0001.

2.2.3. Newcastle Cohort

Data arising from patients within the Newcastle cohort was provided to us by Professor Steven Clifford, University of Newcastle.

Clinical data allocated to individual patient was downloaded and data regarding sample ID, neoplasm histologic grade, overall survival (months) and overall survival status were noted. n=240 (WNT n=28, SHH n=58, G3 n=59 and G4 n =95). High and low expression was determined by the median expression value for each gene. An overall survival status column was generated, with patients who died from their disease were designated '1' and surviving patients were entitled '0'. Log-rank (Mantel-Cox) and Gehan-Breslow-Wilcoxon statistical tests were performed in all cases; *p<0.05, **p<0.01, ***p<0.001, ****p<0.0001.

2.3. Survival analysis and Kaplan-Meier generation

Microsoft Excel was used to sort the data set by gene expression for each gene and find the median gene expression. Median gene expression was used to separate the high and low gene expression. GraphPad Prism 7.0 was used to produce Kaplan-Meier survival curves of all genes in the gene set. Overall survival (months) and overall survival status data for the high and low gene expression groups was entered into the data table. GraphPad Prism was used to generate a survival analysis for each survival curve including a Log-rank/Mantel-Cox (MC) statistical test. *p<0.05, **p<0.01, ***p<0.001, ****p<0.0001

Table 2.1. List of gene names examined

Gene name	Gene description
ALDH18A1 (P5CS)	Aldehyde dehydrogenase 18 family, member A1 (Pyrroline-5-Carboxylate Synthetase)
CDO1	Cysteine dioxygenase type 1
GAD1	Glutamate decarboxylase 1
GCLC	Glutamate—cysteine ligase catalytic subunit
GCLM	Glutamate-cysteine ligase regulatory subunit
GLS	Glutaminase 1
GLS2	Glutaminase 2
GLUD1	Glutamate dehydrogenase 1
GLUL (GS)	Glutamine synthetase
GPX1	Glutathione peroxidase 1
GRM1	Glutamate receptor, metabotropic 1
GRM3	Glutamate receptor, metabotropic 3
GSR	Glutathione reductase
GSS	Glutathione synthetase
OAT	Ornithine aminotransferase
PRODH	Proline dehydrogenase
PYCR1	Pyrroline-5-carboxylate reductase 1
PYCR2	Pyrroline-5-carboxylate reductase 2
SHMT1	Serine Hydroxymethyltransferase 1 (cytosolic)
SHMT2	Serine Hydroxymethyltransferase 2 (mitochondrial)
SLC1A1 (EAAT3)	Excitatory amino-acid transporter 3
SLC1A2 (EAAT2)	Excitatory amino-acid transporter 2
SLC1A3, (EAAT1), (GLAST)	Excitatory amino-acid transporter 1, (Glutamate Aspartate

	Transporter)
SLC1A5	Neutral amino acid transporter B
SLC1A6 (EAAT4)	Excitatory amino-acid transporter 4
SLC1A7 (EAAT5)	Excitatory amino-acid transporter 5
SLC6A1 (GAT1)	GABA transporter 1
SLC7A11	Cystine/glutamate transporter (xCT)

2.4 RNA Silencing

To assess the knockdown in expression of GLS1 and GLS2, cells were seeded at 2.5 x 10^5 onto 12-well plates in standard culture conditions. After 24 h, cells were transfected following manufacturer's instructions with non-targeting RNA (siNT) and siRNA targeting GLS1 (siGLS1) and GLS2 (siGLS2) (Dharmacon ON-TARGETplus human siRNA; D-001810-10, L-004548-01-0010 and L-012500-01-0010, respectively) at 25 nM using DharmaFECT 1 transfection reagent (Thermo Fisher Scientific, T2001-01) for the ONS-76 and UW228.3 cell line and Lipofectamine2000 for the DAOY line.

Table 2.2. Table of transfection conditions

Gene target name	Product information	siRNA sequence	Concentration
Non-targeting (NT)	Dharmacon,	D-001810-10-05	25nmol
GLS1	Dharmacon SMARTpool	CCUGAAGCAGUUCGAAAUA	25nmol
GLS2	Dharmacon SMARTpool	GCUGAAGCAGUGCGCAACA	50nmol
GAC1	Dharmacon ON-TARGET	GGAAGUCUGGGAGAGAAUU	25nmol
GAC2	Dharmacon ON-TARGET	CUAUGAAAGUCUCCAACAUU	25nmol
KGA1	Dharmacon ON-TARGET	CCCAAGGACAGGUGGAAUAUU	25nmol
KGA2	Dharmacon ON-TARGET	CUGGAAGCCUGCAAAGUAAUU	25nmol

24 h, 48 h and 72 h post transfection, cells were lysed for protein to evaluate efficiency of gene knockdown. All transfections were carried out 48 h post seeding and all experiments were terminated approximately 72 h from transfection.

2.5 mRNA extraction

Total RNA was extracted from the ONS-76, DAOY and UW228.3 cell lines using the RNeasy Mini Kit (Qiagen, 74104) according to the manufacture's protocol. Cells were lysed in RLT buffer (350 µL), scraped and collected. 350 µL of 70% ethanol was added to each sample and were subsequently transferred to RNeasy Mini spin columns and centrifuged for 15 secs at 8000 G. RW1 Buffer (350µL) was added to each column and centrifuged for 15 secs at 8000 g. Buffer RW1 (350µL) was added to each column and centrifuged for 15 seconds at 8000 g. Buffer RPE (500 µL) was added to each column and centrifuged for 15 seconds at 8000 g. Buffer RPE (500 µL) was added to each column and centrifuged for 2 minutes at 8000 g. RNase-free water (30 µL) was added to each column and centrifuged for 1 minute at

8000 g to elute the RNA. The quality of the extracted RNA was assessed with a ND-1000 Nanodrop.

2.6 Quantitative real-time PCR

Following extraction, 1 µg RNA per sample was subjected to reverse transcription using Moloney Murine Leukemia Virus Reverse Transcriptase (MMLV-RT) kit (Promega, M1701). 10 µL of the resulting cDNA was used with TaqMan® gene expression master mix (AB, 4369016) for quantitative real-time PCR using AB 7500 Real Time PCR System. The following primers and probes were used: *GLS1* (Hs01014020_m1), *GLS2* (Hs00998733_m1), KGA (Hs04969278_s1), GAC (Hs01022163_m1) and *ACTIN* (Hs00157387_m1) (ThermoFisher Scientific). The expression of GLS1, GLS2, KGA and GAC were normalised to actin as housekeeping gene. Comparative analysis across samples was calculated using the $2^{-\Delta\Delta CT}$ method.

Table 2.3 Table of Taqman probes for qPCR

Gene target name	Product number	Application
Actin	Hs00157387_m1	FAM-MGB
GLS1	Hs01014020_m1	FAM-MGB
GLS2	Hs00998733_m1	FAM-MGB
GAC	Hs01022163_m1	FAM-MGB
KGA	Hs04969278_s1	FAM-MGB

2.7 Immunoblotting

Cells were washed with 1x PBS and lysed directly into 100 µL 1x Laemmli buffer (Sigma-Aldrich, S3401-1VL), heated at 100^{o}C for 10min, and loaded on 12% acrylamide gels for SDS-PAGE. Following SDS-PAGE, proteins were transferred electrophoretically onto 0.1 µm nitrocellulose membrane (GE Healthcare, 10600000) at 100 V for 90 min. The blots were blocked in PBST buffer containing 5% (w/v) non-fat dry milk for 1h, and then incubated with the following specific primary antibody diluted in blocking buffer at 4^{o}C overnight (see table for antibody spec). All antibodies were diluted in 5% milk. Membranes were washed three times in PBST and incubated with HRP-conjugated secondary antibody for 1 h at room temperature (Cell Signalling secondary anti-mouse #7076 and anti-rabbit #7074 were both diluted 1:4000 in 5% milk). Membranes were washed three times and developed using EZ-ECL enhanced chemiluminescence detection kit (BI, 20-500-120). All western blots are representative of two experiments unless otherwise indicated.

Table 2.4 **Antibodies used for western blotting**

Antibody	Species	Concentration	Supplier (product code)
Anti-GLS1	Rabbit	1:3000	Abcam, ab93434
Anti-GLS2	Mouse	1:500	Abcam, ab150474
Anti-PYCR1	Rabbit	1:5000	Proteintech, 13108-1-AP
Anti-PYCR2	Rabbit	1:1000	Proteintech, 17146-1-AP
Anti-Actin	Mouse	1:2000	Sigma, A4700
Anti-Mouse	Goat	1:4000	Cell signalling, 7074S
Anti-Rabbit	Horse	1:4000	Cell signalling, 7076S

2.7.1 Western blot densitometry

Western blot band density was analysed to further assess protein knockdown. Developed blots were scanned and imported into imageJ. The density of the protein bands for each sample was normalised to the density of the corresponding Actin band and plotted in GraphPad Prism 7.0.

2.8 Mitochondria isolation.

Isolation was carried out according to Frezza et al, 2007.

$10x10^6$ cells were frozen and subsequently thawed (to increase yield). Cells were then resuspended in 2-3ml of IBc buffer (10% Tris/MOPS, 1% EGTA/Tris, 20% 1M sucrose and 69% MiliQ H_2O) and transferred to a glass vial. The sample was homogenized at 1600rpm for 5mins on ice, washed with 1ml IBc buffer and subsequently transferred to centrifuge tubes. Homogenates were centrifuged at 800g for 8mins at 4◦C and supernatants were transferred into fresh centrifuge tubes. The supernatants were then centrifuged at 10000g for 15mins in order to pellet the mitochondria. The protein concentration of the mitochondria (pellet) and cytosolic fraction (supernatant) were determined using a Pierce™ BCA Protein Assay Kit (Thermofisher, 23225).

2.9 High-resolution respirometry

High-Resolution Respirometer (Oroboros Oxygraph-O2k) was used to determine the oxygen consumption of intact MB cells. $2X10^6$ of ONS-76, DAOY and UW228.3 cells were resuspended in approximately 2.5mL of DMEM/F12. Cell suspensions were then added to individual respirometer chambers for approximately 10 min to allow the respiratory flux to reach steady state levels.

The following parameters (Figure 2.1 A) were measured: Routine oxygen consumption (no use of inhibitors); ATP synthase-independent respiration in the presence of oligomycin, which allows for the measurement of oxygen consumption uncoupled to ATP synthesis (leak); Oxygen consumption inhibited by the presence of oligomycin (coupled); Oxygen consumption with carbonyl cyanide-4-(trifluoromethoxy) phenylhydrazone (FCCP- titrated in 1 µM steps) to measure the maximal oxygen consumption rates upon stimulation of the electron transfer system efficiency (ETS); residual oxygen consumption (ROX) in the presence of rotenone (NADH dehydrogenase inhibitor) and antimycin A (AA) (cytochrome bc1 inhibitor). Data acquisition and analysis were carried out with DatLab (Oroboros Instruments, Innsbruck, Austria). An example respirometry acquisition can be seen in Figure 2.1 B.

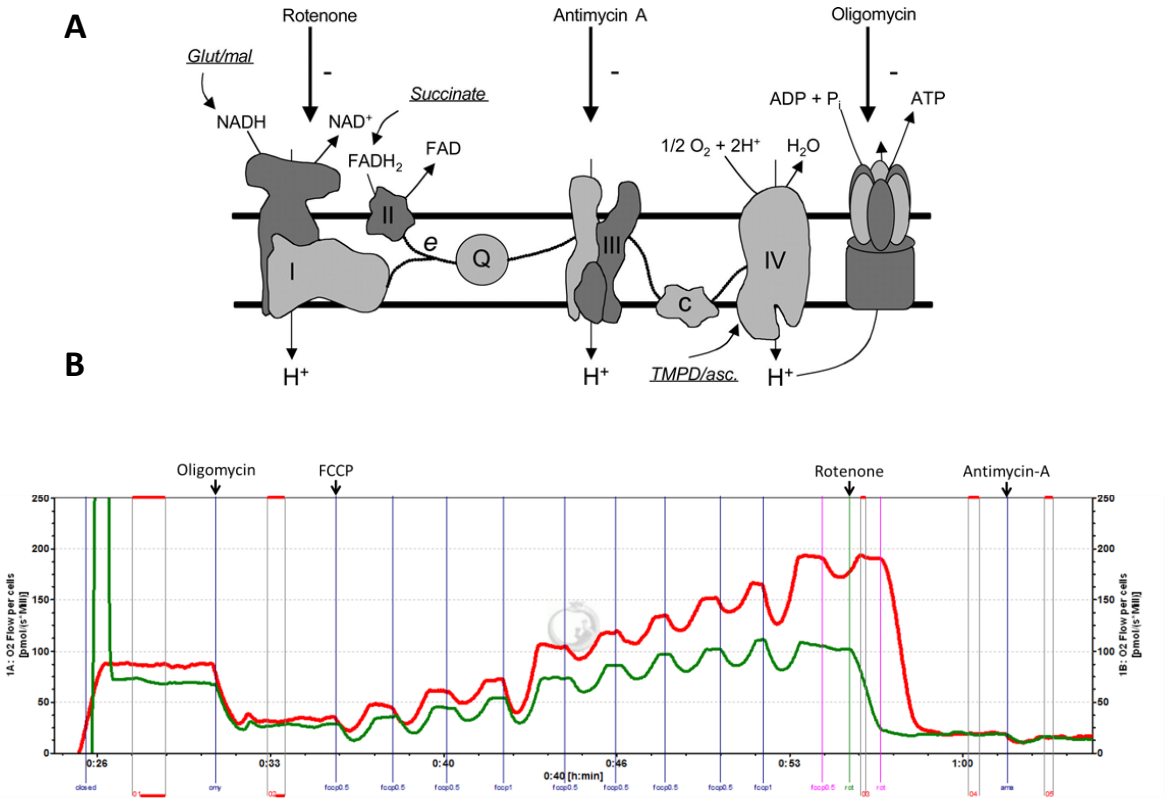

Figure 2.1. High-resolution respirometry. A) Inhibiting specific complexes in the electron transport chain. B) example data demonstrating high-resolution respirometry of the ONS-76 cell line with either DMSO (in red) or BPTES (in green).

2.10 Immunohistochemistry

5 µM sections cut from 6 paraffin-embedded SHH-MB tumour samples were mounted on SuperFrost® Plus slides (ThermoFisher Scientific, 10143560). The following antibodies and a VECTASTAIN® ELITE® ABC Kit (PK-6100) were used for immunohistochemistry with 3,3'-Diaminobenzidine (DAB) as a chromogen. Slides were first placed in xylene for 10 minutes, in order to dewax the sample. Rehydration of the tissue was achieved by placing slides in 100% EtOH for 10mins and then gradually introducing the sample to water (25% for 2min, 50% for 2min and 100% for 10min). Slides were immersed in 0.3% hydrogen peroxide (1:100 dilutions of 30% H_20_2 in dH_20) for 15 minutes and then washed in water for 10mins. Heat induced epitope retrieval was achieved by incubating tissue in citrate buffer (0.63g sodium citrate, 0.125g citric acid and 500ml dH20) for 20min at 96°C using a water bath. Slides were left to cool at room temperature for 30min and washed in water. Blocking of non-specific proteins was achieved by adding horse serum for 1 h and primary antibody concentrations (refer to table 2.5) were subsequently added for 1 h. Slides were washed in PBST for 30mins before being incubated in secondary antibody (depending on primary antibody species) for 30min. Samples were incubated with VECTASTAIN ABC reagents for 30 min. DAB (3, 3'-diaminobenzidine) chromogen was applied to slides for a predetermined amount of time. Finally, the slides were further washed for 30min and then counterstained with hemotoxylin for 10min. Table 2.1 shows the antibodies, dilution and antigen retrieval method employed for Immunohistochemistry staining of CAIX and SLC7A11.

Table 2.5 Antibodies used for IHC staining of hypoxia marker (CAIX) and the glutamate-cystine antiporter (SLC7A11)

Antibody	Supplier (product code)	Dilution	Antigen retrieval method
Anti-CAIX	Abcam (ab15086)	1:200	Heat retrieval in citrate buffer (pH6.0)
Anti-SLC7A11	Abcam (ab37185)	1:200	Heat retrieval in citrate buffer (pH6.0)

Samples were then mounted using DPX and Images were acquired with a Leica DM400B microscope with Leica Application Suite software version 2.8.1, and a Leica DFC420C camera (Leica).

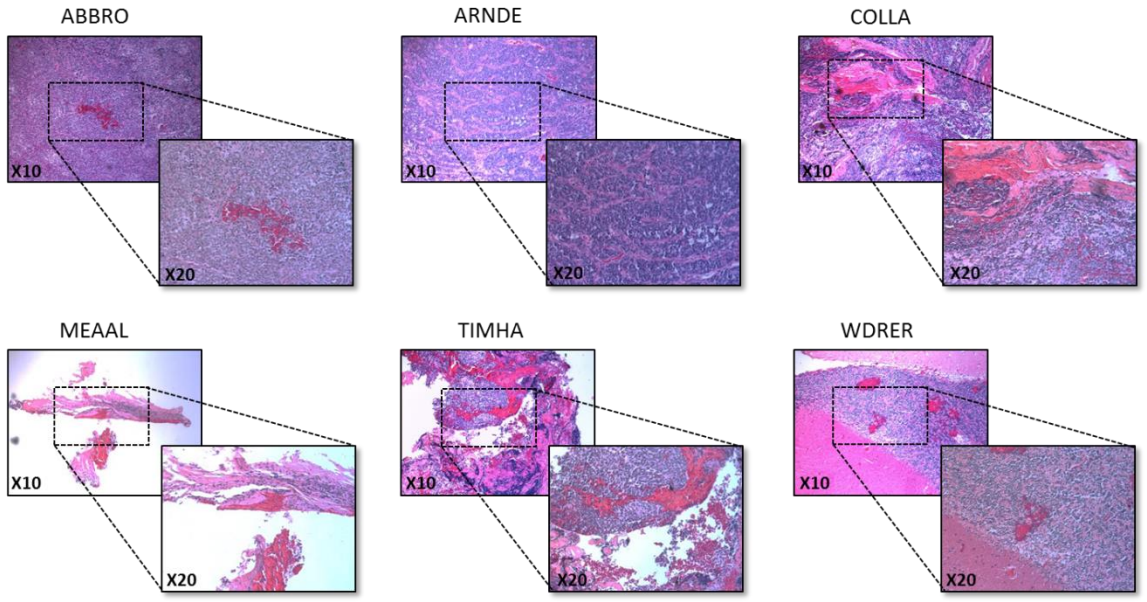

Figure 2.2. H&E staining of MB patient tissue. All patient samples were confirmed as being SHH-derived MB tumours, at the Birmingham children's hospital (BCH).

2.11 Stable isotope Tracing

Basic formulation DMEM media (Sigma, D5030) was supplemented with the relevant tracer $^{13}C_6$ glucose (Sigma, 389374) or $^{13}C_5$ glutamine (Sigma, 605166) at 10 mM and 2 mM respectively, along with the same concentration of corresponding unlabelled glutamine or glucose. All tracing experiments were conducted for 24 h and commenced 24 h post seeding.

2.11.1 GC-MS

Cells were seeded at 10 x 10^4 onto 6-well plates in standard culture conditions and were transfected after 24 h with non-targeting RNA (siNT) and siRNA targeting GLS1 (siGLS1), GLS2 (siGLS2), GAC (siGAC) or KGA (siKGA). Concentrations of siRNA can be seen in table 2.2. After overnight incubation, media was changed to basic formulation DMEM (flux media) containing 2mM $^{13}C_5$ glutamine for a further 24h. For hypoxic experiments, relevant plates were transferred to hypoxia (1 % O_2) chambers for 24h.

At the conclusion of tracer experiments, cells were washed twice with ice-cold 0.9% saline solution and subsequently quenched with 0.5 mL pre-chilled methanol (-20^{o}C). After adding an equal volume of ice-cold HPLC-grade water containing 0.5 µg/mL D6-glutaric acid (C/D/N ISOTOPES INC, D-5227), cells were collected with a cell scraper and transferred to tubes containing 0.5 mL of chloroform (-20^{o}C). The extracts were shaken at 1400 rpm for 15 min at 4^{o}C and centrifuged at 16,000 *g* for 15 min at 4^{o}C. Equal volumes of the upper aqueous phase was collected and evaporated in GC glass vials under vacuum at -4^{o}C using a refrigerated CentriVap Concentrator (Labconco). Metabolite derivatization was performed using an Agilent autosampler. Dried polar metabolites were dissolved in 15 µl of 2% methoxyamine hydrochloride (Sigma-Aldrich, 226904) in pyridine (Thermo Fisher Scientific,

25104) at 45°C. After 60 min, an equal volume of 2,2,2-trifluoro-N-methyl-N-trimethylsilyl-acetamide + 1% chloro-trimethyl-silane (Sigma-Aldrich, T228575) was added and metabolites were incubated for 30 min at 45°C.

GC-MS analysis was performed using an Agilent 6890GC equipped with a 30 m DB-35MS capillary column. The GC was connected to an Agilent 5975C MS operating under electron impact ionization at 70 eV. The MS source was held at 230°C and the quadrupole at 150°C. The detector was operated in scan mode and 1 µL of derivatised sample was injected in splitless mode. Helium was used as a carrier gas at a flow rate of 1 mL/min. The GC oven temperature was held at 80°C for 6 min and increased to 325°C at a rate of 10°C/min for 4 min. The run time for each sample was 59 min. For determination of the mass isotopomer distributions (MIDs), spectra were corrected for natural isotope abundance. Data processing from raw spectra to MID correction and determination was performed using MetaboliteDetector software (Hiller *et al.*, 2009).

2.12 SRB assay

Cells were fixed in 20% (v/v) ice-cold trichloroacetic acid solution (TCA) (Sigma-Aldrich, T0699) for 20 min at 4°C. Plate wells were washed with water and once dry, intracellular protein was stained using 0.4% (w/v) sulfohodamine B (SRB) (Sigma-Aldrich, 230162) in 1% acetic acid for 10 min at room temperature. After washing with 1% acetic acid to reduce non-specific staining, SRB was dissolved in 50 mM Tris/HCl pH 8.8 once dry. 100 µL/well was aliquoted for quantification by absorbance at 495 nm on FLUOstar Omega (BMG LabTech).

Final sample absorbance values were determined by calculating the mean blank-corrected absorbance for each replicate, where 50 mM Tris/HCl pH 8.8 alone was used as the blank.

2.13 Glutathione measurements.

2.13.1 1D-^{1}H NMR

2×10^{6} cells were plated onto three 15 cm dishes (high cell numbers are required for NMR) and cultured in DMEM-/HAMS/F12 media. When roughly 80% confluent, cells were extracted for 1D-^{1}H NMR spectroscopy. Extractions were performed as per GC-MS protocol, however volumes of methanol, water and chloroform were increased to 1.2ml, 0.5ml and 1.2ml, respectively.

Extracted samples where then dried and then resuspended in 60 µL 100 mM sodium phosphate buffer (pH 7.0) containing 500 µM TMSP [(3-trimethylsilyl)propionic-(2,2,3,3-d4)-acid sodium salt] and 10% D2O. Samples were vortexed, sonicated for 10min and centrifuged briefly twice, prior to being transferred to 1.7mm NMR tubes using an automatic Gilson 215 Liquid Handler (Bruker Biospin).

1D-^{1}H NMR spectra were acquired using a 600- MHz Bruker Avance III spectrometer (Bruker Biospin, UK) with a TCI 1.7 mm z-PFG cryogenic probe at 300 K. Spectral widths were set to 7,812.5, with 16,384 complex data points being acquired. Each sample was automatically tuned, matched and then shimmed (1D-TopShim) to a TMSP line width of <2 Hz before acquirement of first spectrum. Spectra were analysed using Chenomx NMR suit software, where concentrations of glutamine, glutamate and glutathione were determined.

2.13.2 Determining the GSH/GSSG ratios

Cells were seeded at 10 x 10^{4} on a 12-well plate in standard culture conditions and were transfected after 24 h with non-targeting RNA (siNT) and siRNA targeting GLS1 (siGLS1), GLS2 (siGLS2), GAC (siGAC) or KGA (siKGA). Concentrations of siRNA can be seen in table 2.2.

A Glutathione assay kit (Cayma, 703002) was used to measure GSH:GSSG in all three MB cell lines, as per manufacturers guidelines.

2.14 Hypoxic incubation

To achieve hypoxia cells were incubated in a hypoxic incubator (Don Whitley, H35 Hypoxystation), at 1% O_2, 5% CO_2, balance N_2, 37^{o}C and 75% humidity, for the length of time indicated in the figure legend.

2.15 Dose response treatments:

Treatment conditions are described below. Each treatment was optimised using SRB dose response curve to acquire the IC50s in each cell line. Control samples were either treated with H2O or DMSO, depending on the treatment given.

2.15.1 H_2O_2 treatment

15 x 10^4 cells were plated onto 12-well plates in standard culture conditions. Cells were incubated with media containing 10, 50, 100, 300 and 500 µM H_2O_2 12h later. Cells were fixed using the SRB method as described above and the optimum concentration of 50 µM was established for further experiments.

2.15.2 X^{CT} transporter inhibitor- Sulfasalazine (SSZ)

Cells were seeded at 15 x 10^4 onto 12-well plates in standard culture conditions and incubated for 24 h. Cells were treated with 10 µM, 25 µM, 50 µM, 100 µM, 250µM, 500 µM and 1mM SSZ and left for 48h. Cells were fixed using the SRB method as described above and the optimum concentration of 250 µM for 48 h was established for further experiments.

2.15.3 Cisplatin

15 x 10^4 cells were plated onto 12-well plates in standard culture conditions. Cells were incubated with media containing 5, 10, 25, 50, 100 µM cisplatin 24h later. Cells were fixed using the SRB method as described above and the optimum concentration of 25 µM was established for further experiments.

2.15.4 Irradiation

20 x 10^4 cells were plated onto 10 cm dishes in standard culture conditions. Cells were exposed to varying Gy of radiation using a Cs-137 Irradiator (Model CIS IBL 437). Cells were fixed 48 h after, using the SRB method as described above and the optimum exposure of 12 Gy was established for further experiments.

2.15.5 BPTES

15 x 10^4 cells were plated onto 12-well plates in standard culture conditions. Cells were incubated with media containing 1, 5, 10, 25 and 50 µM BPTES 4, 8 and 24h later. Cells were fixed using the SRB method as described above and the optimum concentrations of 25 µM, 15 µM and 10 µM were established for 4, 8 and 24h experiments, respectively.

Table 2.6. Summary of treatments

Treatment	Concentration used	Treatment time
H_2O_2	500 µM	12 h
SSZ	250 µM	48 h
Cisplatin	25 µM	24 h
Irradiation	12 Gy	12min
BPTES	10, 15 or 25 µM	24, 8 or 4 h

2.16 Measuring changes in cell viability- AnnexinV/PI cell death assay

2.16.1. Sample preparation

Cells were seeded at 5 x 10^4. Cells were transfected after 24 h with non-targeting RNA (siNT) and siRNA targeting GLS1 (siGLS1) or GLS2 (siGLS2). Concentrations of siRNA can be seen in table 2.2. Cells were subsequently treated as per previous methods (refer to table 2.6). Positive control and single stain samples were given 500 µM H_2O_2 (30% w/w: Sigma, H1009) 2 hours prior to the experimental procedure, to ensure appropriate cell death (+VE control). Following treatment, cells were washed with 1x PBS and trypsinised. Media was then added to neutralise trypsin activity for 20 minutes before being centrifuged and removed. Samples were resuspended in 500 µl 1x AnnexinV Binding Buffer (BD, 556454) prior to incubation with 1 µL 1:1000 PI (Life Technologies, V13242) and 5 µL AnnexinV-FITC (BD, 556419) for 10 minutes.

2.16.2. Data collection

Analysis was achieved on the LSRFortessa X-20 flow cytometer. Forward scatter (FSC), side scatter (SSC), FITC (530 nm wavelength) - which measures AnnexinV- and PE (575 nm wavelength) - which measures PI- signals were determined. FITC and PE laser intensities were set so the signal intensity of the unstained control sample was below 103. Cross channel bleeding was checked through single stain control samples treated with AnnexinV-FITC or PI only. 10000 events were collected for further analysis.

2.16.3. Data analysis

Analysis was achieved using the FlowJo software. AnnexinV-FITC and PI gates were set using the control population at approximately 90% viability. The percentage of AnnexinV-FITC and

PI negative cells represent the viable cell population. Early stage apoptosis is represented by Increased AnnexinV-FITC, with late stage apoptosis is represented by increased staining in both AnnexinV-FITC and PI. Cells undergoing necrosis were defined as those with increased PI staining. The viable cell population for each control was used to measure alterations in cell viability between samples. The data was analysed using a one way ANOVA with a Tukey post-hoc test. *p<0.05, **p<0.01, ***p<0.001, ****p<0.0001.

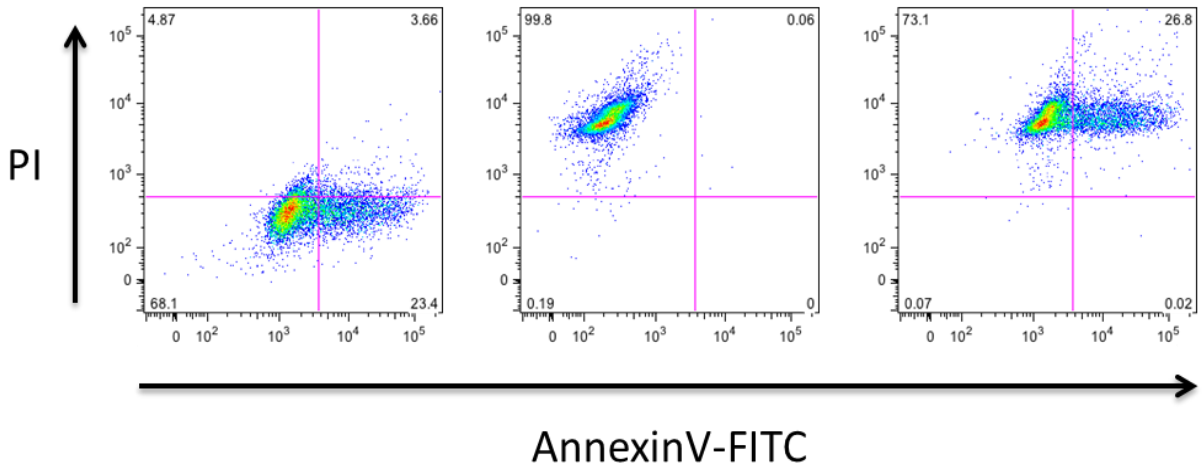

Figure 2.3. Example of flow cytometry staining controls for the Annexin-V/PI cell death assay. (left) single stain control for AnnexinV-PE, (middle) single stain control for PI, double positive control for both stains.

2.17. Collagen staining

5 µM sections cut from 6 paraffin-embedded SHH-MB tumour samples were mounted on SuperFrost® Plus slides (ThermoFisher Scientific, 10143560). The following antibodies and a VECTASTAIN® ELITE® ABC Kit (PK-6100) were used for immunohistochemistry with 3,3'-Diaminobenzidine (DAB) as a chromogen. Slides were first placed in xylene for 10 minutes, in order to dewax the sample. Rehydration of the tissue was achieved by placing slides in 100% EtOH for 10mins and then gradually introducing the sample to water (25% for 2min, 50% for 2min and 100% for 10min). Van Gieson reagent was then applied to slides for 5mins, then subsequently dipped in 100% IMS X3 for 2mins each. Slides were then dehydrated and mounted using depex.

2.18. Statistical Analysis

Samples sizes and reproducibility for each figure are denoted in the figure legends. Unless otherwise noted, all experiments are representative of at least three biologically independent experiments in technical triplicate. All error bars represent mean +/- S.E.M, unless stated differently in the figure legend. Statistical significance was determined by either a one-way ANOVA or two-tailed Student's t-test using GraphPad Prism 6, where *P < 0.05; **P < 0.01; and ***P < 0.001.

Chapter 3

Metabolic pathways involved in glutamate synthesis and utilisation in Medulloblastoma

3.1 Introduction

Glutamine acts as a vital amino acid in cancer where by it is able to serve as a carbon and nitrogen source in metabolic pathways including; ATP production, the regulation of ROS homeostasis (via glutamate by forming glutathione), and biosynthetic reactions. Many of these effects are regulated by glutamine-derived glutamate, which is largely controlled through GLS enzymes. The GLS family comprise of two isozymes, GLS1 and GLS2, each with their own individual splice variants. GLS1 is commonly highly expressed in tumour cells, where it has been shown to aid cellular proliferation and oncogenic transformation (Song *et al.*, 2017). Conversley, GLS2 is thought to be tumour suppressive, with reduced expression observed in a number of tumours (Szeliga *et al.*, 2014). However, the role of GLS2 in cancer is arguably more complicated as there are some types of cancer where increased GLS2 expression is observed, conferring resistance to current therapies (Hu *et al.*, 2010).

Glutamate, the product of glutaminase activity, has diverse roles within the cell, where it can be utilised as an amino acid, donate its amine group for the biosynthesis of non-essential amino acids (NEAAs), donate amino groups to α-keto acids for essential amino acids, or glutamate can contribute towards other amino group-requiring macromolecules, such as nucleotides (Newsholme *et al.*, 2003). In addition, glutamate is required to maintain the pool of intracellular glutathione (GSH), both as a component of the tripeptide and availability of the other two substrates, by driving the biosynthesis of glycine and the import of cystine (for cysteine). Metabolism is important in cancer, and it has been observed that glutamate is a marker of survival in patients with MB tumours, regardless of subgroup (Wilson *et al.*, 2014). Furthermore, the implications of glutamine metabolism have been

revealed more recently in MB, where cell lines derived from MB tumours are addicted to glutamine.

In this chapter we investigate the significance of genes involved in glutamine and glutamate metabolism and their associated metabolic pathways with regards to their expression and their impact on patient survival. We achieve this by assessing several gene databases from available online geo data sets (geo: GSE42658 and geo: GDS4471) and a larger patient cohort provided by Steve Clifford, University of Newcastle. The aim of this was to identify important, novel metabolic genes, in which we could study further. Through *in vitro* investigations we aim to reveal important aspects of glutamate metabolism within MB cell lines.

3.2 Results

3.2.1 Genes encoding glutamine and glutamate related pathway genes are deregulated in MB.

Previous studies by others have suggested that glutamine and glutamate metabolism may be altered in MB, and moreover the degree to which it is altered may correlate with patient survival (Wilson *et al.*, 2014). We therefore assessed the expression of several glutamine-related metabolic genes and the result of this on patient survival, using three independent databases (Newcastle cohort and an online database, GEO: GSE42658 and GEO: GDS4471, respectively). We noted that in all cases, expression of the transporters responsible for glutamate uptake, EAAT1 (Figure 3.2.1) and EAAT2-4 (supplementary figure 1) were reduced, while the neutral amino acid transporter SLC1A5, responsible for the transport of glutamine into tumour cells, was significantly increased (Figure 3.2.1), suggesting MB tumours may prefer *de novo* glutamate synthesis rather than exogenous uptake. Furthermore, the expression of these transporters proved to be prognostic, with low EAAT1 and high SLC1A5 being predictive of a worse overall survival in MB patients (Figure 3.2.1). We also investigated genes more directly involved in glutamine catabolism (GLS1, GLS2 and GLUD1) and anabolism (GLUL). GLS1 expression was highest in the SHH-MB subgroup when compared to the other three conventional groups, although, when compared to normal cerebellum (CB) we found increased expression in all MB tumour types (Figure 3.2.1). We observed GLS2 expression was highest in Grp4 MB, but no differences were observed when compared to CB. GLUD1, which allows the NAD(P)+ dependent release of the amino group of glutamate to form αKG, is an important enzyme which contributes towards TCA anaplerosis. Our results revealed a striking and significant alteration in GLUD1 expression, where its expression in decreased in the SHH, Grp3 and Grp MB subgroups, which have a more aggressive phenotype than the WNT group (Cavalli *et al.*, 2017). We also observed

decreased expression in MB tumours compared to CB, which interestingly held up as prognostic in patients, with low expressing patients having a significantly poorer overall survival (OS) compared to their higher GLUD1 expressing counterparts (Figure 3.2.1). Glutamine synthetase (GLUL) is an ATP-dependent enzyme which catalyses the condensation of ammonium to glutamate, forming glutamine. In many cancers, the intricate balance equilibrium between glutamine anabolism and catabolism is vital. We therefore, investigated GLUL in MB and showed no significant changes in expression when compared across MB subgroups or CB control.

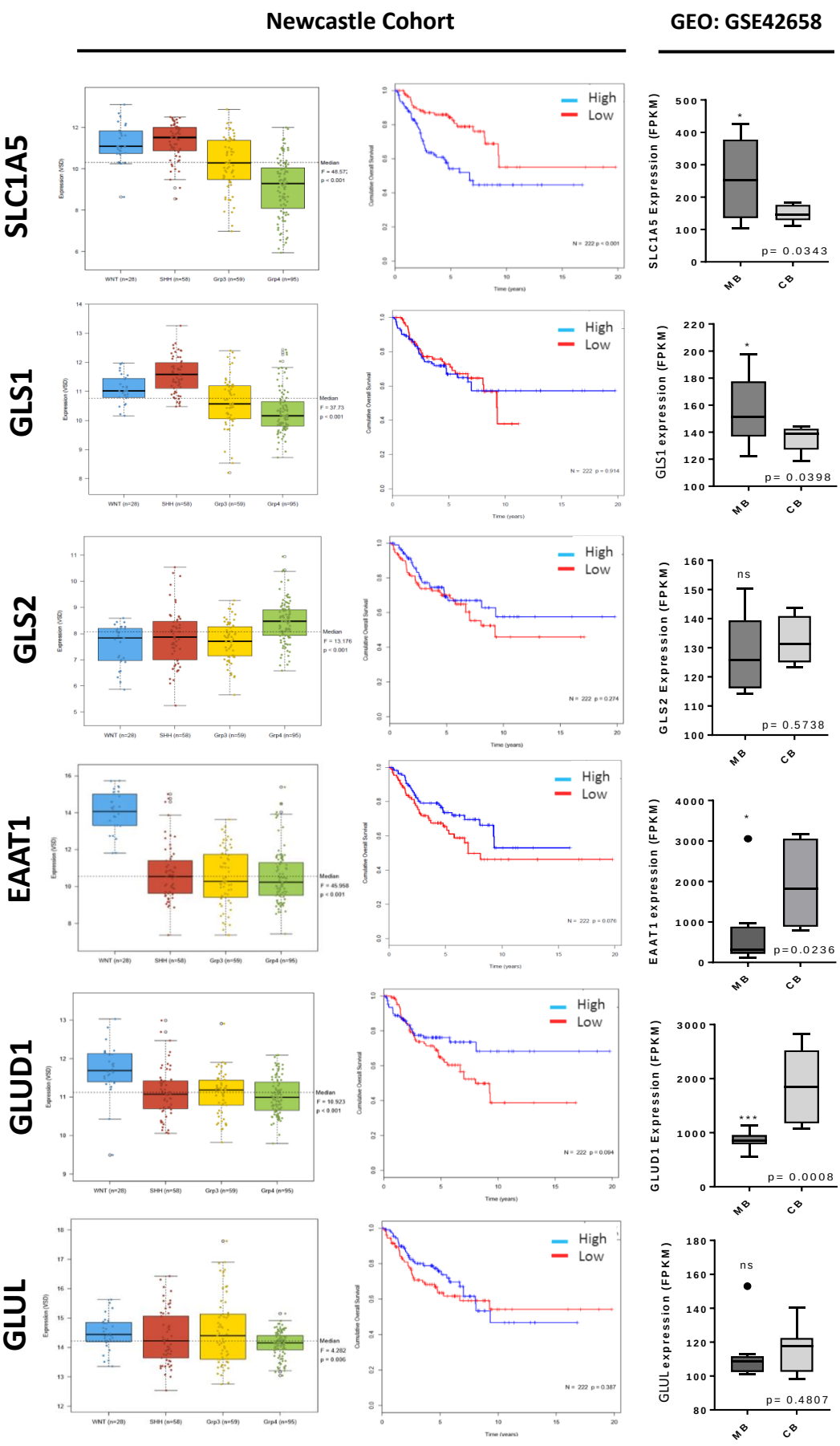
Newcastle Cohort
GEO: GSE42658
SLC1A5
GLS1
GLS2
EAAT1
GLUD1
GLUL
High
Low
SLC1A5 Expression (FPKM)
p= 0.0343
GLS1 expression (FPKM)
p= 0.0398
GLS2 Expression (FPKM)
ns
p= 0.5738
EAAT1 expression (FPKM)
p=0.0236
GLUD1 Expression (FPKM)
p= 0.0008
GLUL expression (FPKM)
ns
p= 0.4807
MB
CB

Figure 3.2.1. Expression of glutamine-related genes was associated with survival in MB tumours. A) RNA expression data compared across subgroups of MB and representative Kaplan-Meier survival curves of the MB Newcastle cohort. n=240 (WNT n=28, SHH n=58, G3 n=59 and G4 n =95). High and low expression was determined by the median expression value for each gene. Log-rank (Mantel-Cox) statistical test was performed in Kaplan-Meier survival graphs. Unpaired two-tailed t-test statistical tests were performed in mRNA expression data graphs; *p<0.05, **p<0.01, ***p<0.001, ****p<0.0001.

3.2.2 Increased glutamine catabolism over glutamine anabolism predicts survival in MB patients.

To determine the importance of glutamine catabolism or anabolism in MB tumours, we also analysed survival data from a publically available GEO data set (GDS4471). When using a median expression cut off value, a correlation was found between overall survival of MB patients and expression of GLS1, where increased expression significantly decreased survival. Moreover, we observed a strong trend with GLUL expression, with low expressing patients having a poorer overall survival. To further elucidate this, we utilised gene expression ratios GLS1:GLUL and (GLS1+GLUD1)/GLUL, which give a read out of glutamine catabolism versus anabolism and is generally considered as a valid representation of such (Yang *et al.*, 2014). We establish that opposing activities of glutamine catabolism and glutamine anabolism, in our dataset, act as a biomarker for predicting survival in MB patients. We found that patients with high GLS1/GLUL and (GLS1 + GLUD1)/GLUL ratios had significantly poorer prognoses than patients with lower ratios (Figure 3.2.2). These data were further strengthened through proteomic analysis of the GLS: GLUL in MB tumours (Figure 3.2.3).

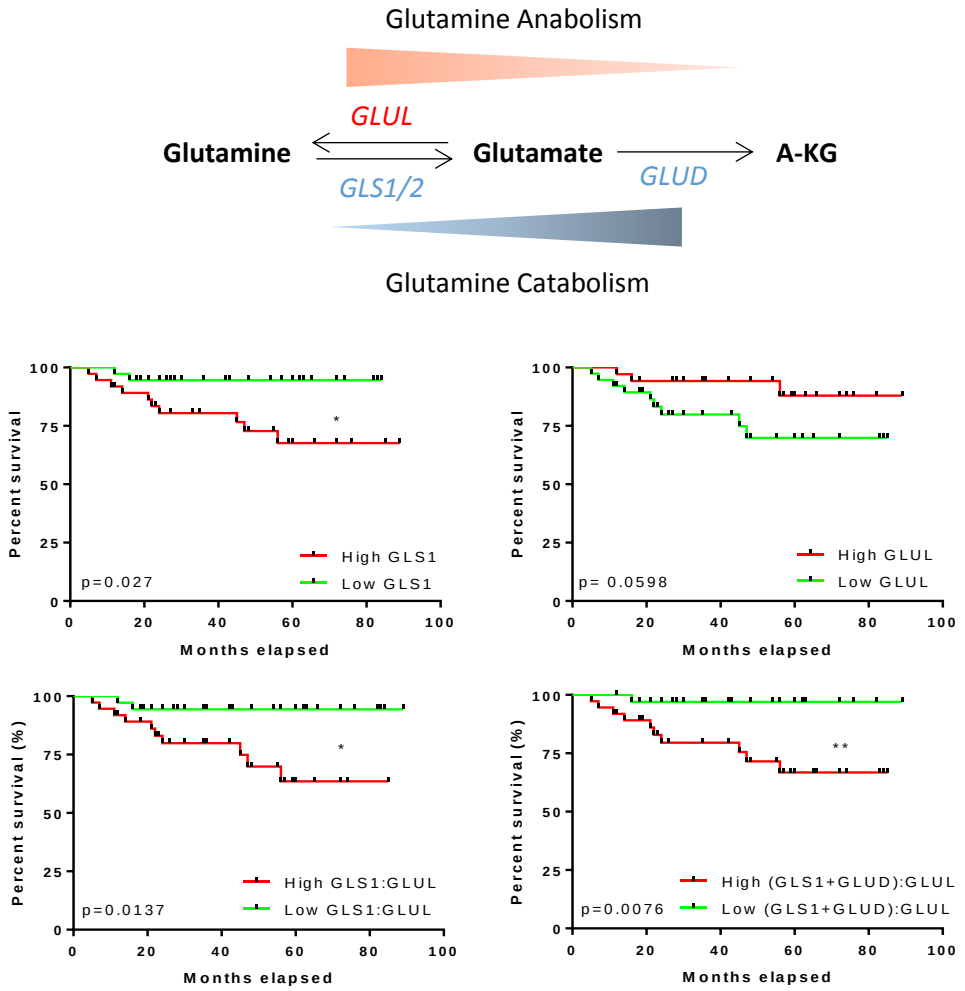

Figure 3.2.2. Kaplan-Meier of GLS1 / GLUL mRNA ratio is associated with survival in MB patients. Analysis of GLS1/ GLUL mRNA ratio reveals increased glutamine catabolism is associated with a worse overall survival. Clinical and mRNA expression data, from MB patients, was extracted from an online NCBI Geo repository (accession number: GDS4471). This Expression profiling array, included 76 samples, each belonging to the separate MB subgroups; WNT (n=8), SHH (n=11), G3 (n=16) and G4 (n=39). High and low expression was determined by the median expression value for each gene. Log-rank (Mantel-Cox) statistical test was performed in Kaplan-Meier survival graphs. Unpaired two-tailed t-test statistical tests were performed in mRNA expression data graphs; *p<0.05, **p<0.01, ***p<0.001, ****p<0.0001.

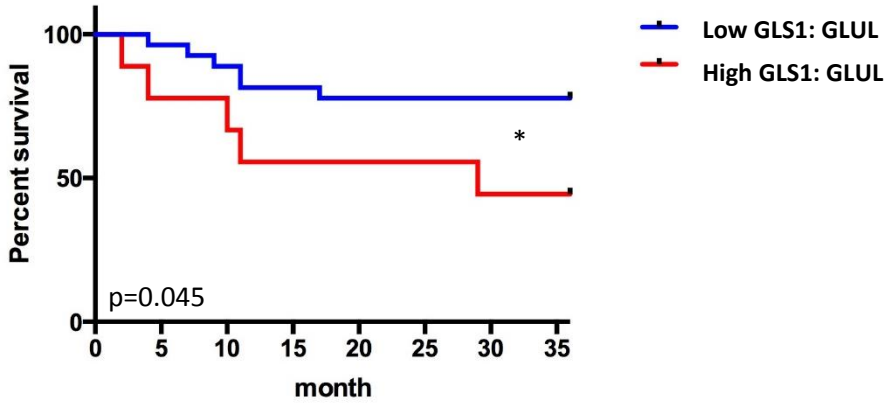

Figure 3.2.3. Kaplan-Meier of GLS1 / GLUL protein ratio associated 3 years survival. Proteomic analysis of GLS1/ GLUL ratio reveals increased glutamine catabolism is associate with a worse overall survival. High (n=9) and low (n=27) groups were determined by Last quartile (log10-ratio>1, 5). * p=0.045. Data generated by Ayrault Olivier's group, institut-curie, 2018.

3.2.3. Glutaminase expression in MB cell lines.

To investigate the expression of GLS isozymes in the model cell lines, DAOY, UW228.3 and ONS-76, a quantitative real-time PCR analysis was performed. Significant differences in the expression of these enzymes were observed between the cell lines, with ONS-76 exhibiting the lowest GLS1 but highest GLS2 expression, and UW228.3 with the highest GLS1 but lowest GLS2 expression (figure 3.2.4 B). Having acquired mRNA expression of GLS1 and GLS2 in the MB cell lines, we further explored these enzymes by means of protein expression by immunoblot analysis (figure 3.2.4 A). GLS1 protein expression was similar across all cells lines, differing only in the DAOY cells. Furthermore, we observed several protein bands for GLS1, which we believe two of the bands to be specific towards the two splice variants (KGA and GAC), due to their reduced expression upon RNA knockdown with siGLS1 (Supplementary figure 2). GLS2 protein expression however, was only observed in the ONS-

76 and DAOY cell lines, with ONS-76 expressing the greatest amount. Overall, GLS2 protein expression is minimal in MB cell lines.

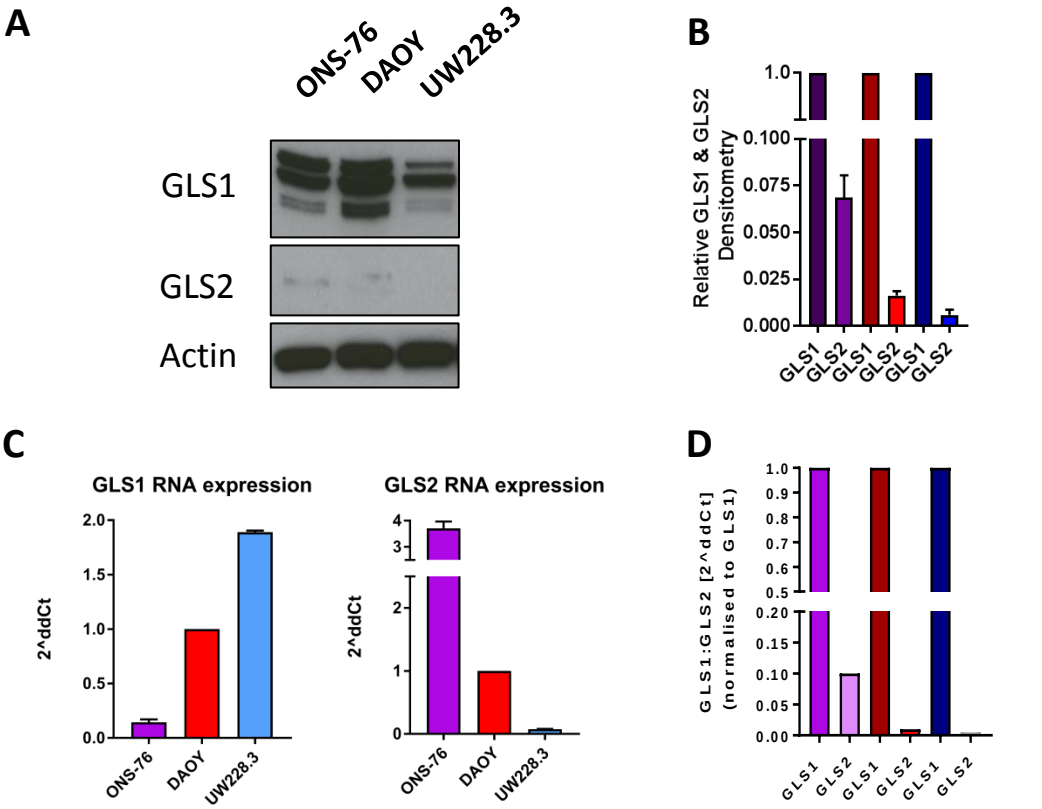

Figure 3.2.4. Glutaminases are differentially expressed between MB cell lines. A) Immunoblot analysis of GLS1 and GLS2 show different protein expression between ONS-76, DAOY and UW228.3 cell lines. Actin was used as a loading control. B) Densitometry values from immunoblot. C) Glutaminase mRNA expression was assessed by qPCR.

3.2.4 MB cell lines are addicted to glutamine.

To understand glutamine dependence in MB cells, we first analysed cell proliferation, by means of an SRB growth assay, of three MB cell lines (ONS-76, DAOY and UW228.3) under complete medium (2mM glutamine) and varying degrees of glutamine deprived conditions (0-1mM). All three cell lines show a dependency on glutamine to sustain optimal growth, with complete glutamine deprivation leading to reduced growth in the ONS-76 and UW228.3 (Figure 3.2.5 A and C) cell lines and cell death after 24h in the DAOY line (Figure 3.2.5 B). Our data therefore demonstrate a reliance on glutamine in the MB cell lines tested. The structure of glutamate is similar to that of glutamine, lacking only an amide group. We investigated whether the addition of a methylated form of glutamate, N-Methyl-L-glutamic acid, which efficiently delivers glutamate into cell, could rescue growth in cell lines cultured in 0mM glutamine. Our results conclude that N-Methyl-L-glutamic acid is unable to rescue growth, suggesting an importance for *de novo* glutamate synthesis from gln (Figure 3.2.5 D). In parallel, we also observed a requirement for exogenous glucose in all three cell lines (Figure 3.2.5 D).

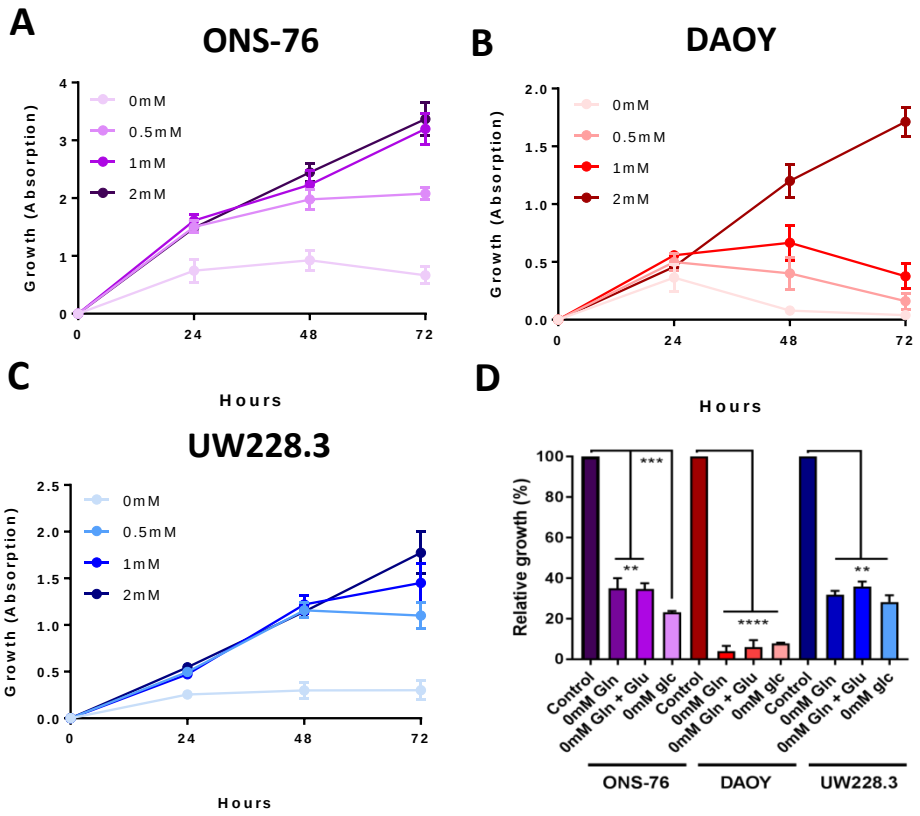

Figure 3.2.5. MB cell lines require glutamine for growth. A-C) SRB growth curves of ONS-76, DAOY, and UW228.3 cell lines incubated with 0, 0.5, 1 or 2mM glutamine for 3 days (72 h). Incubation in 0mM glutamine significantly decreased the growth rate of all three cell lines, with the DAOY cell line showing heightened reliance on glutamine. D) SRB relative growth of MB cell lines incubated with 0mM glutamine, 0mM glutamine + 2mM methyl-glutamate or 0mM glucose. Glutamate is unable to rescue growth in 0mM glutamine conditions. Glucose is vital for MB cell line growth. Data shown as mean ±SEM, representative of 3 independent experiments and analysed with an unpaired t-test; *p<0.05, **p<0.01, ***p<0.001, ****p<0.0001

3.2.5 MB cell lines show increased glutamine catabolism and low glutamine anabolism

To further understand the importance of glutamine, we explored the relative use of glutamine catabolism versus its anabolism within our three cell lines, by measuring the incorporation of ^{13}C-U-glutamine into glutamate (representative of GLS activity), alpha-ketoglutarate (representative of GLUD and transaminase activity) and back into glutamine (representative of GLUL activity). In the presence of ^{13}C-U-glutamine for 24h we observe high m+5 labelling into both glutamate and alpha-ketoglutarate (Figure 3.2.6), suggesting a high flux of glutamine catabolism into these downstream metabolites.

Two carbons of glucose are commonly utilised in the synthesis of glutamine, however, no m+2 label incorporation into glutamine was observed when cells where fed with ^{13}C-U-glucose (Figure 3.2.7 A), which suggest a lack glutamine synthetase activity. Furthermore, we observed minimal levels of m+1, m+2, m+3 and m+4 isotopologues of glutamine from ^{13}C-U-glutamine in the ONS-76 cell line (Figure 3.2.7 A), suggesting partial GLUL activity in these cells. However, labelling with ^{13}C-U-glutamine reveals only the recycling of the carbon backbone, of which glutamine, glutamate and αKG share identical carbons. These metabolites alter in their nitrogen composition, with the deamidation of glutamine resulting in a loss of the amide nitrogen, and a loss of the amine nitrogen when glutamate is deaminated to αKG. We therefore labelled with $^{13}C_5$, $^{15}N_2$-glutamine to better appreciate GLUL activity. Our data further support a lack of GLUL activity with low m+6 and no m+5 labelled glutamine observed (Figure 3.2.7 C). Taken together, these results are indicative of increased glutamine catabolism over glutamine anabolism in the MB cell models.

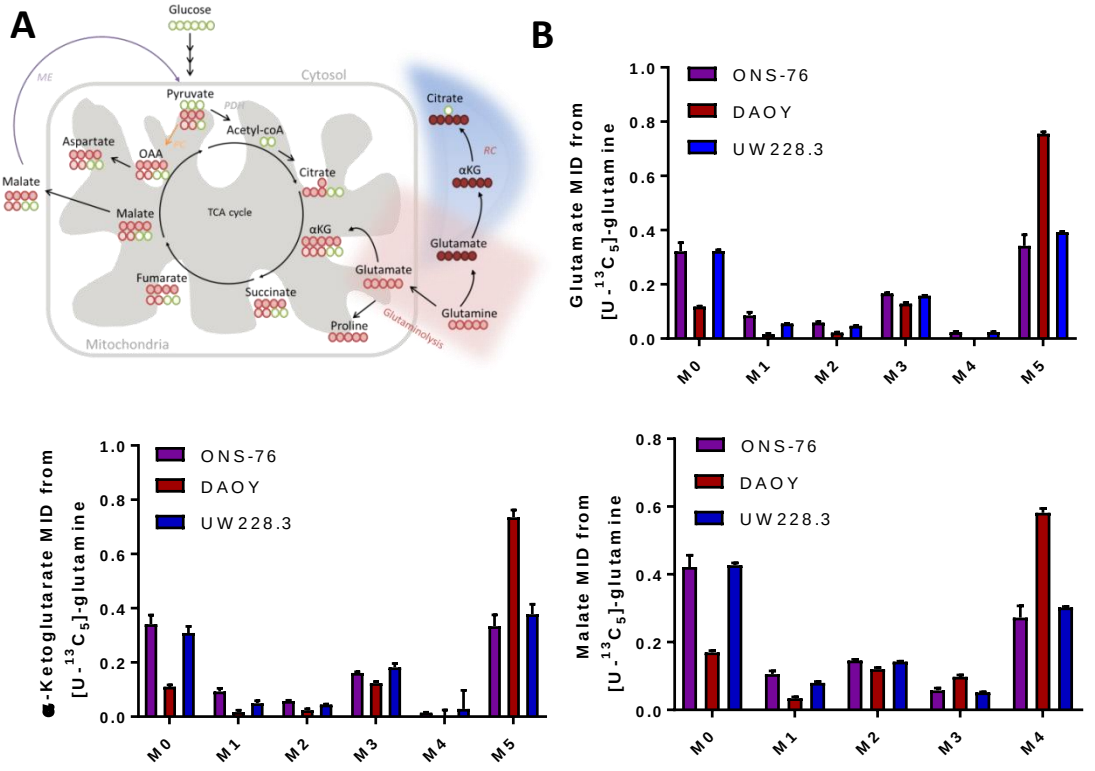

Figure 3.2.6. MB cell lines undergo glutamine catabolism. Analysis of the mass isotopomer distribution (MID) of glutamine- derived metabolites. A) Glutamine catabolism can be assessed through MID analysis of downstream metabolite; glutamate (via GLS activity), α-KG (via GLUD1 activity) and malate (indicative of TCA cycle metabolism). B) Extensive ^{13}C label incorporation is observed in glutamine-derived metabolites after 24 h incubation with ^{13}C-U-glutamine. Data is performed in technical triplicate, mean +/- S.D. Statistical significance determined using two-tailed unpaired Student's t-test; *p<0.05, **p<0.01, ***p<0.001, ****p<0.0001

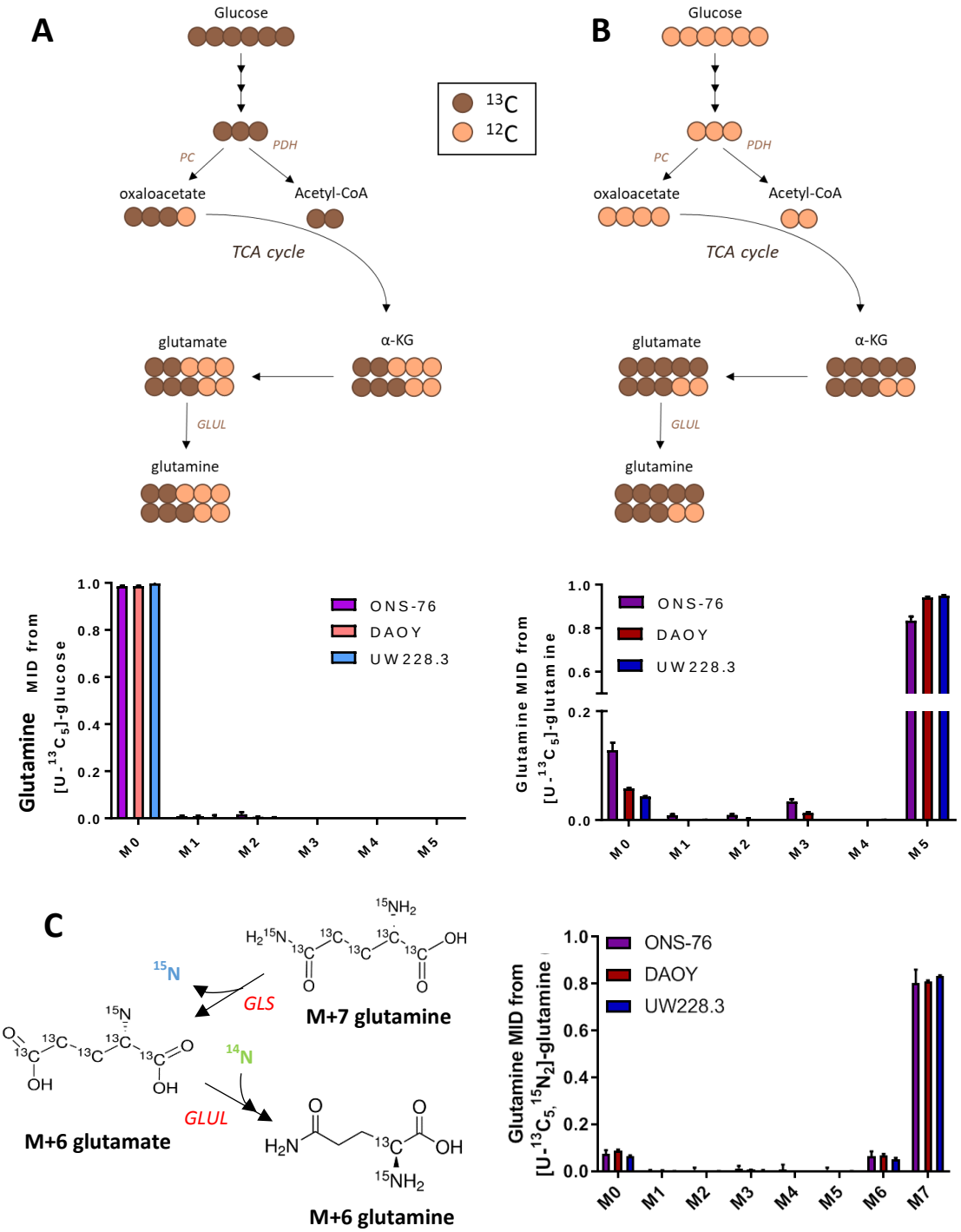

Figure 3.2.7. Low glutamine synthase activity in MB cells. Analysis of the mass isotopomer distribution (MID) of glutamine to assess GLUL activity. Mass isotopologues (m+0, m+1, m+2, m+3, m+4 and m+5) correspond to ion fragments containing different ^{13}C atoms. A) No 13C label incorporation is observed in glutamine after 24 h incubation with ^{13}C-U-glucose, suggesting no glucose-derived glutamine via GLUL activity. B) Glutamine-derived metabolites can be converted back to glutamine through GLUL activity. Minute ^{13}C label incorporation is observed in glutamine after 24 h incubation with ^{13}C-U-glutamine, suggestive low GLUL activity. Data is performed in technical triplicate; mean +/- S.D. Statistical significance determined using two-tailed unpaired Student's t-test; *p<0.05, **p<0.01, ***p<0.001, ****p<0.0001

3.2.6 GLS1 is the primary functioning glutaminase

The conversion of glutamine to glutamate is predominantly catalysed through glutaminase enzymes, of which two isoforms exist- GLS1 and GLS2. We previously identified GLS1 as being highly expressed in our cell lines, while GLS2 expression was low in the ONS-76 and DAOY cell line and no expression was observed in the UW228.3 line (Figure 3.2.4). We further investigated the relative activities of these two isoforms by knocking-down either GLS1 or GLS2 in the MB cell line models. Knock-down was achieved using short interfering RNA (siRNA), attaining significant reduction in mRNA of both GLS1 splice variants; KGA and GAC and protein expression, and a reduction in GLS2 protein and mRNA (Supplementary figure 2). To investigate the metabolic changes accompanying GLS1 knockdown, the mass isotope distribution (MID) of metabolites after incubation with uniformly-labelled-^{13}C glutamine ($^{13}C_5$-U-glutamine) was measured. Upon GLS1 KD, the m+5 isotopologue of glutamate (which represents a read-out of the direct synthesis of glutamate from glutamine) was significantly decreased, consistent with reduced GLS1 activity. We observed no changes in label incorporation into glutamate upon GLS2 knock-down, suggesting our cell lines do not utilise this isoform of GLS under basal conditions. Furthermore, siGLS1 but not siGLS2 significantly reduced the growth of all three cell lines (Figure 3.2.8 B), further indicating a preference of the GLS1 isoform in MB.

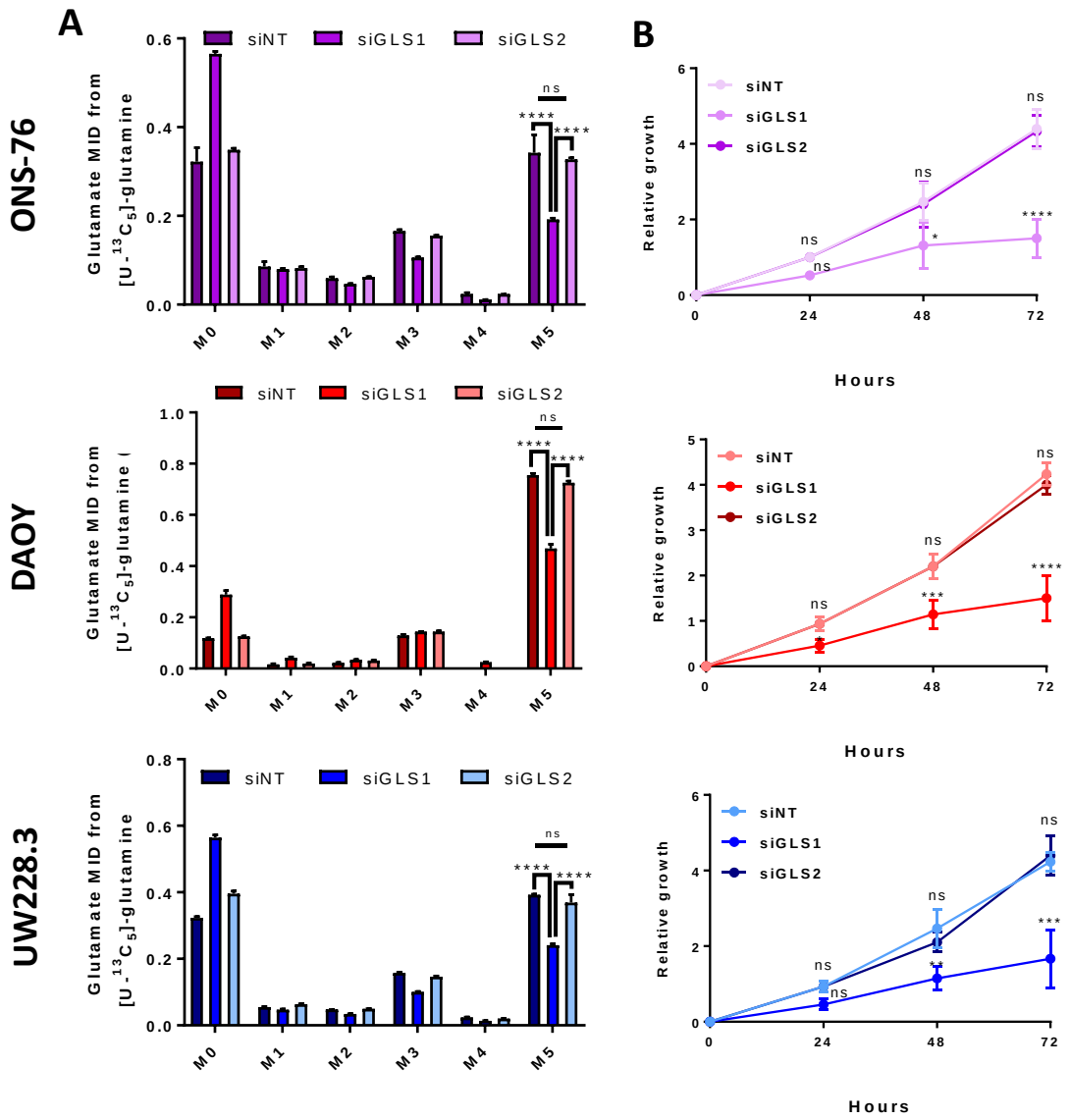

Figure 3.2.8. GLS1 is the actively used glutaminase in MB. Analysis of the mass isotopologue distribution (MID) of glutamine- derived glutamate. A) Significant reductions in ^{13}C label incorporation is observed in siGLS1 treated MB cell lines after 24 h incubation with ^{13}C-U-glutamine compared to siNT and siGLS2, suggestive of favoured GLS1 activity. B) Relative growth curves of ONS-76, DAOY, and UW228.3 cell lines incubated with siNT, siGLS1 or siGLS2 for 3 days (72 h). Treatment with siGLS1, but not siGLS2 significantly decreased the growth rate of all three cell lines. Data is performed in technical triplicate, mean +/- S.D. Statistical significance determined using two-tailed unpaired Student's t-test; *p<0.05, **p<0.01, ***p<0.001, ****p<0.0001

3.2.7 Reduced glutamate impairs oxygen consumption

Our observations that decreased glutamate synthesis reduces MB cell line growth led us to hypothesise that glutamate may be important for TCA cycle metabolism, where mitochondrial respiration is a key element of cell growth. To understand the contribution of glutamate to mitochondrial respiration, we performed a high-resolution respirometry assays using OXPHOS modulators in intact MB cells treated with DMSO or BPTES (a GlS1 inhibitor). Treatment with BPTES significantly reduced the Routine oxygen consumption of all three cell lines (Figure 3.2.9), suggesting an important role for glutamate in maintaining OXPHOS under basal conditions. In order to evaluate the dependence of respiratory complexes on oxygen consumption (OC), we used membrane permeable compounds that affect mitochondrial function.

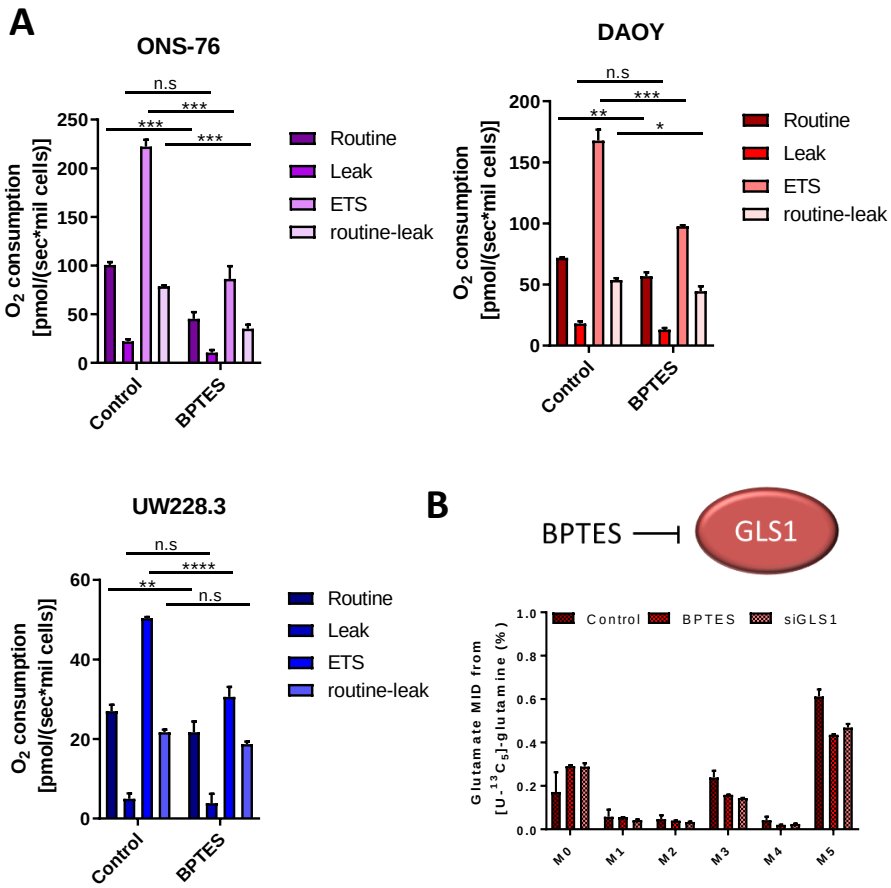

Figure 3.2.9. Glutamate promotes mitochondrial metabolism in MB. A) Bar graph representing the results of the various states measured with high-resolution respirometry (error bars ± SEM of 3 independent experiments). B) Mode of action for BPTES. Treatment with BPTES reduces glutamine-derived glutamate to the same extent as siGLS1.

Subsequently, we measured the 'leak' OC (ATP synthase-independent respiration in the presence of oligomycin). Our results show that BPTES treatment has no impact on leak OC, suggesting glutamate is not used in mitochondrial-independent OC. We further measured the maximal oxygen consumption rates (ETS) through FCCP uncoupling and show significantly decreased OC with BPTES treatment. Routine/leak represents the OC attributed to electron transport chain (mitochondrial) activity only, where our results demonstrate that glutamate is heavily utilised.

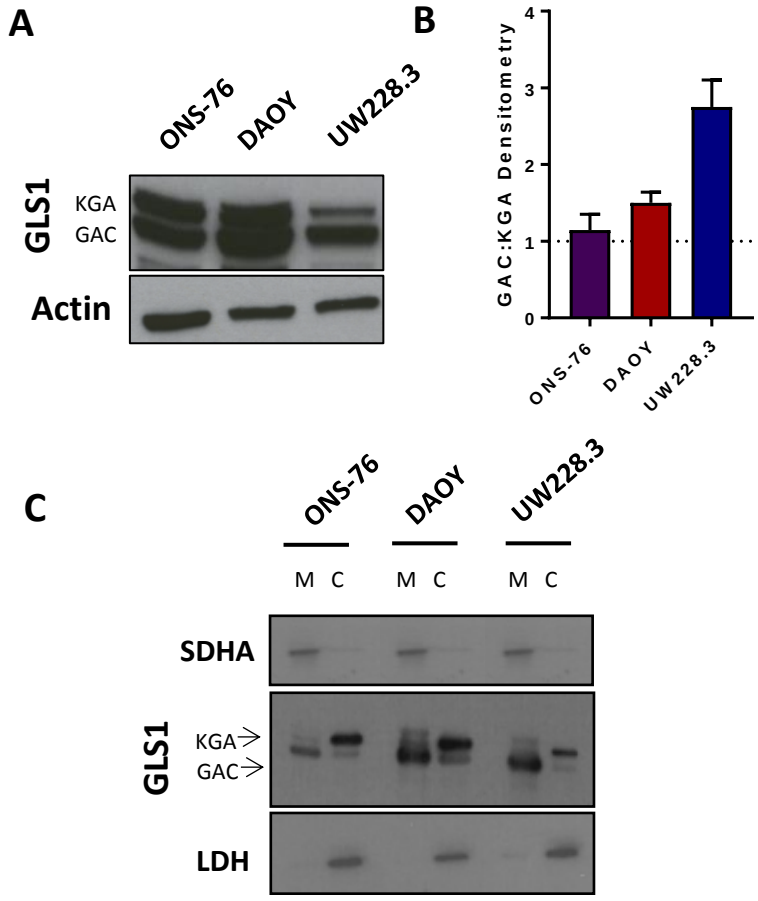

Figure 3.2.10. GLS1 splice variants, KGA and GAC expression and localisation differences. A) Immunoblot analysis of KGA and GAC protein in the ONS-76, DAOY and UW228.3 cell lines. B) Quantification of immunoblot by densitometry analysis. C) Immunoblot analysis of fractionated (mitochondrial and cytosolic) MB cell lines. LDH (lactate dehydrogenase) was used as a cytoplasmic marker. SDHA (succinate dehydrogenase) was used as a mitochondrial marker. (n=1)

3.2.8 Relative expression and localisation of the GLS1 splice variants

GLS1 is typically referred to as a mitochondrial enzyme. However, more recently it has been shown to also exist in the cytosol, with the two splice variants, KGA and GAC, being differentially restricted to each compartment – the former to the cytosol and the latter, the mitochondria. The relative expressions of the KGA and GAC splice variants have not previously been identified in the setting of MB. We therefore investigated the expression and localisation of each isozyme in the MB cell lines, and observed that although both variants were expressed, GAC appeared to be the major isoform in the DAOY and UW228.3 cell lines, while no differences were observed in the ONS-76 line (Figure 3.2.10 A and B). In order to investigate whether the variants were differentially localised, mitochondrial and cytosolic (including nuclear) fractions were generated and immunoblotted as before. It was found that, consistent with the literature on other cancer types (Cassago *et al.*, 2012), KGA localised mainly to the cytosol, while GAC was predominantly mitochondrial, although some expression was observed in the cytosolic fraction of the DAOY cell line (Figure 3.2.10 C).

To investigate the importance of these enzymes in MB biology, we measured the effect of GAC and KGA knockdowns (Figure 3.2.11) on relative growth in two of our cell lines, ONS-76 and DAOY. Our results highlight differences in dependencies of cells on each splice variant, with siGAC resulting the largest reduction in growth (figure 3.2.12), suggesting MB cell lines prefer the GAC isoform to sustain growth. To further understand their relative importance, we examined the metabolic changes accompanying KGA or GAC knockdown, through mass isotope distribution (MID) analysis, using ^{13}C fully labelled glutamine ($^{13}C_5$-U-glutamine). Upon knockdown of either GAC or KGA, the m+5 isotopologue of glutamate was significantly decreased (Figure 3.2.13), consistent with reduced GLS1 activity observed with siGLS1. Our

results reveal siGAC decreased label incorporation to a larger extent than with siKGA, suggesting increased GAC activity compared to KGA. The same is apparent for αKG and key TCA intermediates: succinate and malate and in oxidative-derived citrate (m+1 to m+4). We observed no additional effect on m+5 citrate (reductive-derived) when siGAC is compared with siKGA, suggesting an additional impact of KGA when citrate is made in the cytosol, or alternatively a reduced impact of GAC on cytosolic-derived citrate.

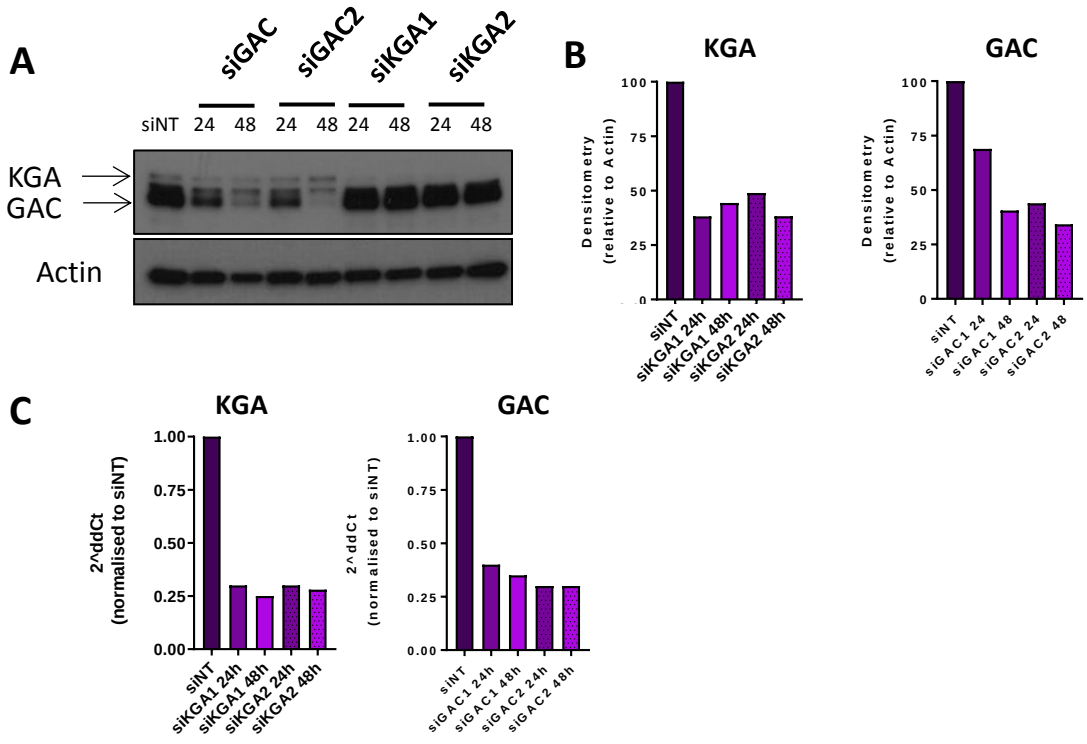

Figure 3.2.11. Successful knock down of GLS1 splice variants. Successful knock down of GLS1 variants KGA and GAC protein was validated for all experimental conditions. A) Immunoblotting demonstrates protein knock down of KGA and GAC by two independent siRNA transcripts 24 and 48 h post transfection. B) Densitometry analysis of KGA knockdown immunoblot. C) qPCR confirming reduction of KGA and GAC RNA transcripts, using two independent siRNA sequences. (n=2)

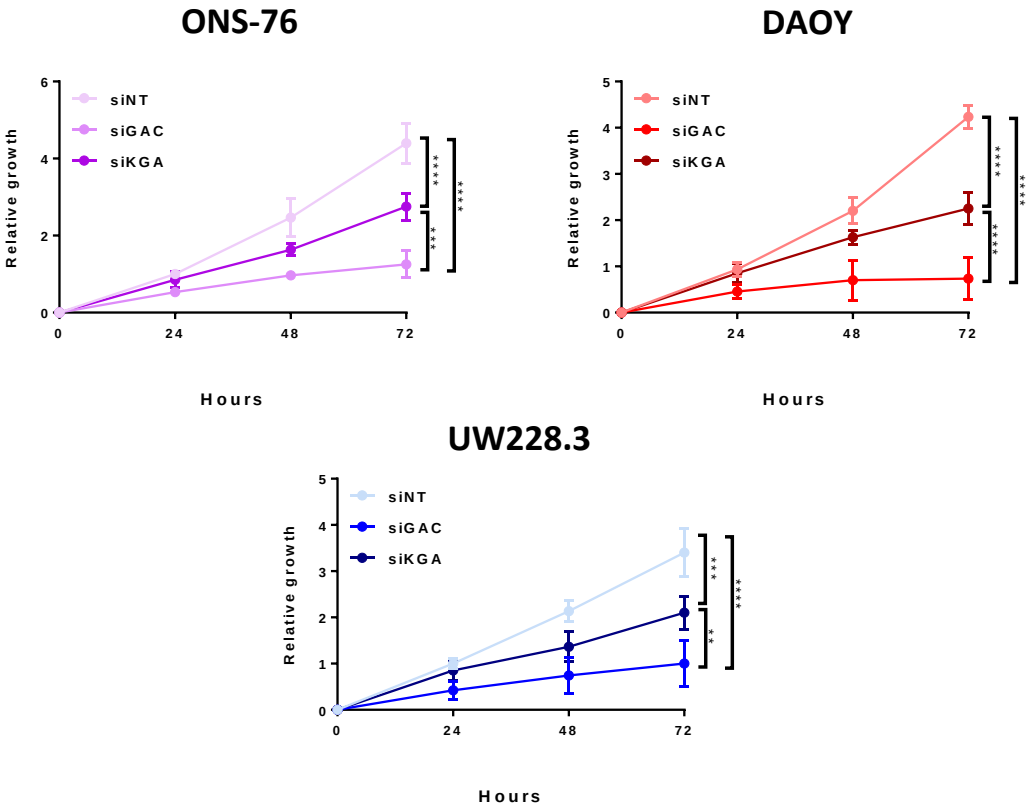

Figure 3.2.12. The effect of GLS1 splice variants, KGA and GAC on MB growth. Relative growth curves of ONS-76, DAOY, and UW228.3 cell lines incubated with siNT, siKGA or siGAC for 3 days (72 h). Treatment with siKGA and siGAC significantly decreased the growth rate of all three cell lines, compared to siNT control, with siGAC showing the largest reduction in growth. Data is performed in technical triplicate with 3 independent experiments, mean +/- S.D. Data analysed with an unpaired t-test; *p<0.05, **p<0.01, ***p<0.001, ****p<0.0001

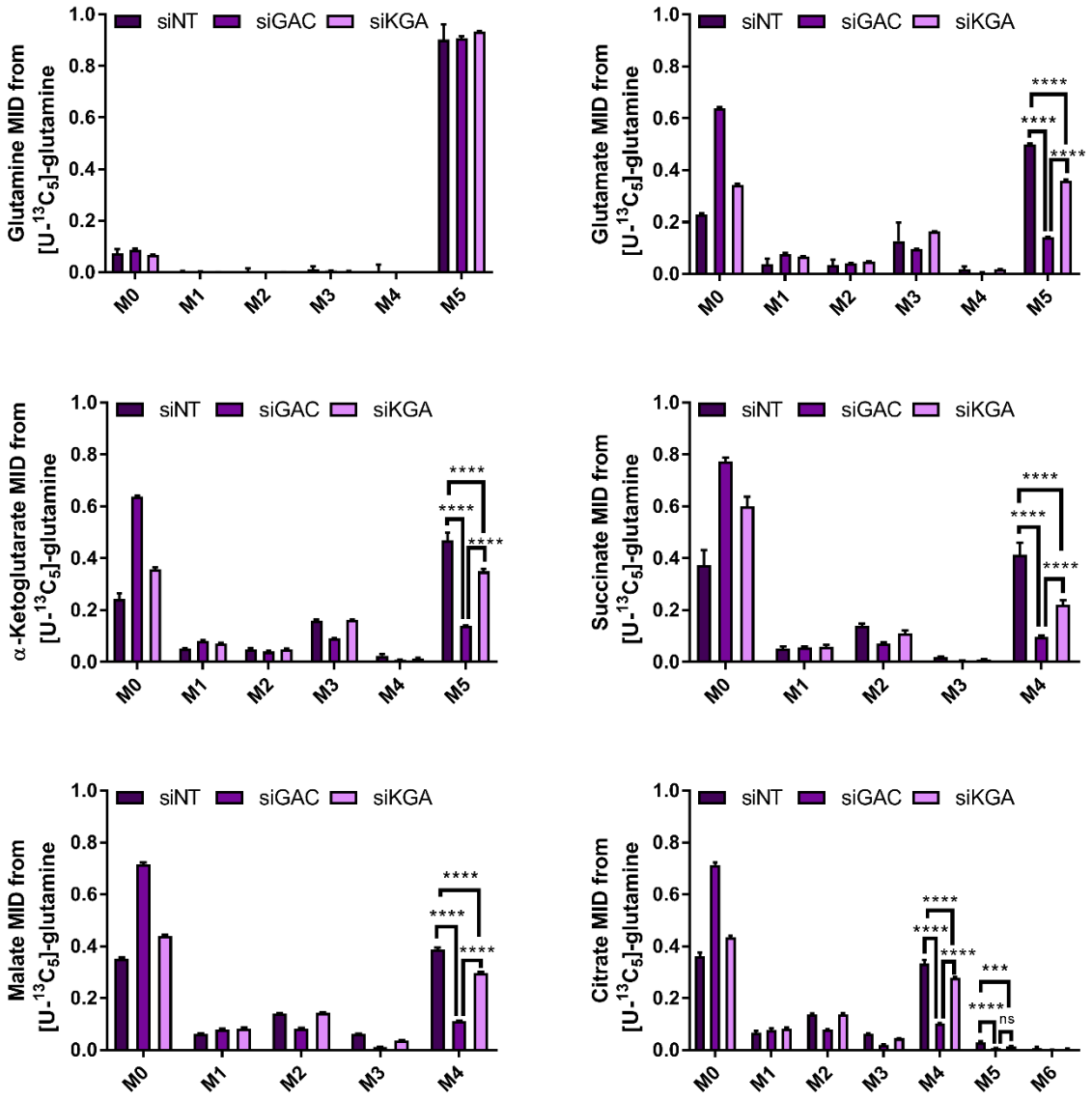

Figure 3.2.13. GAC activity is preferred in MB. Analysis of the mass isotopologue distribution (MID) of glutamine- derived glutamate. A) Significant reductions in ^{13}C label incorporation is observed in siGLS1 treated ONS-76 line after 24 h incubation with ^{13}C-U-glutamine compared to siNT and siGLS2, suggestive of favoured GLS1 activity. Data is performed in technical triplicate, mean +/- S.D. Statistical significance determined using two-tailed unpaired Student's t-test; *p<0.05, **p<0.01, ***p<0.001, ****p<0.0001

3.2.9 Glucose metabolism is increased after GLS1 knock-down.

Glucose and glutamine are major anabolic carbon sources in most tumours, with our results suggesting they both have important roles in MB cell growth. There is evidence to suggest that loss of one carbon source can be somewhat compensated by enhanced metabolism of the other. However, it has also been shown that glucose metabolism may be negatively impacted upon glutaminase inhibition (Pan *et al.*, 2015). We utilised both ^{13}C-U-glucose and ^{13}C-U-glutamine to investigate the metabolic alterations induced by GLS inhibition in the MB cell lines. Upon entry of pyruvate into the mitochondria, there are two means of entry to the TCA cycle; the oxidative decarboxylation of pyruvate to acetyl CoA by PDH, and carboxylation of pyruvate by PC forming oxaloacetate as a result. Both of these pathways may yield αKG and subsequently glutamate via further TCA metabolism. The unique MIDs produced from ^{13}C-U-glucose can reveal the relative activities of PDH (m+2 citrate) and PC (m+3 citrate) (Figure 3.2.14 A). We therefore incubated MB cells with siGLS1 with $^{13}C_6$-U-glucose, and found that m+2 and m+3 glutamate isotopologues were increased compared to control conditions, suggestive of relatively increased glucose-derived glutamate synthesis, via PDH and PC activity, respectively. We also noted significant increases in m+4 and m+5, indicating further TCA cycle activity resulting in glutamate synthesis (figure 3.2.14 B). Glucose contribution towards glutamate biosynthesis was shown to almost double after siGLS1, suggesting increased glucose metabolism is utilised in an attempt to compensate for reduced glutamate and therefore highlighting the importance of glutamate synthesis in MB cell lines (figure 3.2.14 C). However, glutamate concentrations were not rescued by heightened glucose metabolism (Figure 3.2.14 D).

We subsequently measured the different contributions of glutamine and glucose towards the biosynthesis of glutamate in all three MB cell lines. Through the use of both ^{13}C tracer metabolites, we were able to establish the total carbon contribution of glucose and glutamine towards glutamate synthesis. Unsurprisingly, we found around 50% of glutamate was derived from glutamine in the ONS-76 cell lines, 60% observed in the UW228.3 line and a contribution of 80% in the DAOY cell line, highlighting the differential dependencies on glutamine between our MB cell lines (figure 3.2.15 C). Furthermore, our results show a smaller contribution of glucose towards glutamate synthesis, with 15%, 5% and 18% observed in the ONS-76, DAOY and UW228.3 lines respectively (figure 3.2.15 C).

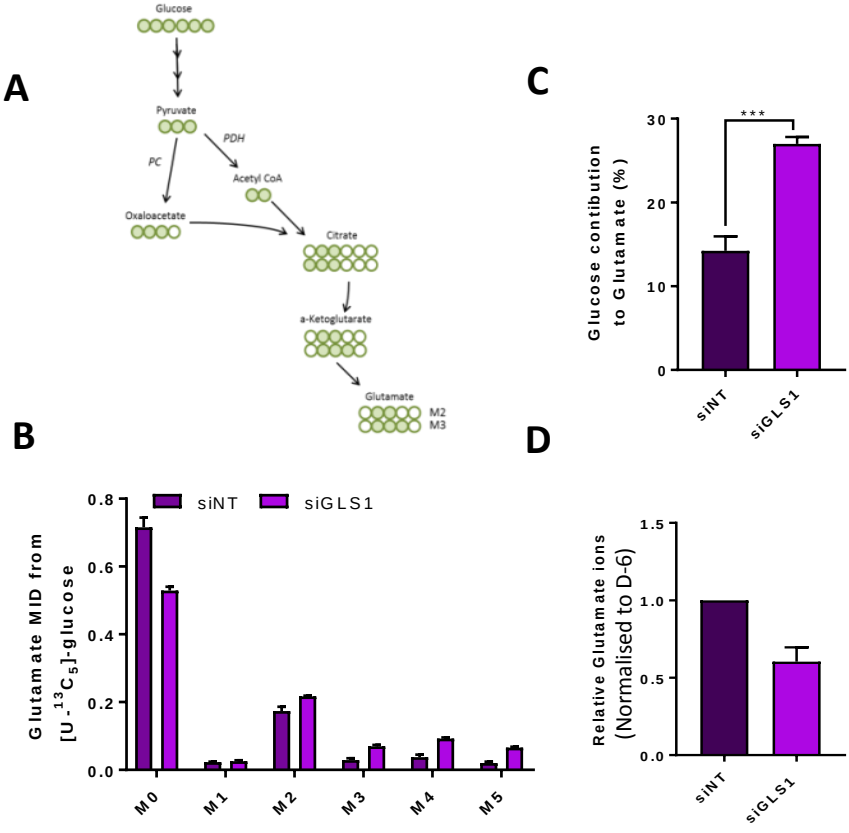

Figure 3.2.14. Glucose attempts to rescue glutamate concentrations when GLS1 activity is impaired, through increased pyruvate carboxylase activity. A) M+5 Incorporation of [U-13C5]-glutamine into glutamate is decreased upon KD of GLS1. B) [U-13C5]- glucose incorporation into glutamate is increase upon KD of GLS1. C) Despite increased contribution of glucose to glutamate; steady state levels show an inability of glucose to rescue glutamate concentration with siGLS1. (n=3)

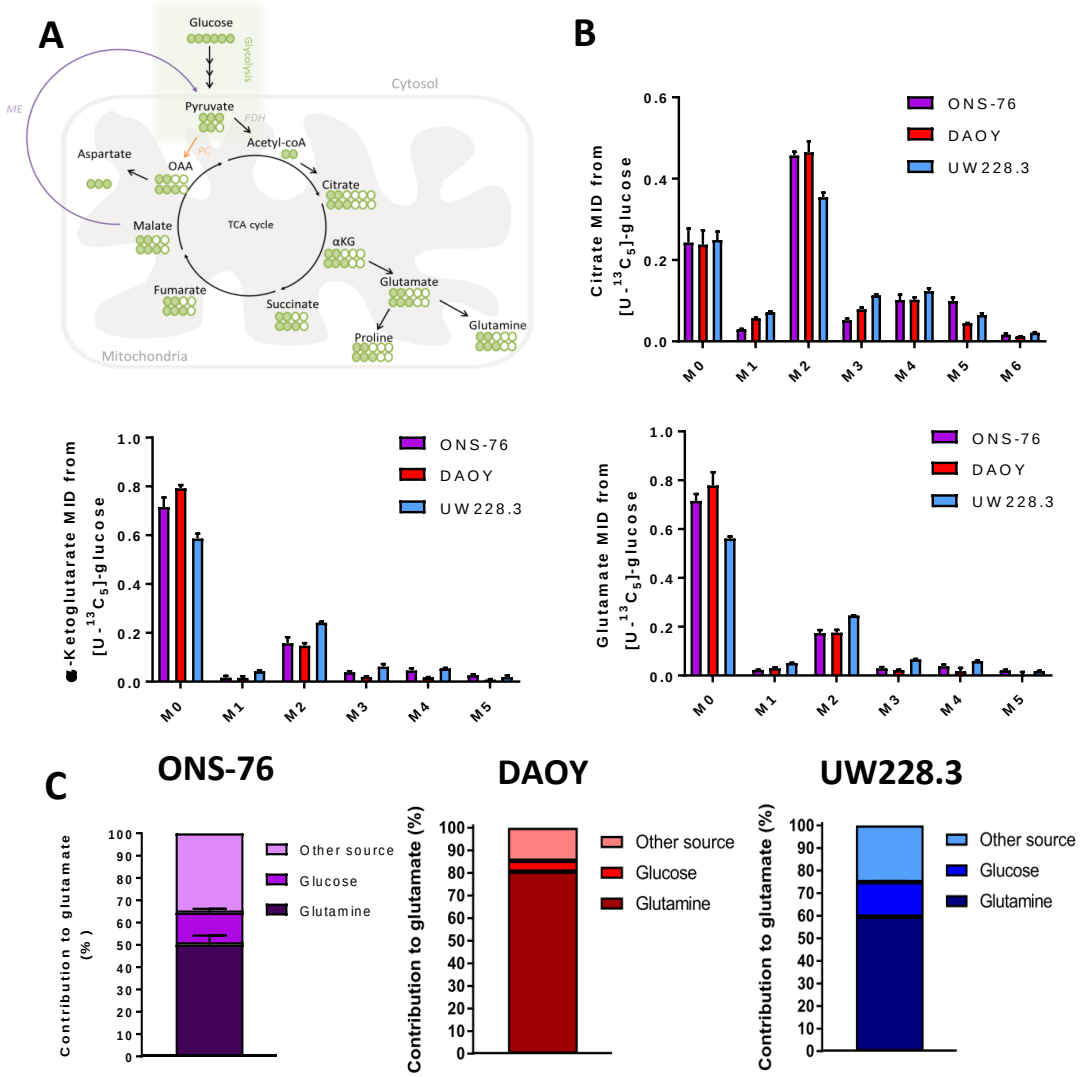

Figure 3.2.15. Utilisation of glucose in MB cell lines. A) Label incorporation of glucose into downstream metabolites. B) Analysis of the mass isotopologue distribution (MID) of glucose- derived metabolites. C) Total carbon contribution of glucose and glutamine towards glutamate synthesis. (n=3)

3.2.10 Glutamate is exported from MB cell lines.

We have shown that MB cell lines demonstrated high glutamine use, and that neither glutamate feeding, nor enhanced glucose metabolism could compensate in glutamine-depleted conditions. As glutamate concentrations were previously shown to negatively correlate with outcomes in MB patients (Wilson *et al.*, 2014), we investigated the

concentrations of glutamate in MB cell lines and their environment. This is particularly important, as the patient study was unable to define whether the glutamate levels measured were cellular or stromal. We show that although intracellular concentrations of glutamate are consistently in the low micromolar range (Figure 3.2.16 B), extracellular concentrations of glutamate were relatively high, especially so in the DAOY cell line, given that the medium contained no exogenous glutamate (Figure 3.2.16 C). To examine the source from which the glutamate was synthesised by cells, we cultured them in the presence of stable isotope-labelled ^{13}C-U-glutamine, and monitored the synthesis and excretion of ^{13}C-labelled glutamate. We found that at least 50% of the extracellular glutamate was labelled from glutamine – with over 75% observed in the DAOY cell line (Figure 3.2.16 D). Our results are the first to suggest that glutamate is exported from MB cells.

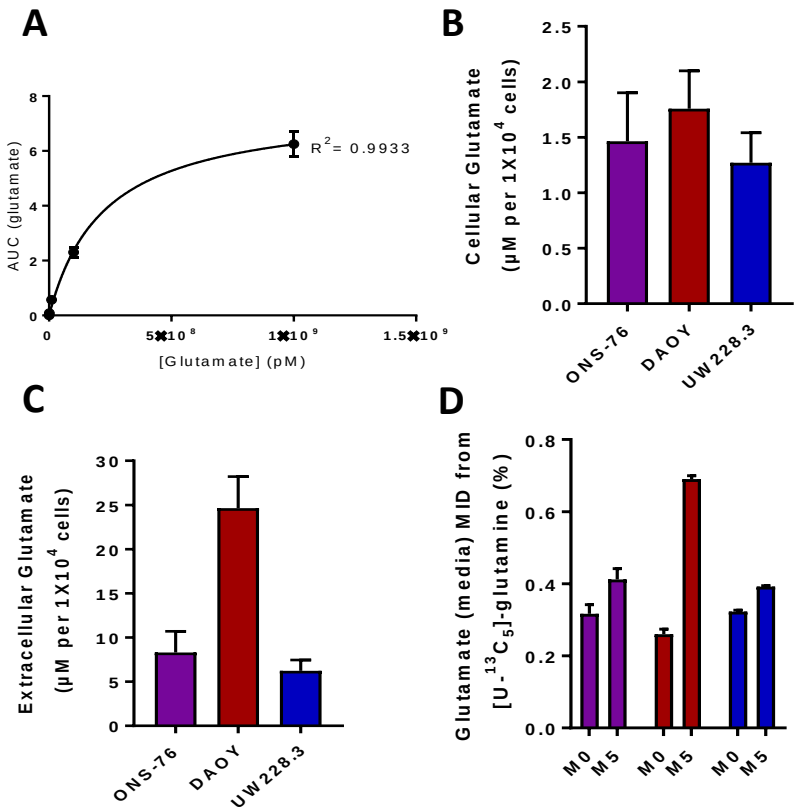

Figure 3.2.16. Assessing intracellular and extracellular glutamate concentrations. A) Glutamate concentration curve was generated using calibration series of glutamate standards by GC-MS. B) Cellular glutamate concentrations in the ONS-76, DAOY and UW228.3 cell lines. C) Extracellular (media) glutamate concentrations reveal extensive glutamate release in the DAOY cell line. D) MID analysis of extracellular glutamate after 24 h incubation with ^{13}C-U-glutamine tracer. (n=3)

3.2.11 SLC7A11 is expressed in MB, which pairs glutamate export with cystine import.

Glutamate export has been implicated in glioma cell growth and invasion (Takano *et al.*, 2001), with an important role for the glutamate/cystine transporter SLC7A11 (X^{CT}) being reported (Polewski *et al.*, 2016). However, the role of SLC7A11 has not been previously shown in MB. We demonstrate SLC7A11 protein expression in both MB tumours (Figure 3.2.17 A) and cell lines (Figure 3.2.17 C), suggesting a role for this anti-porter in MB biology. To further assess the importance of SLC7A11 in the MB cell lines, we inhibited this system using sulfasalazine, SSZ – a well-described inhibitor of this transporter. After treatment, we observed decreased intracellular concentrations of cysteine (Figure 3.2.17 D), consistent with reduced SLC7A11 activity. We also found that SSZ treatment reduced cell growth in all three lines (Figure 3.2.17 E), suggesting that interfering with glutamate/cystine transport may be beneficial in the treatment of MB tumours. Importantly, this effect was abolished by the addition of the reducing agent, 2-mercaptoethanol (2-ME) to cells, which facilitates the uptake of cystine independently of the xCT transporter by reducing cystine to cysteine, allowing its uptake through an alternative transporter.

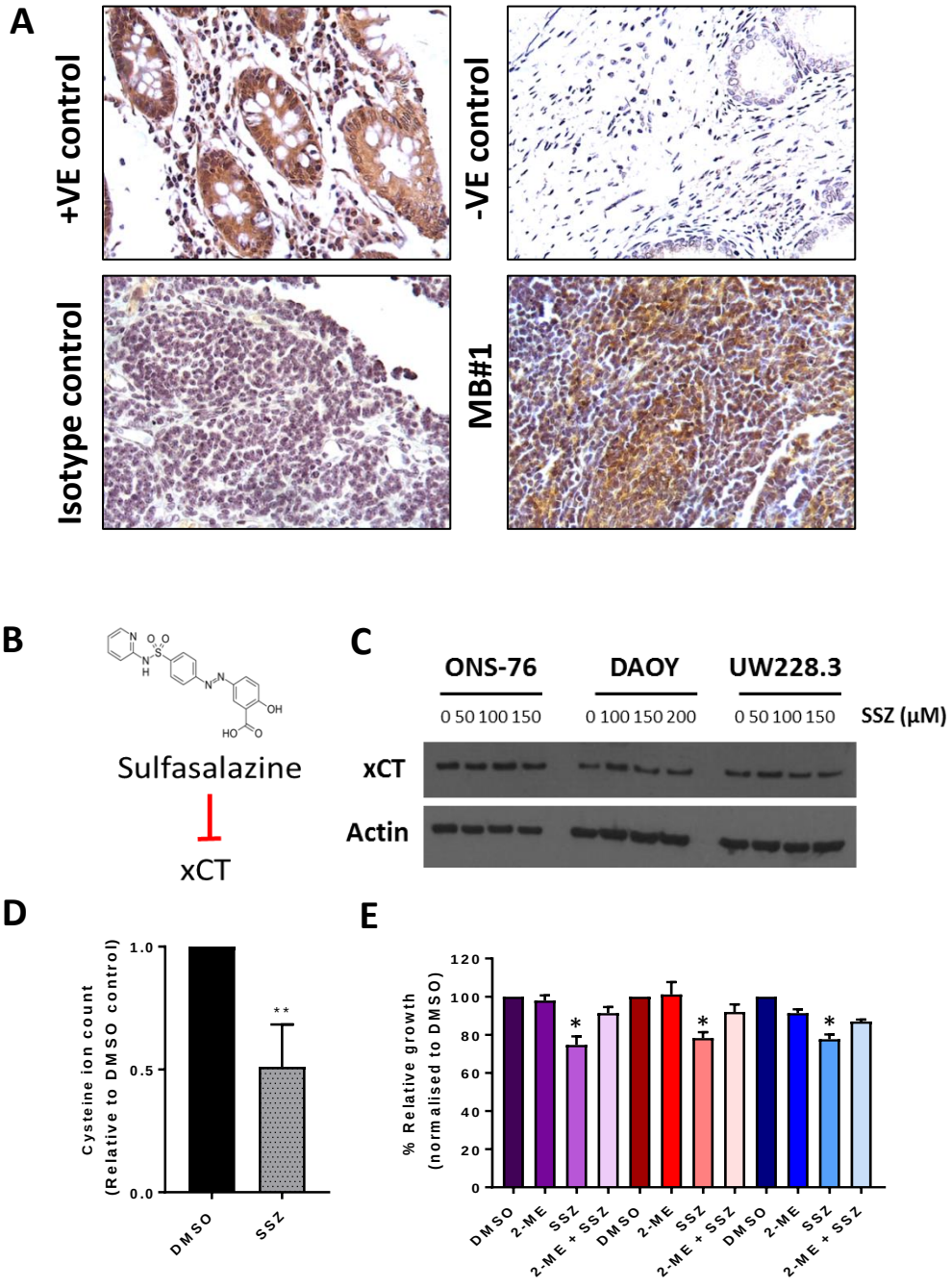

Figure 3.2.17. The glutamate/cystine antiporter, SLC7A11 is expressed in MB tumours and cell lines. A) Immunohistochemical analysis of SLC7A11 expression in MB tumours. Colon tissue was used as a positive control for SLC7A11 staining and Lung tissue was used as a negative control. B) Treatment with Sulfasalazine (SSZ) inhibits SLC7A11 activity. C) SLC7A11 expression in MB cell lines. D) Decreased cysteine ion count after SSZ treatment. (n=3) E) Relative growth of MB cell lines treated with 2-ME, SSZ or 2-ME + SSZ compared to DMSO control. (n=3)

3.2.12 Genes encoding proline biosynthesis predict survival in MB patients

Our results highlight the importance of glutamate, separate to its function in feeding the TCA cycle. We therefore explored other avenues in which glutamate may exert its effects. One of the many metabolic pathways in which glutamate plays a role is in the synthesis of proline, which has recently been highlighted as an important pathway in some cancers (Phang *et al.*, 2015). We therefore assessed the expression of several proline-related metabolic genes and the result of this on patient survival, using two independent databases (Newcastle cohort and online database, GEO: GSE42658). We noted that in all cases, expression of the proline biosynthetic genes (ALDH18A1, PYCR1 and PYCR2) were increased, while PRODH, responsible for the breakdown of proline, was significantly decreased (Figure 3.2.18). Furthermore, the expression of these genes proved to be prognostic, with high ALDH18A1 and PYCR1, and low PRODH being predictive of a worse overall survival in MB patients. These results suggest proline biosynthesis is heightened in MB tumours.

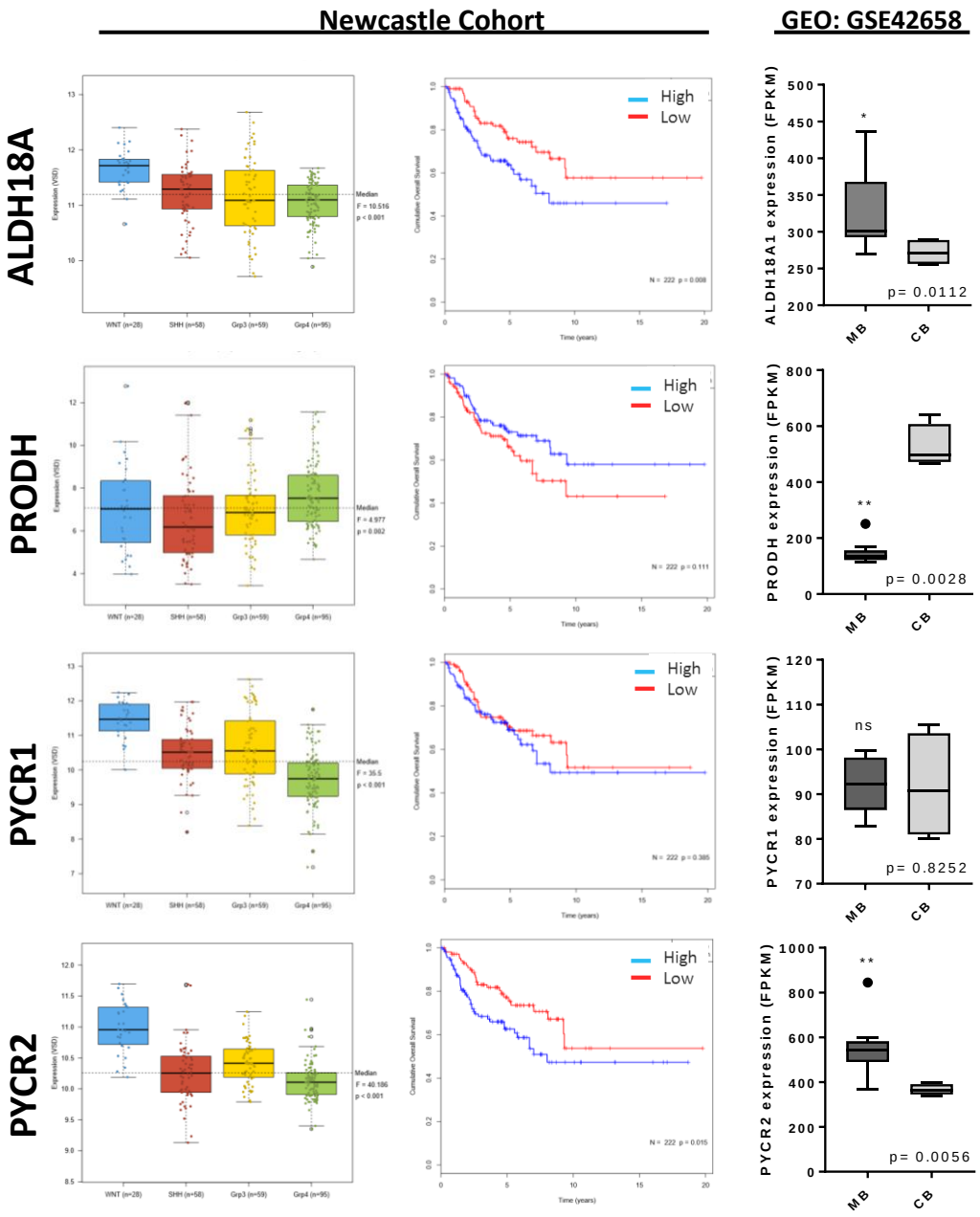

Figure 3.2.18. Expression of proline metabolic-related genes was associated with survival in MB tumours. A) RNA expression data compared across subgroups of MB and Representative Kaplan-Meier survival curves of the MB Newcastle cohort. n=240 (WNT n=28, SHH n=58, G3 n=59 and G4 n =95). High and low expression was determined by the median expression value for each gene. Log-rank (Mantel-Cox) statistical test was performed in Kaplan-Meier survival graphs. Unpaired two-tailed t-test statistical tests were performed in mRNA expression data graphs; *p<0.05, **p<0.01, ***p<0.001, ****p<0.0001.

3.2.13 Proline biosynthesis in MB cell lines

After establishing an important correlation of proline-related genes expression in MB tumours with patient outcomes, we investigated the role of proline metabolism further in the MB cell lines. As proline metabolism activity can be dictated by expression of related enzymes, we measured the relative expression of: pyrroline-5-carboxylate synthetase (ALDH18A1), pyrroline carboxylate reductase 1 (PYCR1) and 2 (PYCR2) (Figure 3.2.19 A) between cell lines. Enzyme expression was observed in all of our lines, where ONS-76 had relatively higher expression of all three enzymes (Figure 3.2.19 B), as confirmed by densitometry analysis (Figure 3.2.19 C). Although indicative, protein expression does not fully reveal metabolic pathway activities. We therefore, investigated the extent of proline biosynthesis by means of ^{13}C-U-glutamine incorporation into proline. Our results suggest

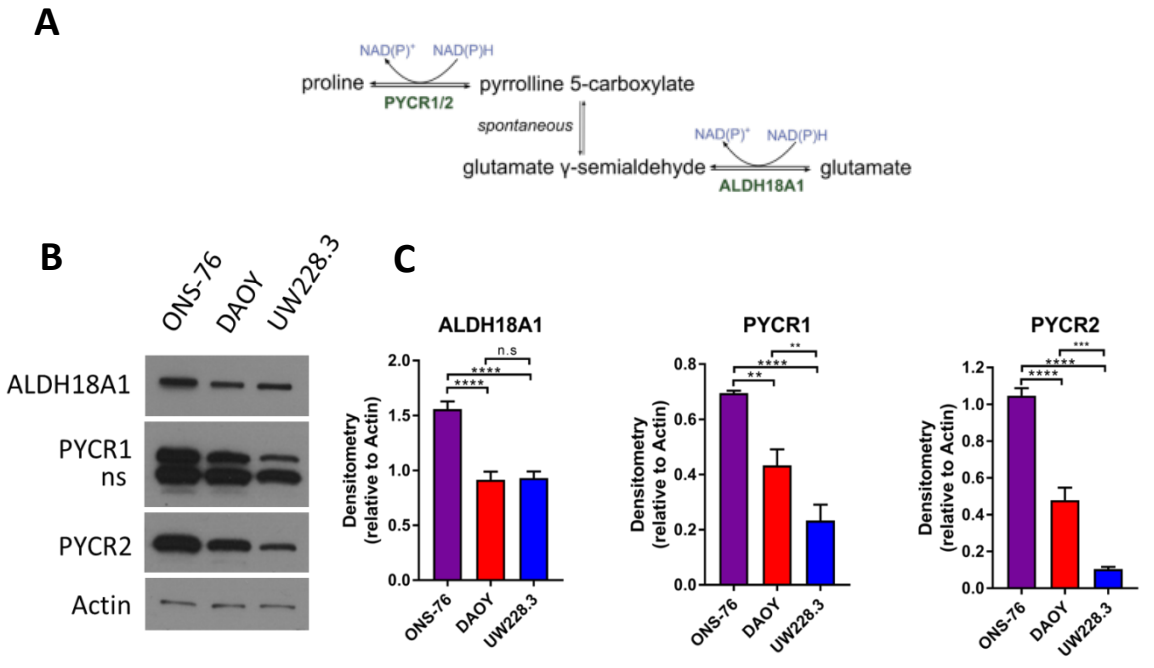

Figure 3.2.19. MB cell lines express proline biosynthetic enzymes. A) Enzymes involved in the biosynthesis of proline. B) Protein expression of enzymes involved in proline metabolism, in MB cell lines. Gene expression of enzymes involved in the biosynthetic pathway. Experiments performed in technical and biological triplicate. Data is mean +/- S.E.M. Significance determined by one-way ANOVA; *p<0.05, **p<0.01, ***p<0.001, ****p<0.0001

heightened glutamine-derived proline biosynthesis in our cell lines, with up to 50% label incorporation observed after 24 h (Figure 4.2.20).

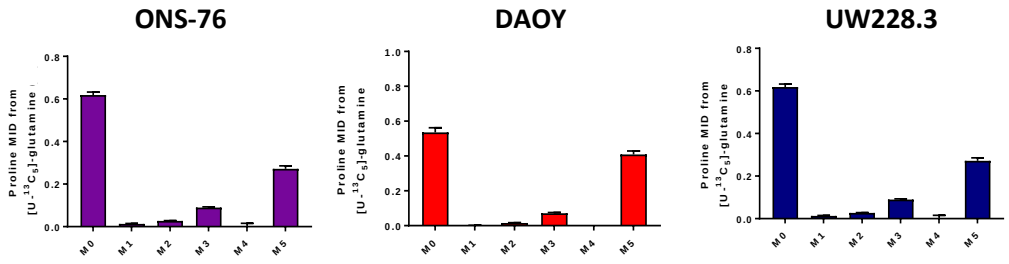

Figure 3.2.20. Glutamine- derived proline synthesis in MB. Analysis of the mass isotopologue distribution (MID) of glutamine- derived proline. (n=3)

3.2.14 Proline biosynthesis helps control intracellular glutamate

Another source of proline is through the metabolism of arginine. Arginine can be hydrolysed by ARG1 to ornithine, which subsequently may be converted to proline through ornithine aminotransferase (OAT) activity. As the most abundant amino acid in brain tissue, arginine, or arginine-derived ornithine may also be used in proline biosynthesis in MB cells. To investigate this, we used a competition assay between arginine and ^{13}C-U-glutamine or ornithine and ^{13}C-U-glutamine, where we would expect ^{13}C label incorporation into proline to decrease if the competing metabolite is used to synthesise proline. Surprisingly, we find no change between arginine addition and control (Figure 3.2.21 A), suggesting this metabolite is not used in proline biosynthesis. However, we observe a significant decline in labelled proline when ornithine was added to the medium (Figure 3.2.21 B), indicating a strong role of ornithine in proline biosynthesis. Our data also reveals an increase in glutamate ions upon ornithine addition (Figure 3.2.21 C), suggesting that in the absence of ornithine, proline is a significant product of glutamate. No changes in proline ions were seen

(Figure 3.2.21 D), possibly suggesting that ornithine and glutamate contribute equally to proline synthesis, when ornithine concentrations are present. It is surprising to observe differences between arginine and ornithine, given that they are so closely interrelated. We therefore hypothesised that there must be a reduced potential of our cell lines to synthesise ornithine from arginine, through ARG1. We investigated the expression of ARG1 in MB tumours and observed reduced ARG1 RNA compared to CB control (Figure 3.2.22). Our data suggest proline synthesis from arginine is reduced in preference for glutamate as the predominant source, which could reduce potentially cytotoxic glutamate concentrations.

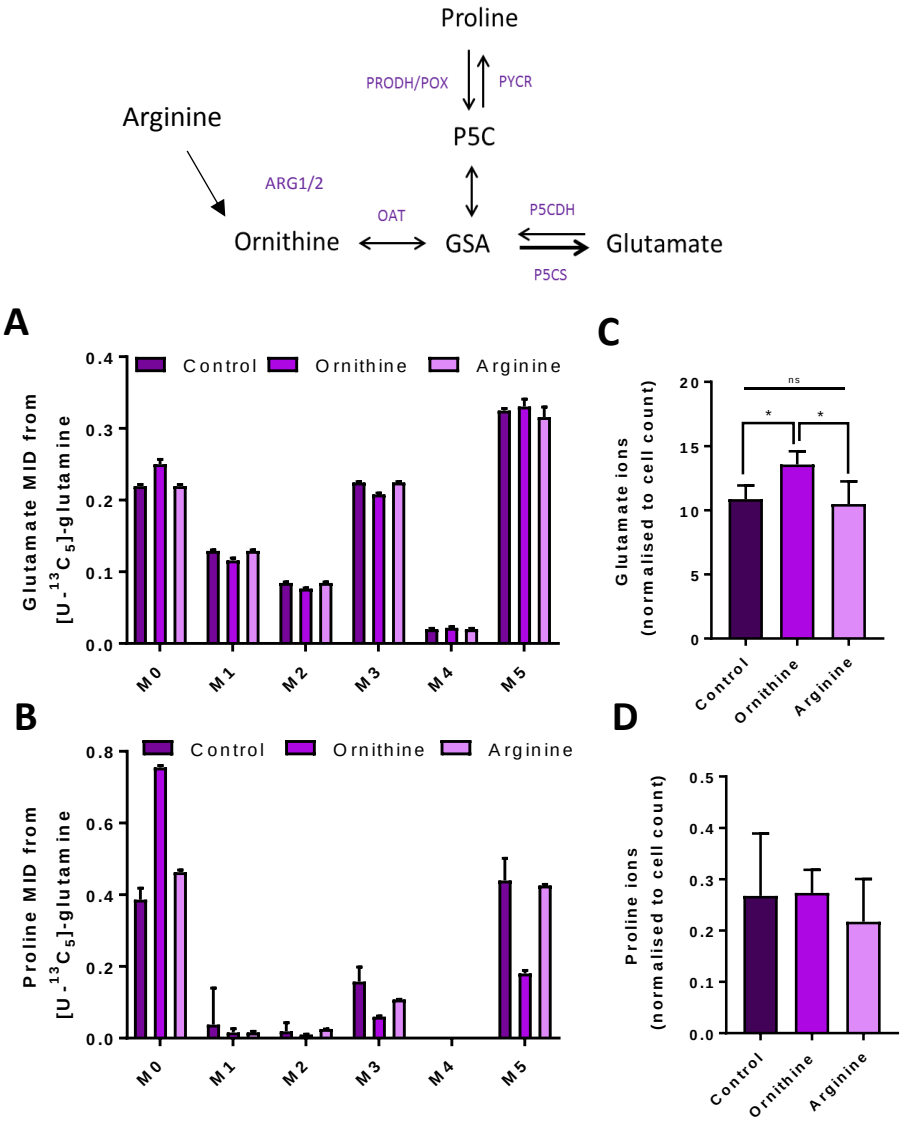

Figure 3.2.21. Ornithine increases glutamate concentrations by relieving glutamate driven proline synthesis. Proline biosynthesis from arginine/ornithine or glutamate. A) Glutamine-derived glutamate does not alter with exogenous arginine or ornithine. B) Glutamate-derived proline is reduced with exogenous ornithine. C) Glutamate ions increase with ornithine treatment. D) Proline ion count is unaffected by ornithine and arginine treatment. Data is performed in technical triplicate, mean +/- S.D. Statistical significance determined using two-tailed unpaired Student's t-test; *p<0.05, **p<0.01, ***p<0.001, ****p<0.0001

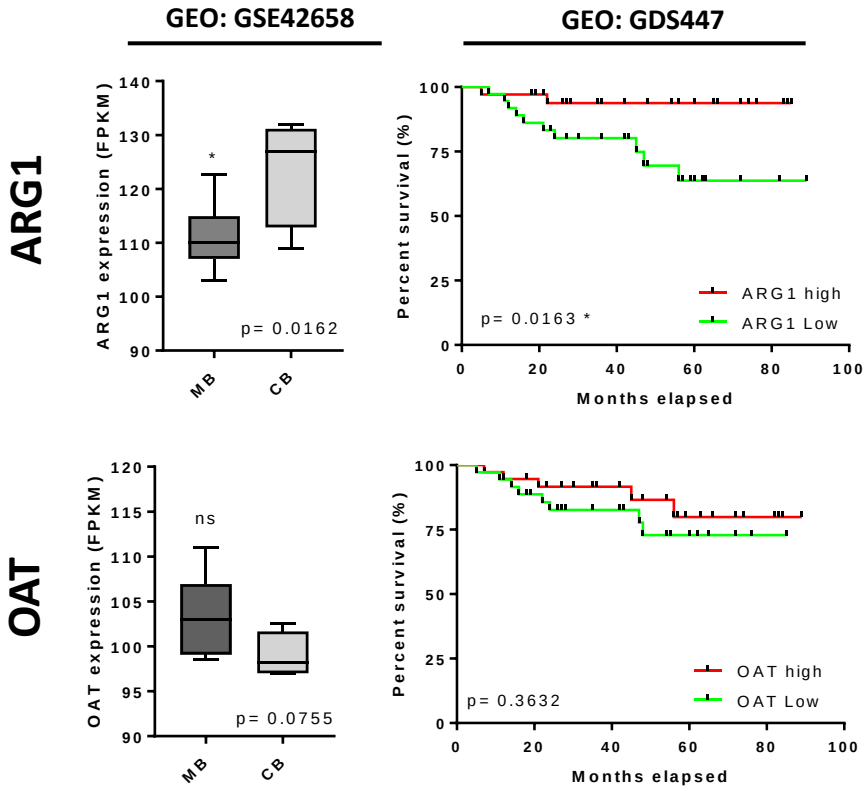

Figure 3.2.22. Expression of proline-related genes was associated with survival in MB tumours. A) Representative Kaplan-Meier survival curves of the online NCBI Geo repository cohort (accession number: GDS4471). This Expression profiling array, included 76 samples, each belonging to the separate MB subgroups; WNT (n=8), SHH (n=11), G3 (n=16) and G4 (n=39). High and low expression was determined by the median expression value for each gene. Log-rank (Mantel-Cox) statistical test was performed in Kaplan-Meier survival graphs. Unpaired two-tailed t-test statistical tests were performed in mRNA expression data graphs ; *p<0.05, **p<0.01, ***p<0.001, ****p<0.0001

3.2. 15 Proline is exported from MB cell lines

Analysis of the culture media revealed glutamine-derived proline is exported from MB cell lines (Figure 3.2.23), suggesting concentrations of proline exceed metabolic demand. Within the microenvironment, proline is essential in the formation of collagen. Research has also revealed a potential role of type one collagen in MB tumours (Liang *et al.*, 2008). To investigate this further, a Van Gieson's stain was used to assess collagen in MB tumours. Immunohistochemical analysis revealed extensive collagenous networks compared to CB control tissue (Figure 3.2.24), strengthening the notion that collagen may be important in MB.

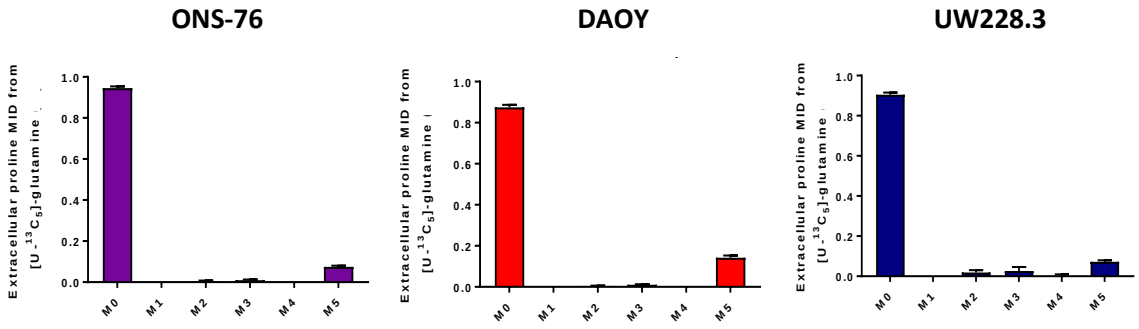

Figure 3.2.23. Proline is exported from MB cells. Analysis of the mass isotopologue distribution (MID) of glutamine- derived proline in the media of cell lines incubated with ^{13}C-U-glutamine for 24 h. (n=3)

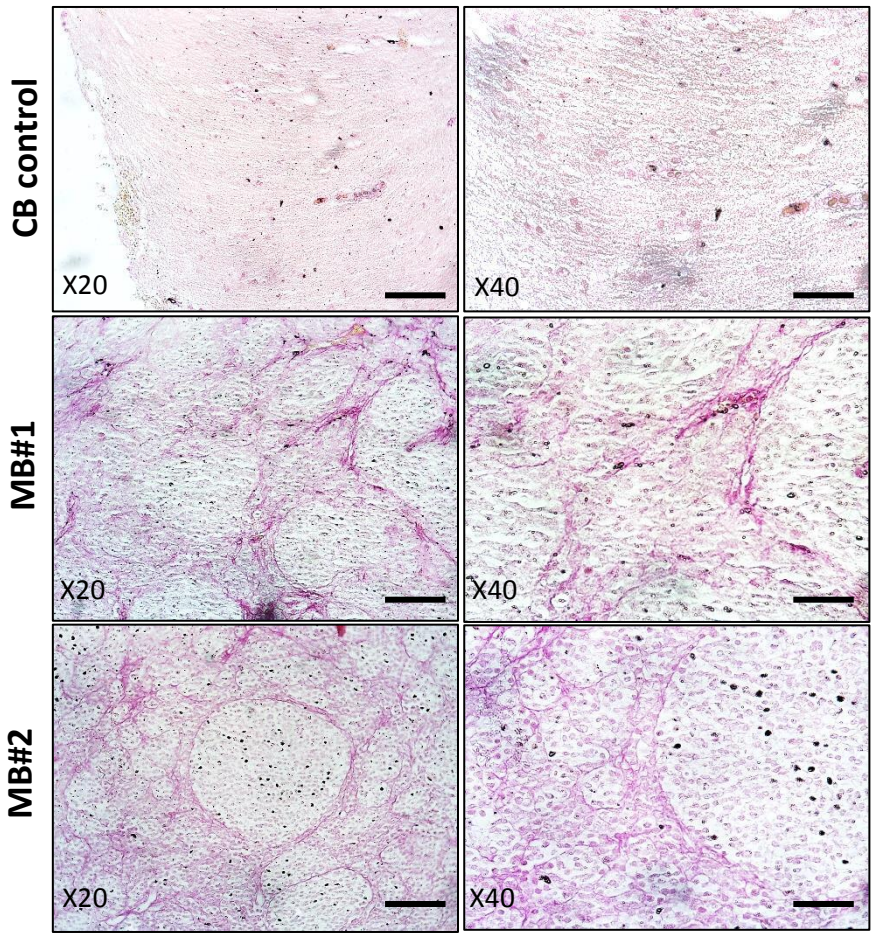

Figure 3.2.24. Histologic illustration of collagen in normal cerebellum (CB) and MB. A Van Geison stain was used to assess the extent of collagen deposits in MB tumours. MB tumour shows increased deposits of collagen compared to CB control tissue, demonstrated by the pink fibres.

3.2.16 Exogenous proline decreases MB cell line growth.

It has been previously reported that exogenous proline can regulate its intracellular biosynthesis, via inhibition of PYCR1/2 (de Ingeniis *et al.*, 2012; Liu *et al.*, 2015). This sensitivity of PYCR to product inhibition led us to investigate whether increasing extracellular proline concentrations (0, 200 and 400 µM) would have a similar effect in the MB cell lines. In order to investigate this, we measured ^{13}C incorporation into proline from glutamine (^{13}C-U-glutamine) when cells were cultured with 0, 200 or 400µM exogenous proline. We observed decreased m+5 proline MID in all three cell lines, suggestive of

reduced glutamine-derived proline (Figure 3.2.25). We further show that exogenous proline resulted in decreased growth in all three cell lines, in a concentration dependent manner, suggesting product inhibition of PYCR is detrimental to MB growth (Figure 3.2.26).

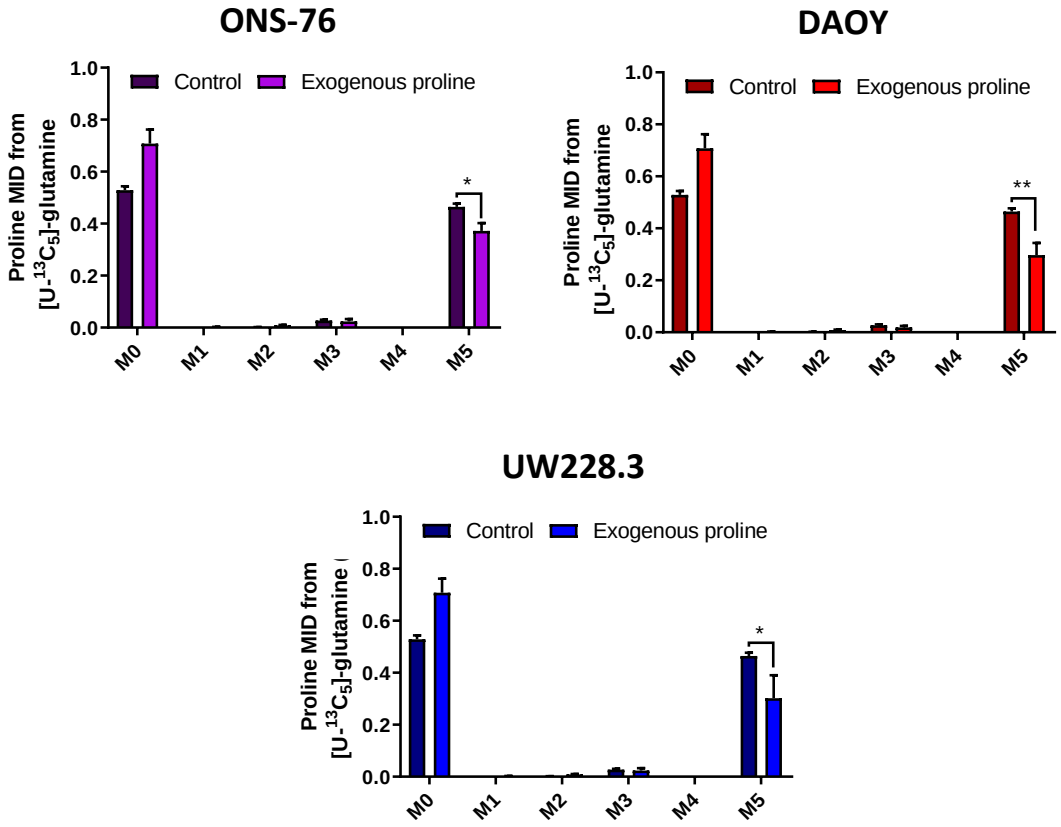

Figure 3.2.25. Exogenous proline reduces glutamine-derived proline. The mass isotopologue distribution (MID) of proline is reduced when cells are cultured in medium containing 200µM proline. GC-MS data is mean +/- S.D from three technical replicates; *p<0.05, **p<0.01, ***p<0.001, ****p<0.0001

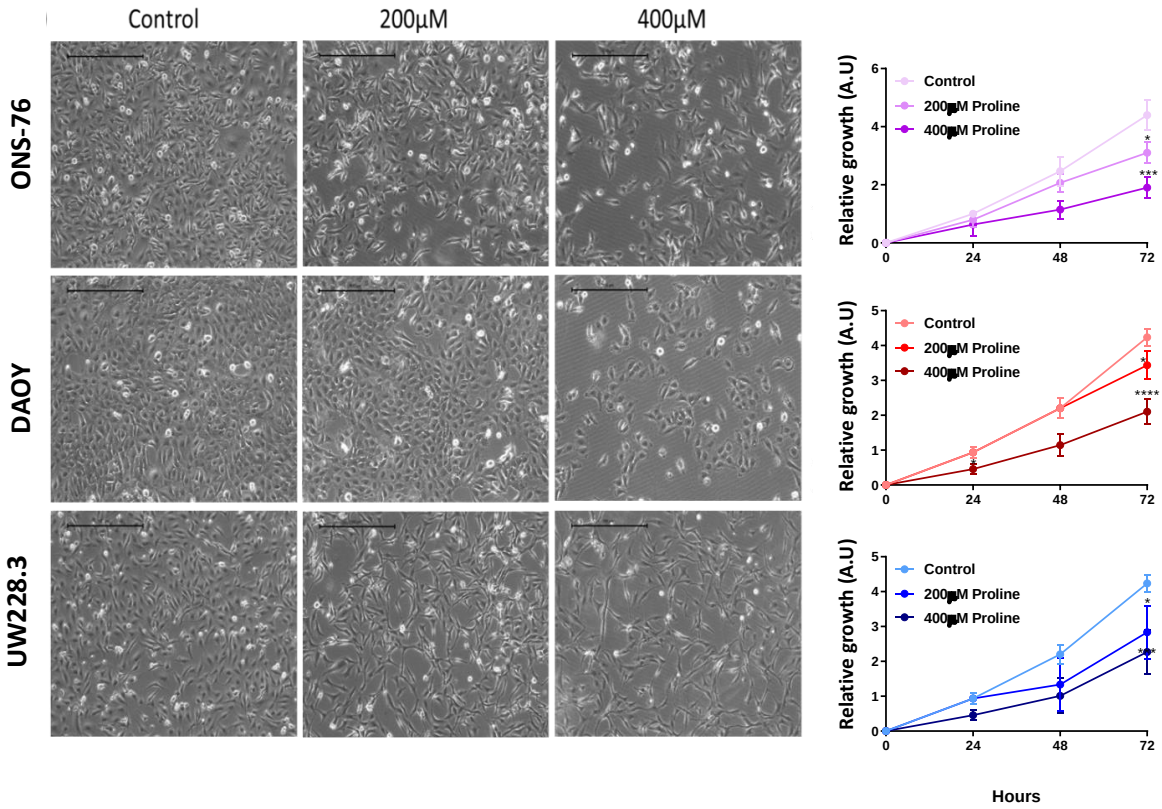

Figure 3.2.26. Exogenous proline reduces MB cell line growth. MB cell line growth is reduced when cells are cultured in medium containing 200 or 400µM proline. . A) Reduced growth was determined by light microscopy. B) Growth was further assessed by an SRB proliferation assay. Data is performed in technical triplicate with 3 independent experiments, mean +/- S.D. Data analysed with an unpaired t-test; *p<0.05, **p<0.01, ***p<0.001, ****p<0.0001

3.2.17 Genes involved in GABA metabolism are predictive of survival in MB patients

Glutamate plays a significant role in neurotransmission, both directly as an excitatory neurotransmitter and indirectly through the synthesis of the inhibitory neurotransmitter, GABA. We therefore investigated the expression of several GABA-related metabolic genes in MB tumours. We observed decreased expression of the main biosynthetic gene, GAD1 when compared to CB, suggesting decreased *de novo* synthesis of GABA in MB tumours (Figure 3.2.27). Furthermore, the expression of GAD1 proved to be prognostic, with high expressing patients having a lower overall survival compared to their low GAD1 expressing counterparts. These results suggest GABA biosynthesis is reduced in MB tumours. Further mRNA expression analysis revealed additional disruption of genes involved in GABA

metabolism, with the major transporter involved in GABA uptake, SLC6A1 and the GABAergic receptor, GABRA2 both being downregulated in MB tumours compared to CB control tissue. These findings further strengthen the fact that MB tumours favour low GABA concentrations, downregulating GABA metabolism and synthesis.

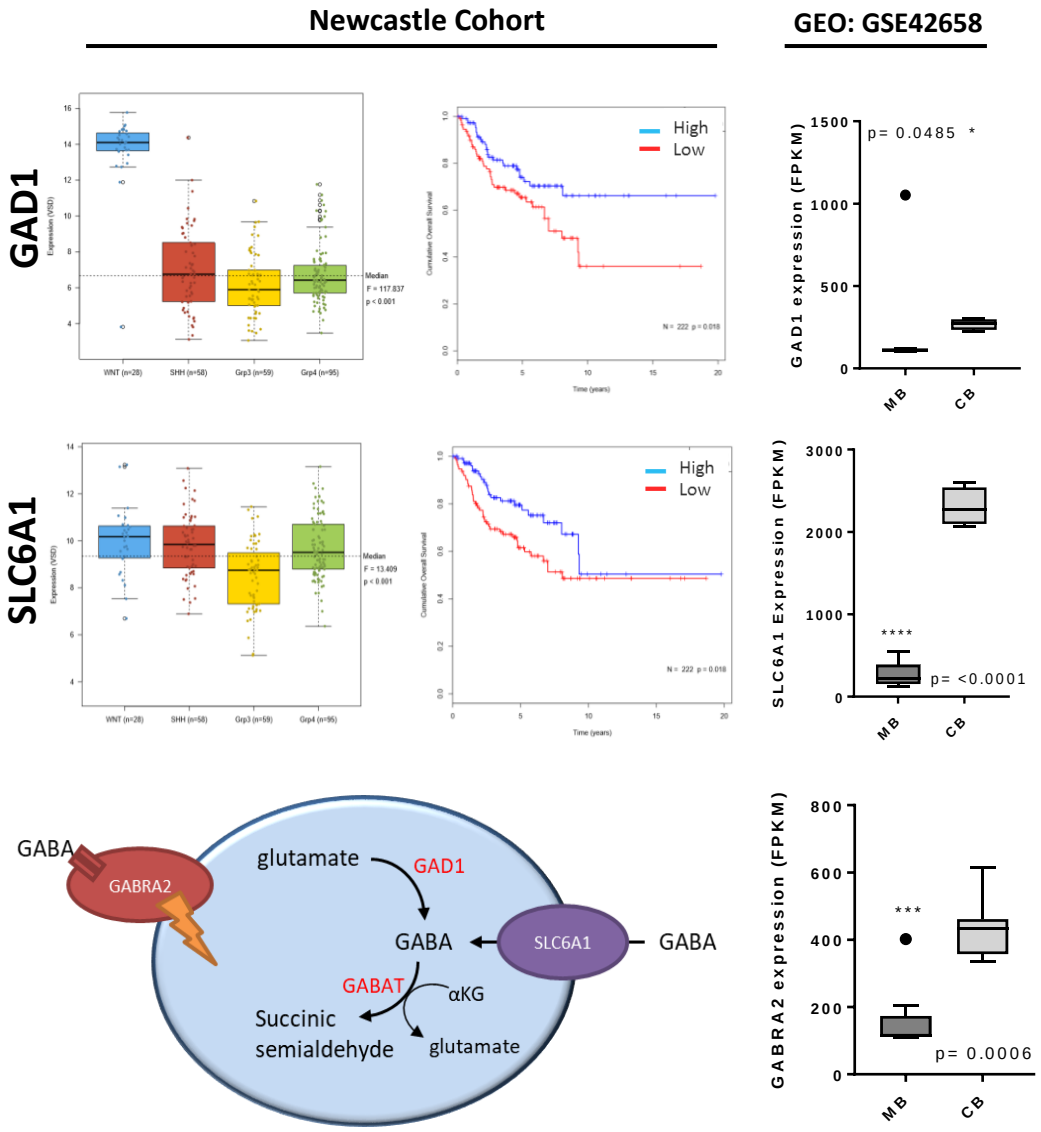

Figure 3.2.27. Expression of GABA-related genes was associated with survival in MB tumours. A) RNA expression data compared across subgroups of MB and representative Kaplan-Meier survival curves of the MB Newcastle cohort. n=240 (WNT n=28, SHH n=58, G3 n=59 and G4 n =95). High and low expression was determined by the median expression value for each gene. Log-rank (Mantel-Cox) statistical test was performed in Kaplan-Meier survival graphs. Unpaired two-tailed t-test statistical tests were performed in mRNA expression data graphs; *p<0.05, **p<0.01, ***p<0.001, ****p<0.0001.

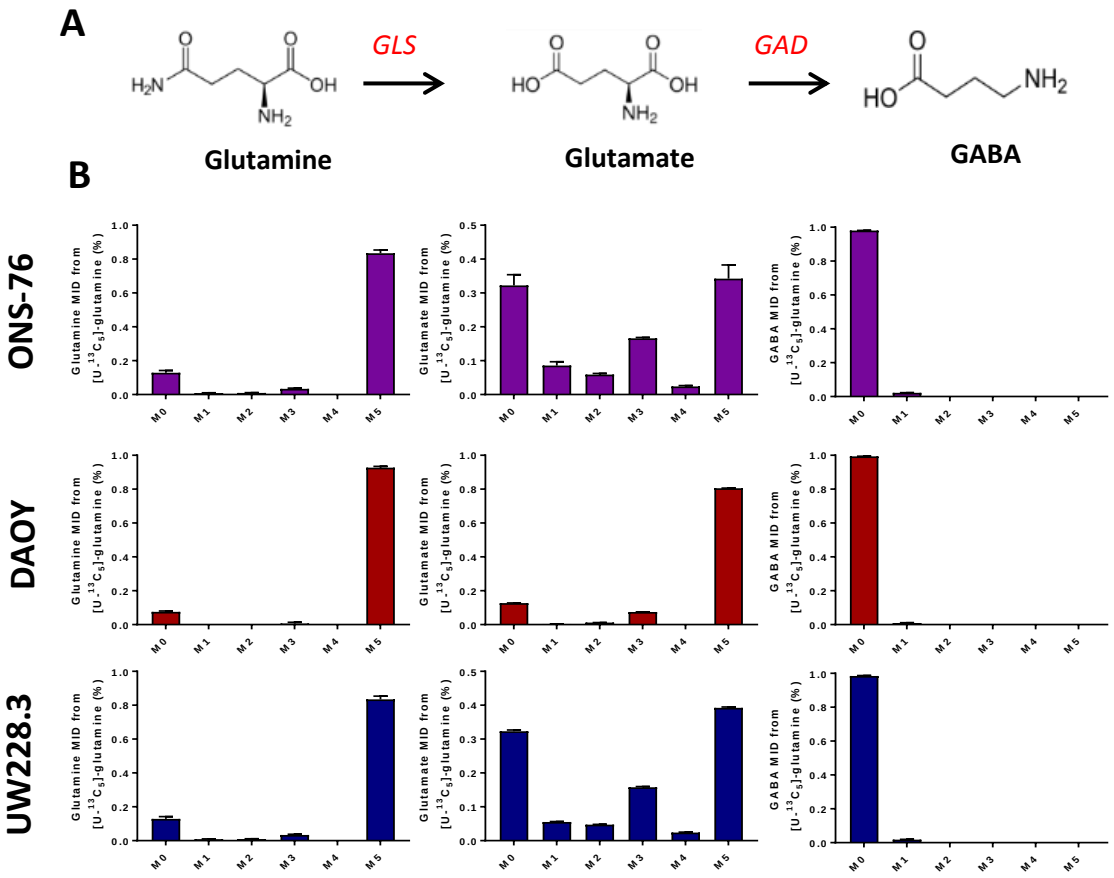

Figure 3.2.28. De novo GABA biosynthesis is abolished in MB cell lines. A) Glutamate is a direct precursor for *de novo* GABA synthesis. B) No ^{13}C label incorporation into GABA when MB cell lines are incubated with 13C-U-glutamine 24 h, suggesting a block in GABA biosynthesis. (n=3)

3.2.18 MB cell lines block GABA biosynthesis

GABA is synthesised from glutamate via GAD enzyme activity (Figure 3.2.28 A). We investigated the extent of glutamine-derived GABA biosynthesis in our MB cell lines, by means of measuring ^{13}C-U-glutamine incorporation into GABA. Our results suggest a block in glutamine-derived GABA biosynthesis in our cell lines, with only slight m+1 label incorporation observed after 24 h (Figure 3.2.28 B). Our results align with our previous findings that GAD1 is significantly reduced in MB tumours.

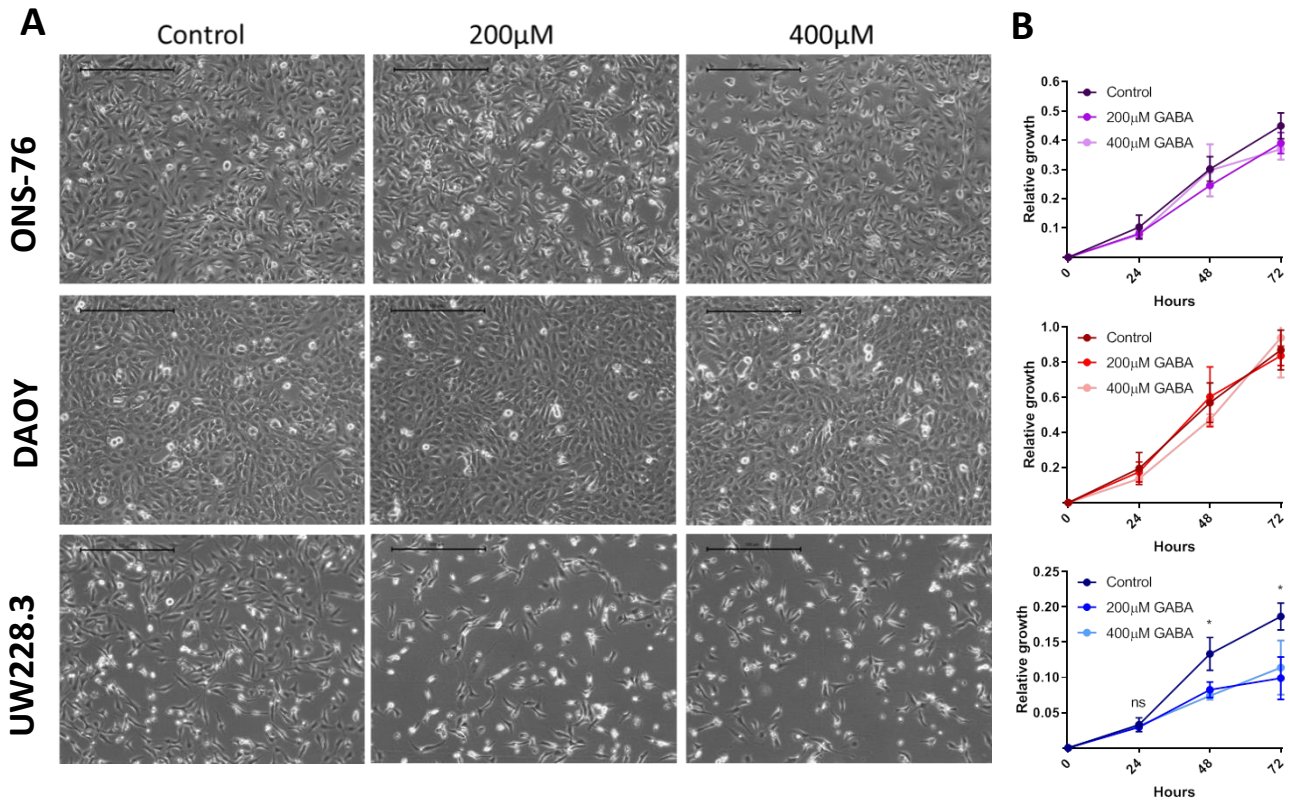

Figure 3.2.29. Exogenous GABA reduces growth in the UW228.3 cell line. UW228.3 cell line growth is reduced when cells are cultured in medium containing 200 or 400µM GABA. A) Reduced growth was determined by light microscopy. B) Growth was further assessed by an SRB proliferation assay. Data is performed in technical triplicate with 3 independent experiments, mean +/- S.D. Data analysed with an unpaired t-test; *p<0.05, **p<0.01, ***p<0.001, ****p<0.0001

3.2.19 Exogenous GABA reduces growth in the UW228.3 cell line.

We would predict that MB cells have reduced GABAergic properties, due to the reduced receptor expression observed in tumours. We therefore incubated all three cell lines with exogenous concentrations of GABA (0, 200 and 400 µM) to investigate this further. Indeed, we see no changes in cell growth in the ONS-76 and DAOY cell lines, although, exogenous GABA reduces growth in the UW228.3 cell lines (Figure 3.2.29), suggesting an ability of these cells to react to GABA.

3.3 Discussion

3.3.1 Introduction

The metabolism of two major energy sources, glucose and fatty acids have previously been well described in MB (Gershon et al. 2013; Tech et al. 2015). It was not until more recently, however, that a significant role for glutamine metabolism has been shown in these tumours (Niklison-Chirou *et al.*, 2017), with glutamate concentration also being identified as a prognostic marker in MB patients (Wilson *et al.*, 2014). These data highlight the potential role of glutamine and glutamate in MB tumours, although not surprising given that glutamine metabolism has been shown as critical for normal tumour function in many different tumour types (Daye and Wellen, 2012). Furthermore, as a number of therapies are being trialled toward targeting glutamine metabolism, it is important to understand how its metabolism may be altered specifically in MB.

3.3.2 Genes involved with glutamine metabolism are altered in MB patient tumours.

The data presented investigate for the first time the expression of metabolic genes and their clinical consequences in MB patients. We noted that in all cases, expression of the glutamate uptake transporters EAAT1 (Figure 3.2.1) and EAAT2-4 (supplementary Figure 1) were reduced, while the neutral amino acid transporter SLC1A5, responsible for the transport of glutamine into tumour cells, was significantly increased. Furthermore, the expression of these transporters proved to be prognostic, with low EAAT1 and high SLC1A5 being predictive of a worse overall survival in MB patients (Figure 3.2.1). It has been previously shown that EAAT-2 expression is decreased in high-grade glial tumours when compared with normal brain or even low-grade astrocytomas (de Groot *et al.*, 2005). The

same group also revealed that EAAT-2 expression was inversely correlated with tumour grade. It is interesting therefore that we observed reduced EAAT expression in MB. Although we see reduced expression of EAAT-2, this does not correlate with survival in patients and only EAAT-1 and EAAT-3 expression affected clinical outcomes. It is no surprise that we observe heightened SLC1A5 expression as tumours typically favour glutamine uptake. SLC1A5 has been shown to be overexpressed in several tumours including, prostate (Carr *et al.*, 2010), colorectal (Huang, Zhao, *et al.*, 2014), aggressive subtypes of breast cancer (Kim *et al.*, 2013) and gliomas (Vastrad and Vastrad, 2018). Our data suggests that MB tumours prioritise glutamine uptake and subsequently utilise *de novo* glutamate synthesis rather than exogenous uptake.

We also investigated genes involved in glutamine catabolism (GLS1, GLS2 and GLUD1) and anabolism (GLUL) in MB tumours. GLS1 expression was highest in the SHH-MB subgroup when compared to the other three conventional groups, although when compared to normal cerebellum (CB) no expression differences were observed. Previous studies in colorectal tumours (Huang, Zhang, *et al.*, 2014) have shown increased expression of GLS1 in tumours compared to normal tissue, suggesting a role for GLS1 in cancer progression. Increased glutamine transporter expression and high glutamate concentrations reported *in vivo* (Wilson et al., 2014) may be expected to translate to enhanced GLS1 expression in MB tumours. Indeed, results obtained from the GEO repository (GEO: GSE42558) showed changes in GLS1 expression between MB and CB, although no significance was observed for GLS1 expression and patient survival in the Newcastle cohort. Despite this, using another online expression database (GEO: GDS4471) we show high expressing GLS1 patients have a

worse overall survival than low GLS1 expressing patients (Figure 3.2.2). Our proteomic data further reveal an importance of GLS1 expression in predicting survival (Figure 3.2.3).

We further show no expression changes in GLS2 in MB tumours when compared to normal cerebellum. This aligns with several other tumour types, with studies rarely finding GLS2 overexpression, including gliomas (Martín-Rufián *et al.*, 2014), liver and colon (Zhang *et al.*, 2013). It has been recently suggested that GLS2 has an important role in TAp73-expressing MB tumours. However, TAp73-overexpressing MBs only account for a fraction of these tumours, which may explain the differences in results between our groups.

GLUD1, which allows the NAD(P)+ dependent release of the amine group of glutamate to form αKG, is an important enzyme which contributes towards TCA anaplerosis. Our results revealed a striking and significant alteration in GLUD1, with decreased expression found in the SHH, Grp3 and Grp MB subgroups, which are have a more aggressive phenotype than the WNT group. We also observed decreased expression in MB tumours compared to CB, which interestingly held up as a prognostic indicator in patients, with low expressing patients having a significantly poorer overall survival (OS) compared to their higher GLUD1-expressing counterparts. The use of three independent databases helps strengthen our research, however, patient numbers in the GEO: GSE42558 repository are low (MB n=9 and CB n=4) and may therefore not be as convincing. The Newcastle cohort is much larger and therefore more robust, although normal cerebellar controls are lacking. Furthermore, here we present data as FPKM, although this may have been better presented as TMM (Trimmed mean of m values). We therefore suggest future experiments should use TMM as a quality control tool when plotting counts per gene.

Overall, our findings are novel and encouraging, yet more data will be needed truly appreciate expression patterns and consequences in MB tumours.

3.3.3 Medulloblastoma cells are dependent on glutamine for *de novo* glutamate synthesis.

The importance of glutamate metabolism has previously been demonstrated in gliomas, where extracellular concentrations are neurocytotoxic, allowing for the increased invasion of glioma cells (Ye and Sontheimer, 1999; Takano *et al.*, 2001). Despite this, no studies have focused on glutamate in MB tumour biology. It has been previously reported that MB cells may be glutamine addicted (Niklison-Chirou *et al.*, 2017). Our data further highlights the importance of this metabolite in MB, where we observed increased glutamine transporter expression in MB tumours and additionally demonstrated the requirement of glutamine for optimal cell line growth. Furthermore, we revealed the implications of glutamine catabolism in MB patient survival, with high glutamine turnover leading to worse clinical outcomes. The shift towards increased glutamine metabolism has also been implicated in ovarian tumours (OVCA), with glutamine dependent tumours being more invasive than their glutamine-independent counterparts (Yang *et al.*, 2014). The same group also correlated heightened glutaminolysis with poor survival in OVCA patients, suggesting this mode of analysis may be useful in a number of tumours. We further investigated the relative glutamine turnover between our MB cells lines by incubating them with ^{13}C-U-glutamine for 24 h and investigating carbon incorporation into central carbon metabolites. We found that the DAOY line was the most glutamine dependent cell line, with the highest ^{13}C label incorporation detected in every glutamine-derived metabolite measured. Glutamine could be considered an ‘essential amino’ acid in cancer biology, given its central role in supporting proliferation.

Thus, our observations that MB cells are glutamine addicted are not surprising. We show here however that glutamate is unable to rescue cellular growth upon glutamine starvation, which aligns with our data showing low glutamate import potential in MB tumours, but suggests that glutamine use in these tumours may not be as simple as a requirement for growth. It is important to note that dimethyl glutamate - upon removal of the methyl groups within the cell – can result in the production of methanol, which may be toxic to cells. Therefore, it may be this reason why we do not observe a rescuing phenotype with this treatment.

MB cells may also be particularly reliant on *de novo* glutamate biosynthesis because glutamate, unlike other amino acids, does not efficiently cross the BBB into the CNS (Smith, 2000; Hawkins, 2009). Our data show that through glutaminase inhibition, due to specifically its effect on the GLS1 enzyme (not GLS2) significantly impacts on MB cell line growth. We suggest that *de novo* glutamate synthesis is essential in these cells. Glutamine acts as a "nitrogen reservoir" for cancer cells due to its role in nucleotide synthesis and it may be this property that makes glutamine so important in MB, although we did not explore this in our cell line models. Furthermore, we have not investigated the fate of ammonia in MB, where it is a by-product of GLS activity. Ammonia is commonly thought of as a toxic product of glutaminolysis, but has since been shown to be utilised in cancer cell growth (and therefore may have interesting implications for MB). Glutamine synthetase (GLUL) is an ATP-dependent enzyme which catalyses the condensation of ammonium to glutamate, resulting in glutamine synthesis. In many cancers, the intricate equilibrium between glutamine anabolism and catabolism is vital. For example, reduced GLUL activity has been associated with a more invasive and aggressive phenotype in some cancers. However,

conflicting results have been shown in glioblastoma, where GLUL expression was identified as a negative growth regulator (Yin *et al.*, 2013), yet high GLUL expression has also been reported under reduced glutamine concentrations (Tardito *et al.*, 2015). Our data reveal low GLUL expression and activity in MB, which may suggest a lower demand for glutamine-derived nucleotide synthesis. On the other hand, this may also reflect the sustained increase in glutamine availability in these tumours, thus rendering GLUL obsolete. We suggest that although potentially important for nucleotide synthesis, glutamine is needed for biosynthesis of glutamate, which has several downstream fates in MB.

3.3.4 Glutaminase 1 is the preferred isozyme under basal conditions.

The relative activities of GLS isozymes have been reported in several tumours, where GLS1 has been shown to be highly expressed in tumour cells, aiding proliferation and oncogenic transformation. GLS2, however, is commonly down regulated in tumours and is often described as tumour suppressive (Xiang et al, 2013). It is important to note that this does not apply to all tumour types, and therefore the role of GLS2 in tumorigenesis is unclear. Our results align with these common findings, where we show the expression of GLS1 is far higher than GLS2 in all three MB cell lines. Furthermore, when labelled with ^{13}C-U-glutamine, the labelled pool of glutamate was only significantly decreased after GLS1 knockdown, while we observed no changes in labelled glutamate upon GLS2 knock-down. Our results suggest that under basal conditions, GLS1 activity is higher than GLS2, and was the main determinant of *de novo* glutamate synthesis. The transcription of GLS1 can result in two splice variant products, GAC or KGA. Despite the significant research focus on glutaminases, relatively few of these studies take in to account variations in GAC and KGA in the setting of cancer biology. Our data show clearly the relative expressions of the KGA and

GAC splice variants in MB cell lines, where GAC represents the major splice variant at both mRNA and protein expression levels. As the difference between expression is significantly more enhanced at the mRNA level, it suggests that there is differential regulation of mRNA processing between variants.

3.3.5 Differences were observed in the localisation of GLS1 variants KGA and GAC

Glutaminases are typically referred to as a mitochondrial enzymes, however, more recently it has been shown in breast, prostate and lung cancer cell lines that specific variants of GLS also exist in the cytosol (Cassago *et al.*, 2012). The data presented here show that the GLS1 variants demonstrate different sub-cellular localisations, with KGA predominantly localising in the cytosol, while GAC is typically observed in the mitochondria, with low expression also visualised in the cytosolic fraction of the DAOY cell line. Glutaminases are more complex than previously assumed, with protein structures containing additional motifs and functional domains independent of enzymatic abilities. Both KGA and GAC variants harbour transit peptides which direct them to the mitochondria, yet despite this, our results show cytosolic localization of the KGA variant. The differences observed between GLS variants may be caused by dissimilarities in their C-terminal in which they have 12% sequence homology. It has been predicted that KGA contains three ankyrin repeats, allowing for protein-protein interactions (Li, Mahajan and Tsai, 2006). Cassago and co-workers, through structure-based biochemical techniques, have identified five amino acids in the end sequence of KGA as potentially being a second NR box motif (Cassago *et al.*, 2012), which may further account for differences seen between GLS variants.

GAC activity has been implicated more frequently than KGA in tumours, where overexpression of this enzyme have been detected in gliomas (Szeliga *et al.*, 2008), breast cancer (Elgadi *et al.*, 1999), adenomas and colorectal carcinomas (Turner and McGivan, 2003). It has also been shown that GAC inhibition represses oncogenic transformation (Wang *et al.*, 2010), suggesting that GAC is the main glutaminase variant in tumours. However, there has not been sufficient research to distinguish the key differences between KGA and GAC, which will be crucial in our understanding of tumours. Our data supports the hypothesis that GAC is key in tumourigenesis, through its direct support of cell proliferation in two of the MB cell lines. We further show, through the use of ^{13}C labelled glutamine that siGAC reduced label incorporation into several metabolites to a greater extent than siKGA, indicative of increased GAC contribution to these metabolite pools. However, the metabolites detected by our GC-MS are predominantly TCA cycle intermediates and therefore are synthesised in the mitochondria, thus, making it difficult to distinguish between mitochondrial and cytosolic reactions. Despite this, labelling into citrate allows us to distinguish between reductive and oxidative metabolism, where reductively synthesised citrate from 13C-U-glutamate would yield m+5 labelling (directly from α-KG), while other labelling patterns would reflect oxidative TCA activity. Reductive carboxylation of α-KG to form citrate may occur both in the mitochondria and cytosol, depending on the Isocitrate dehydrogenase (IDH) isoform used. It is therefore interesting to see no significant changes when comparing siGAC and siKGA and could potentially indicate an increased use of KGA in the reductive production of citrate, in the cytosol. We suggest that mitochondrial located, GAC may be more important in TCA anaplerosis, while KGA may be responsible for (but not restricted to) controlling cytosolic concentrations of glutamate and its subsequent reactions. We were unable to comprehensively distinguish cytosolic reactions in this project, although

our collaboration with Dr. Jurre Kamphost will allow us to measure the effect of GLS1 variant knockdown on cytosolic specific reactions. One such reaction of importance which occurs almost exclusively in the cytosol (Although the synthesis of mitochondrial GSH has also been shown (Lluis *et al*, 2005) is the synthesis of GSH. Although unproven, we hypothesise that KGA may be more responsible in the synthesis of GSH, and thus its activity may be increased under conditions of stress. We will explore this further in the following chapter.

3.3.6 The importance of proline biosynthesis in MB tumours

We observed increased expression of the biosynthetic genes (ALDH18A1, PYCR1 and PYCR2), suggestive of enhanced capacity for proline biosynthesis from glutamate. We also found decreased PRODH expression, which is required for the breakdown of proline, and thus strengthens the notion that MB tumours favour proline anabolism. Amplified proline biosynthesis from glutamate may offer a way in which to remove excess mitochondrial glutamate, and aligns with the observation of decreased GLUD1 expression in MB patient tumours. The synthesis of proline also offers a reducing potential from NADH or NADPH to P5C, therefore allowing cells to support redox homeostasis, a vital process in rapidly dividing cells.

Blood to brain transport of arginine, mediated by cationic acid transporter 1 (CAT1), makes it the most abundant amino acid in the brain (Smith, 2000). Nitric oxide (NO) is synthesized from arginine by NO synthase (NOS), and the availability of arginine is one of the rate-limiting factors in cellular NO production. The role of NO in cancers is predominantly unknown, although the importance of arginine itself has been extensively studied. Arginine can be hydrolysed by ARG1 or ARG2 to ornithine, which subsequently may be converted to

proline through ornithine aminotransferase (OAT) activity, which transaminates alpha-ketoglutarate to form glutamate as a byproduct. It has previously been shown that ARG2 is amply expressed in MB tumours, with the downstream metabolite of arginine - polyamine, playing an important role in these tumours (Vardon *et al.*, 2017). We, however, show that ARG1 expression is decreased in MB tumours and the low expression conveys a worse outcome in patients (Figure 3.2.20), suggesting arginine may not be actively used in the biosynthesis of proline in these tumours. This is further highlighted by the fact that our MB cell lines do not require arginine for growth (data not shown). Through competing ^{13}C-tracer experiments, we demonstrated this in the MB cell lines by revealing how arginine is unable to contribute toward proline biosynthesis, despite using relatively high concentrations of arginine (Figure 3.2.19). When ornithine was used as a competing metabolite for ^{13}C-U-glutamine, however, we see a significant reduction in ^{13}C labelled proline (glutamine-derived), suggestive of increased ornithine-derived proline biosynthesis. We might expect the cells to utilise arginine, where this biosynthetic pathway is also beneficial for the circumvention of urea production. However, we found that the MB cell lines (and potentially MB tumours) have reduced ARG1 activity, which could be a way of circumventing ornithine-derived production of proline and preferentially use glutamate-derived proline synthesis to circumvent increased concentrations of mitochondrial glutamate.

Furthermore, we show that the addition of exogenous proline decreases growth in all three cell lines in a concentration dependent manner. We suggest the addition of exogenous proline reduces PYCR activity, reducing proline biosynthesis in our cell lines, which has been previously been shown to be the case in melanoma (de Ingeniis *et al.*, 2012). As a large

source of proline in our cell lines, we would expect glutamate concentrations to increase as a result of reduced proline biosynthesis, which is what we observe when cells are fed with ornithine. We propose this affects the concentration of glutamate, the control of which may be an important mechanism to maintain tumour growth of MB.

Interestingly, de Ingenis et al, showed that PYCR1 contributes predominantly towards glutamate-derived proline synthesis, but may also catalyse ornithine to proline, while PYCR2 is used exclusively for biosynthesis of proline from glutamate (de Ingeniis *et al.*, 2012). Our data suggest that PYCR2 expression – but not PYCR1 – is predictive of survival in MB patients, suggesting that these substrate differences in PYCR isoforms may be important in MB biology (i.e. MB tumours might prefer PYCR2 as it catalyses glutamate to proline). They further showed that PYCRL participates only in production of proline from ornithine. These data support our own, but also highlight gaps in our research, as we did not distinguish between PYCR enzymes in this study. PYCRL is a cytosolic enzyme, which converts ornithine but not glutamate to proline. We would therefore expect this isozyme to have little effect on glutamate-derived proline synthesis.

The export of proline in tumours has also been shown to have a wider acting role, and may be an important and dynamic process in tumour progression (Fang *et al.*, 2014). We observed labelled pools (predominantly m+5) of proline in the media of all three cell lines, when labelled with ^{13}C-U-glutamine. Our results suggest that MB cell lines produce proline in amounts surpassing biomass requirements and excretion could be acting to remove excess glutamate and NADH. Collagen in the extracellular matrix (ECM) is predominantly comprised of proline residues, and may serve as a controlled source for proline (Phang *et al.*, 2015). We have previously shown that exogenous proline may impact MB cell growth,

thus depositing proline into collagen could be advantageous to these tumours by reducing extracellular concentrations. It has been suggested that this may also be a route of survival in quiescent cancer cells, with many formed products being deposited as ECM collagen (Valcourt *et al.*, 2012). Increased collagen deposition and remodelling produces a restructured microenvironment able to support tumour progression by destabilizing cell–cell adhesion and cell polarity, and has even been shown to augment growth factor signalling (Paszek *et al.*, 2005). Continued collagen remodelling may also induce changes in gene expression, proliferation, cell differentiation, migration (Fang *et al.*, 2014) and has been linked with treatment resistance in ovarian cancer (Januchowski *et al.*, 2016). Therefore, our observation of intricate collagen networks within patient tumours (Figure 3.2.22) may have significant implications in MB. More research will be needed to explore this, for instance, although we show general collagen deposition, we did not classify the collagen type. Collagens can be divided into separate 'types', where type I-X are described as a fibrillar class. Type XII and type XXI collagens are fibril associated collagens with interrupted triple helices class. Type XV collagen belongs to the multiple triple helix domains with interruptions class, and type XVII collagen belongs to a class of membrane associated collagens with interrupted triple helices. Different collagen types can have separate roles in cancer biology (Januchowski et al., 2016), thus their classification in MB could be important.

3.3.7 MB cells inhibit GABA synthesis and GABAergic properties.

After finding MB cells lines may synthesise proline as a way of reducing concentrations of potentially excitotoxic glutamate, we hypothesised that these tumours may also use GABA synthesis in a similar fashion. Surprisingly however, we find MB tumours significantly reduce the expression of the main enzyme involved in GABA biosynthesis from glutamate, GAD1.

These data disagree with our previous hypothesis, but present an interesting finding as GABA metabolism is being increasingly studied in the setting of cancers. GABA has been implicated in the proliferation (Takehara *et al.*, 2007), differentiation (Liu *et al.*, 2009), and migration (Shankar and Brastianos, 2014) of cancer cells. Amplified GAD activity and subsequent GABA concentrations have been reported in breast cancer (Shankar and Brastianos, 2014), colon cancer (Miao *et al.*, 2010), gastric cancer (Matuszek, Jesipowicz and Kleinrok, 2001) ,prostate cancer (Christopher, 2011), and glioma (Smits *et al.*, 2012; Pallud *et al.*, 2014). Our results reveal a prominent effect of GABA in MB, with GABA biosynthesis being reduced in MB cell lines and GABA biosynthetic and GABAergic genes being downregulated in MB tumours. Separate to its role in neurotransmission, GABA via GABA-A receptors can negatively regulate proliferation of pluripotent and neural stem cells in adult and embryonic tissue (Young and Bordey, 2009). We further show that the addition of exogenous GABA reduces the growth of the UW228.3 cell lines, suggesting these cells retain GABAergic characteristics. The ONS-76 and DAOY cell lines did not elicit the same response, which may be a consequence of reduced GABA receptors and transporters, reflecting the low mRNA expression levels observed in MB tumours. This negative effect on stem cells growth may reveal why MB tumours may be selected to reduce concentrations of reactivity to this metabolite/ligand, and we suggest that MB tumours and cell lines may reduce GABA concentrations to prevent negative growth/differentiation effects elicited by this metabolite.

3.3.8 Glutamate exported is coupled to cystine import, via SLC7A11 anti-porter activity.

The export of glutamate has been studied in the setting of cancers, where several tumours have been shown to release high concentrations of glutamate (Ye and Sontheimer, 1999;

Seidlitz *et al.*, 2009; Fazzari *et al.*, 2015). One of the best studied tumour for the release of glutamate is glioblastoma, where studies have implicated extracellular glutamate with increased uptake of cystine via the SLC7A11 antiporter (Huang *et al.*, 2005), increased invasion through paracrine glutamate signalling (Piao, Lu and de Groot, 2009), and exported glutamate has more recently been shown to alter tumour associated macrophages (Choi *et al.*, 2015). We found that the DAOY cell line exports glutamate at a concentration almost 4-fold higher than the ONS-76 and UW228.3 cell lines, yet intracellular concentrations are relatively equal. The enzymatic properties of glutaminase may suggest one benefit to the heightened release of glutamate in DAOY cell line. GLS1 is potently inhibited by glutamate, thus, reduced intracellular glutamate as a result of glutamate export could increase GLS1 activity, which may help achieve higher glutamine anaplerosis. We do in fact see heightened glutamine flux into TCA metabolites in the cell line. This fits with our previous hypothesis that MB cell lines utilise proline biosynthesis as a means of removing mitochondrial glutamate, thus multiple mechanism may be involved in maintaining an ideal intracellular concentration of glutamate in MB, while also being utilised in potentially vital pathways.

Similar to research conducted in glioblastoma, we observe that glutamate export is coupled with cystine import, suggesting a role for the glutamate/cystine antiporter in MB. The inhibition of SLC7A11 with SSZ resulted in reduced MB cell line growth, suggesting an importance of this anti-porter in MB cell biology. However, the use of SSZ has been previously shown to target several other pathways and thus, the reduced cell growth observed may not be dictated solely by SLC7A11 inhibition. Despite this, the use of SSZ in the treatment of cancers have been demonstrated, where SSZ use in glioblastoma has potential for avoiding or greatly reducing temozolomide-associated toxicity in patients

(Ignarro *et al.*, 2016), suggesting this treatment may be important in other SLC7A11 expressing tumours. We explore the role of SSZ in MB treatment resistance in the following chapter.

3.3.9 Potential advantages of glutamate export in MB, In addition to cystine import.

Our previous data reveal low expression and activity of GLUL, where as a result, cells may be more susceptible to decreases in glutamine concentrations. We have indeed shown in our *in vitro* cell line models that this is the case. One way in which cancer cells have been shown to circumvent this is through the acquisition of glutamine from surrounding stromal cells, with cell of the tumour microenvironment being shown to increase their expression of GLUL (Castegna and Menga, 2018). The release of tumour-derived glutamate has previously been reported to be taken up by stromal cells and subsequently converted to glutamine via GLUL activity (Ye and Sontheimer, 1999). The release of glutamine can subsequently be utilised by tumour cells (Ko *et al.*, 2011). This glutamate-glutamine recycling event allows tumours to sustain a high degree of glutamine uptake, while exporting potentially cytotoxic concentrations of glutamate. This is also particularly important for the heightened glutaminolysis and glutamate exchange for cysteine via SLC7A11.

3.3.10 Summary

In this chapter we highlighted how the expression of certain metabolic genes could impact MB biology. We further built on this information through the use of several *in vitro* techniques to pull apart to importance of glutamine and glutamate, along with other key

metabolites interlinked. We have shown that MB cells require glutamine to sustain optimal growth and the rate in which they utilise glutamine may reflect tumour aggressiveness and may well be prognostic in MB patients.

MB cells have heightened glutamine uptake, of which they subsequently rely on GLS1 for the biosynthesis of glutamate. We have highlighted several potential roles of glutamate in MB, which significantly supports previous *in vivo* data showing glutamate as a prognostic marker (Wilson *et al.*, 2014). In addition to supporting these data, we show the majority of glutamate detected in MB tumours is likely to be extracellular (micro environmental), which may have important clinical consequences.

The tight regulation of intracellular glutamate concentrations are important due to the cytotoxic nature of this metabolite, especially in the brain. We have shown how proline may be an important metabolite in which MB cells use to divert these unwanted excess concentrations. Furthermore, this makes the lack of GABA synthesis interesting where we suggest further research into this metabolite may yield beneficial results for MB.

Chapter 4

Interfering with Glutamate metabolism to further therapeutic options in Medulloblastoma

4.1 Introduction

Whilst the molecular understanding of medulloblastoma has increased greatly in recent years, the translation of this into advances in the treatment of patients with MB have been underwhelming, with surgery, postoperative radiation therapy (RT) and chemotherapy remaining the standard of care (Fossati, Ricardi and Orecchia, 2009). The lack of progress in the development of novel targeted treatments is in part- due to the large proportion of patients that are cured with such therapies, with approximately three-quarters of patients with standard risk disease and around 60% of those with metastatic disease achieving long-term survival (5 or more years). Although these survival rates have increased dramatically over the last few decades, recent improvements have been small and long-term toxicities in survivors is limiting the prospect of intensifying treatment further. Extent of resection is significantly associated with survival in patients with glioblastoma (Lacroix *et al.*, 2001). However, this does not appear to be the case in MB, where a study conducted in 787 patients showed no such correlation of overall survival (OS) or progression-free survival (PFS) when comparing gross total resection with near-total resection (Thompson *et al.*, 2016). This places further emphasis on postoperative radiation and chemotherapy as being key to successful treatment. However, treatment-related toxicities are a significant problem with these therapies, occurring in a large proportion of long term survivors, resulting in a profound deterioration of quality of life (Packer and Vezina, 2008). Several forms of cognitive impairment have been identified in these patients, owing to the disruption of the normal developmental process of the growing brain (Mabbott, 2006). This has, in part, been circumvented by dividing patients into risk categories and reserving high dose radiation and chemotherapy to those patients deemed to be high-risk, while reducing such treatments in

low-risk patients, thereby ensuring decreased toxicities while maintaining high treatment efficacy. Therefore, there is need for alternative approaches to treating these tumours.

Metabolic transformation is a hallmark of tumour biology and may offer potential targets for novel therapies. Since Otto Warburg's observation of increased lactate production in aerobic conditions in cancer cells (Warburg, 1925), significant studies, including clinical trials, have examined the effectiveness of blocking this metabolic pathway to reduce tumour growth, or as a means to sensitising tumours to existing treatment. Such effects have been directed towards inhibiting metabolic phenotypes such as increased glucose uptake (Liu *et al.*, 2012) and tumoural glycolysis (Pelicano *et al.*, 2006). However, a significant problem with these therapies lies in the non-specific nature of targeting glycolysis, highlighting the need for more specific metabolic pathway targeting approaches.

Alongside glucose, glutamine is a critically required nutrient in most if not all tumours. Both are crucial in order to fulfil two essential requirements in proliferating tumour cells. Firstly, ATP production, which is needed for cellular bioenergetics (Le *et al.*, 2012) and secondly, they both provide intermediates for the synthesis of macromolecules (Stumvoll *et al.*, 1999). Glutamine additionally serves as a vital source of nitrogen for amino acid and nucleotide synthesis, and is central to the synthesis of glutathione, a major anti-oxidant couple, and without which cells rapidly die. Indeed, glutathione is central to protection of cells from cytotoxic therapy (Matés *et al.*, 2002). The multiple critical metabolic pathways that glutamine feeds therefore highlights its importance in tumour biology, and specifically the resistance of tumours to certain therapies.

This is underlined by the fact that glutamine use can be predictive of aggressiveness in several tumours, including ovarian (Yang *et al.*, 2014), pancreatic (Son *et al.*, 2013) and

colorectal cancer (Hao *et al.*, 2016). Despite our growing understanding of the role of glutamine in cellular anti-oxidative protection, relatively little progress has been made clinically in targeting its metabolism.

It has previously been shown that cancer cell lines are sensitised to glutamine starvation, including cells derived from small cell lung carcinoma, glioblastoma multiforme and acute myelogeneous leukemia (Wu, Arimura and Yunis, 1978). Glutamine analogues including 6-diazo-5-oxo-L-norleucine (L-DON), azaserine, and acivicin have also been used with varying degrees of success. Preclinical testing of each of these agents displayed significant cytotoxicity in specific tumour types, both in cell lines and in mouse xenograft models (Ahluwalia *et al.*, 1990). Other efforts have been directed towards suppressing glutamine uptake in tumour cells (Fuchs and Bode, 2005), or blocking glutamine-dependent anaplerosis (Thornburg *et al.*, 2008)

In this chapter we explore the impact of inhibiting glutamine and glutamate metabolism in MB cell lines, by means of siRNA knockdowns and compound inhibition. We investigate how this inhibition may affect cell survival and whether or not this may increase the efficacy of treatment in our *in vitro* cell line models.

4.2 Results

4.2.1. Resistance to treatment varies between MB cell lines

We previously observed (chapter 3) that MB cell lines have varying degrees of glutamine dependency. We therefore, hypothesised that these metabolic differences may lead to differential resistance to treatment in our cell lines. To test this, we carried out dose response studies on all three cell lines, using three distinct cellular stressors – gamma irradiation, hydrogen peroxide and cisplatin treatment. Using an SRB assay to quantify the change in cell viability elicited by treatments, we found that the DAOY cell line

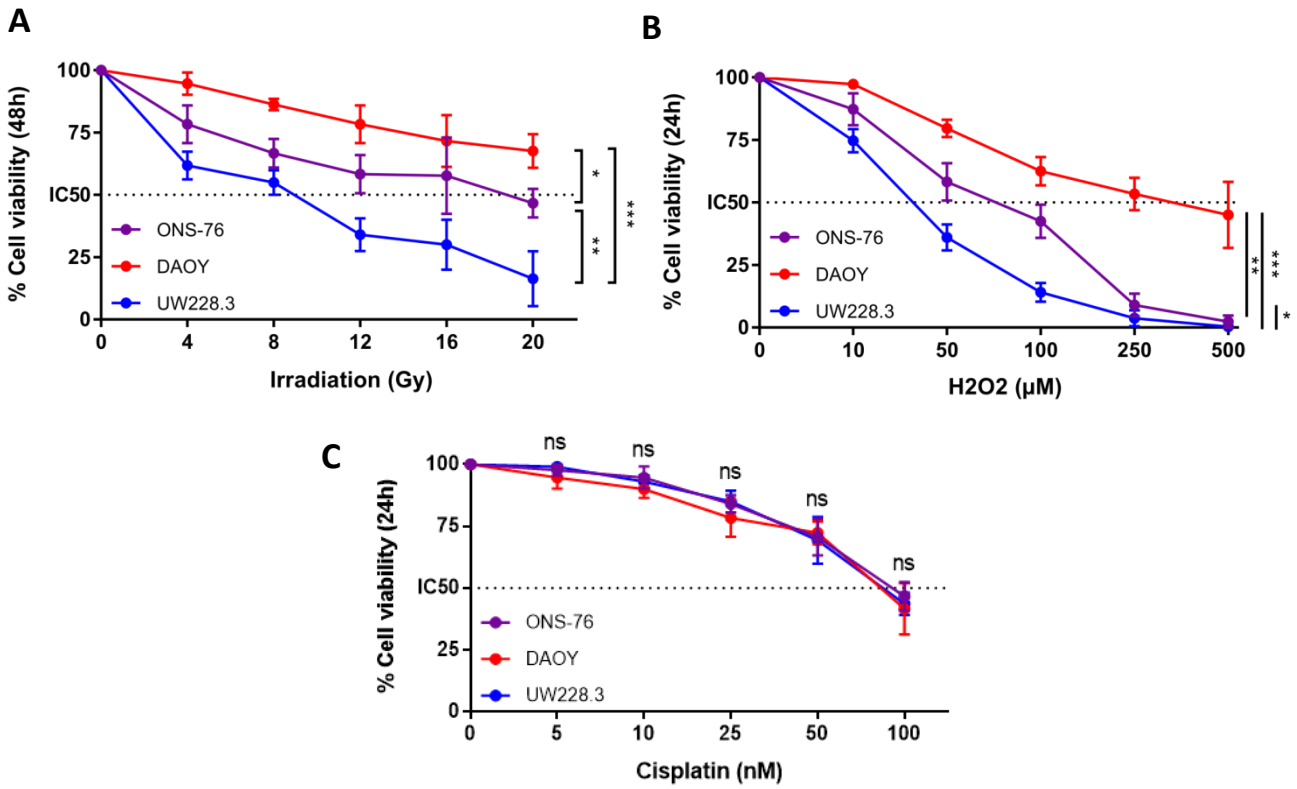

Figure 4.2.1 Medulloblastoma cell lines have varying degrees of treatment resistance. SRB viability assays of ONS-76, DAOY and UW228.3 cell lines when irradiated (0-20Gy), treated with hydrogen peroxide (0-500µM) and Cisplatin (0-100 µM). Cells were then fixed after 24h and assessed for viability. Data presented as mean ±SEM representative of three separate experiments. Significance was determined by performing a one-way ANOVA with Tukey post-hoc test in Graphpad; *p<0.05, **p<0.01, ***p<0.001, ****p<0.0001

demonstrated the highest resistance to irradiation and H_2O_2, with IC50s of; undetermined Gy and 375μM, respectively (figure 4.2.1). ONS-76 cells showed intermediate treatment resistance, while, the UW228.3 cell line was the most sensitive. Interestingly, there was no differential sensitivity observed between cell lines and treatments suggesting that relatively few; perhaps even a single mechanism of resistance was being used by the MB cells.

4.2.2 Starving MB cell lines of glutamine sensitises them to treatment

Our previous findings that MB cell lines require glutamine to sustain competent growth led us to hypothesise that glutamine may also be required for cellular survival. To better understand glutamine dependence in this setting, we investigated MB cell line sensitivity to cisplatin and hydrogen peroxide treatment, under glutamine sufficient and glutamine-deprived conditions. We found that after 12 hours of glutamine starvation, all three MB cell lines became increasingly sensitised to both cisplatin and hydrogen peroxide treatment, with the DAOY cell line showing the largest dependency on glutamine for treatment resistance. This significance was confirmed by two separate assays, an SRB cell viability assay (Figure 4.2.2.A) and with an AnnexinV/PI flow cytometry apoptosis assay (Figure 4.2.2.B). We therefore demonstrated that glutamine is essential for a successful response to cytotoxic agents in the MB cell lines.

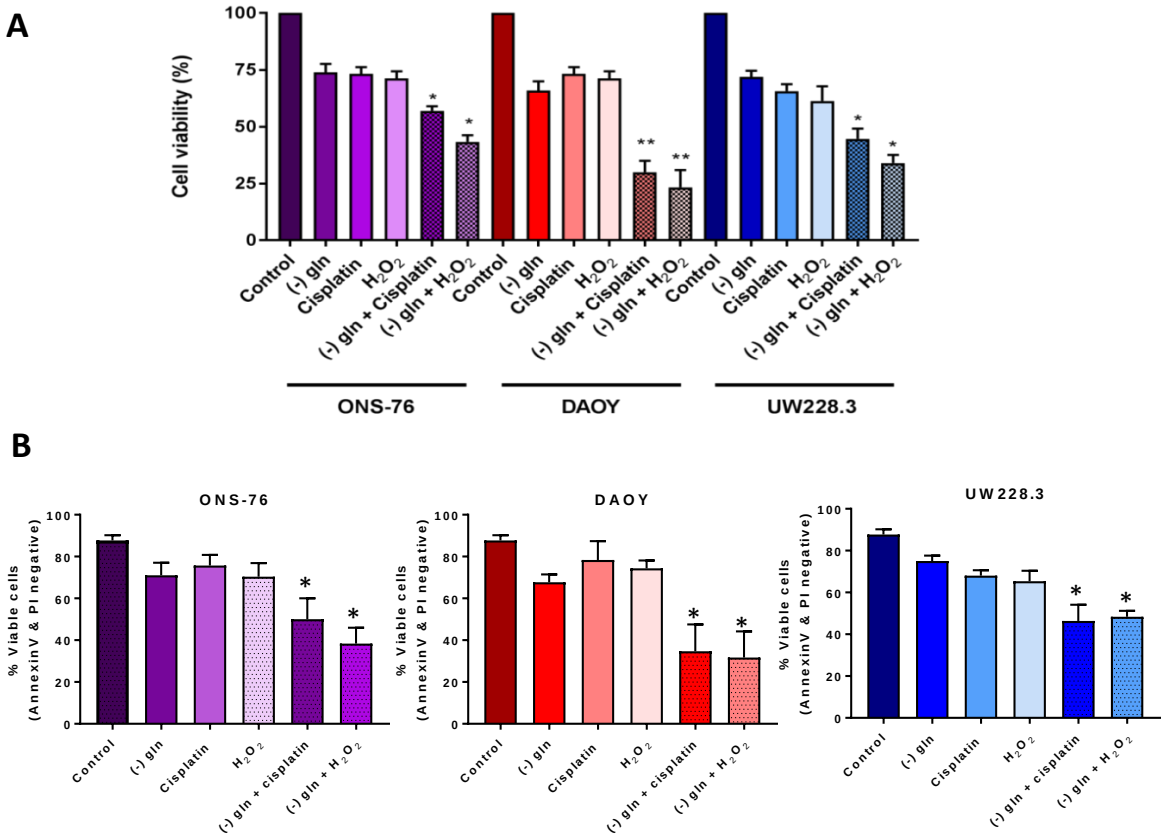

Figure 4.2.2. Glutamine starvations sensitises MB cell lines to treatment. A) An SRB viability assay was carried out to determine the effectiveness of glutamine deprivation on ONS-76, DAOY and UW228.3 cell lines. Cells were cultured in 0mM glutamine for 12h prior to being treated with DMSO, hydrogen peroxide and cisplatin. B) Cell death was further examined using a flow cytometry AnnexinV/PI assay. Cells were cultured in 0mM glutamine for 12h prior to being treated with DMSO, hydrogen peroxide and cisplatin. Data presented as mean ±SEM representative of three separate experiments. Significance was determined by performing a one-way ANOVA with Tukey post-hoc test in Graphpad; *p<0.05, **p<0.01, ***p<0.001, ****p<0.0001.

4.2.3 *De novo* glutamate synthesis drives treatment resistance

After our finding that glutamine is important in the protection against cytotoxic agents, we investigated whether this was driven through the *de novo* production of glutamate. To achieve this, we knocked down the major glutaminase isozyme - GLS1 – and treated with cisplatin or gamma irradiation. These two agents were chosen as they are both very relevant treatments for MB patients. Using an SRB assay, knockdown of GLS1 revealed an increased sensitisation to cisplatin (Figure 4.2.3 A) treatment in the DAOY and UW228.3, similarly to

that seen under glutamine starvation. However, in the ONS-76 cell line, siGLS1 did not sensitise to treatment when assessed by an SRB assay. Knockdown of GLS1 only revealed an increased sensitisation to and irradiation in the UW228.3 line (Figure 4.2.4 A). Furthermore, in contrast to the glutamine depletion experiment, the UW228.3 cell line showed the largest effect, rather than the DAOY cell line.

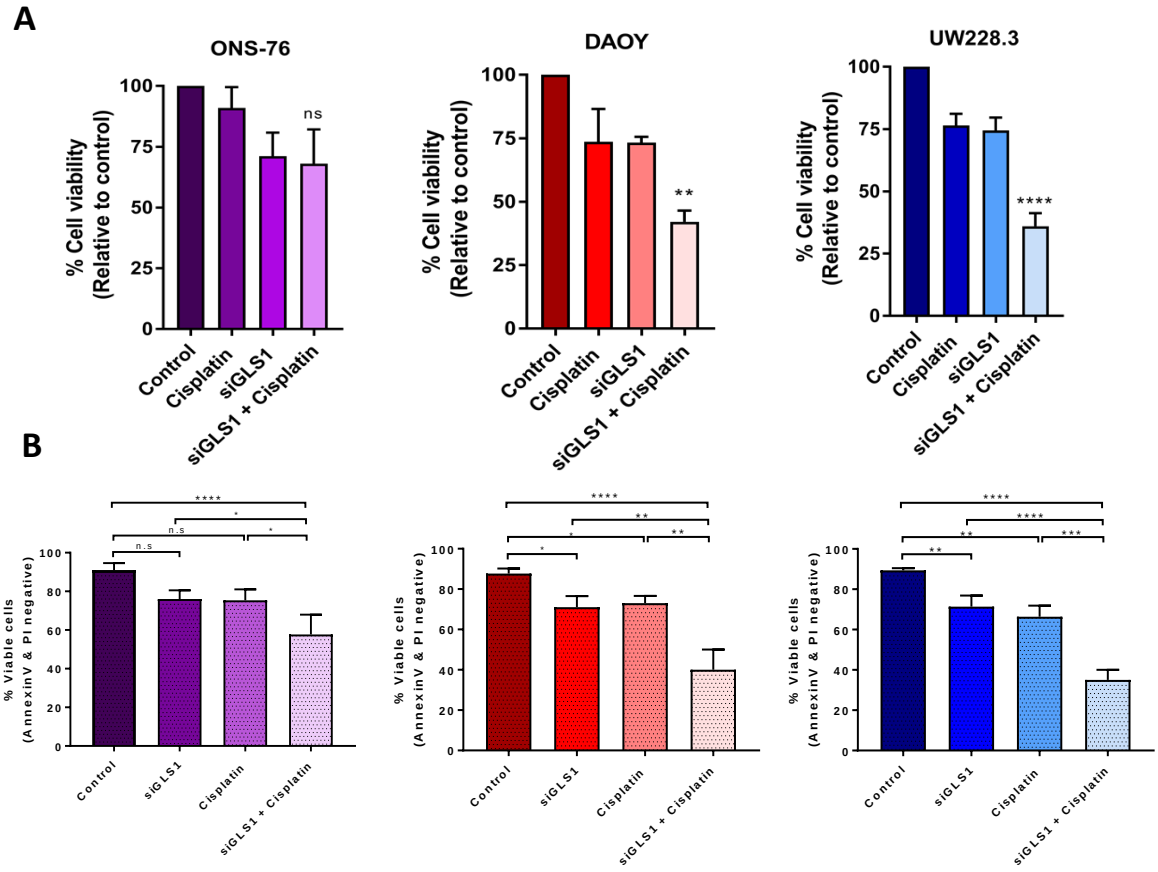

Figure 4.2.3. Knockdown of GLS1 leads to increased cytotoxicity of cisplatin in MB cell lines. A) An SRB viability assay was carried out to determine the effectiveness of GLS knockdown on ONS-76, DAOY and UW228.3 cell lines. Cells were treated with siNT, siNT+cisplatin, siGLS1 and siGLS1+cisplatin. Knockdown of GLS1 decreased the cell viability of all three cell lines to cisplatin treatment. B) Cell death was further examined using a flow cytometry AnnexinV/PI assay. Data presented as mean ±SEM representative of three separate experiments. Significance was determined by performing a one-way ANOVA with Tukey post-hoc test in Graphpad; *p<0.05, **p<0.01, ***p<0.001, ****p<0.0001

The magnitude of the cell death response measured using the SRB assay was examined using an alternative, direct measure of loss of cell viability – annexin V/PI staining of cell and analysis through flow cytometry. A significant reduction of cell viability (in all three lines) was observed using this assay, after either cisplatin or irradiation treatment (Figure 4.2.3B and 4.2.4B).

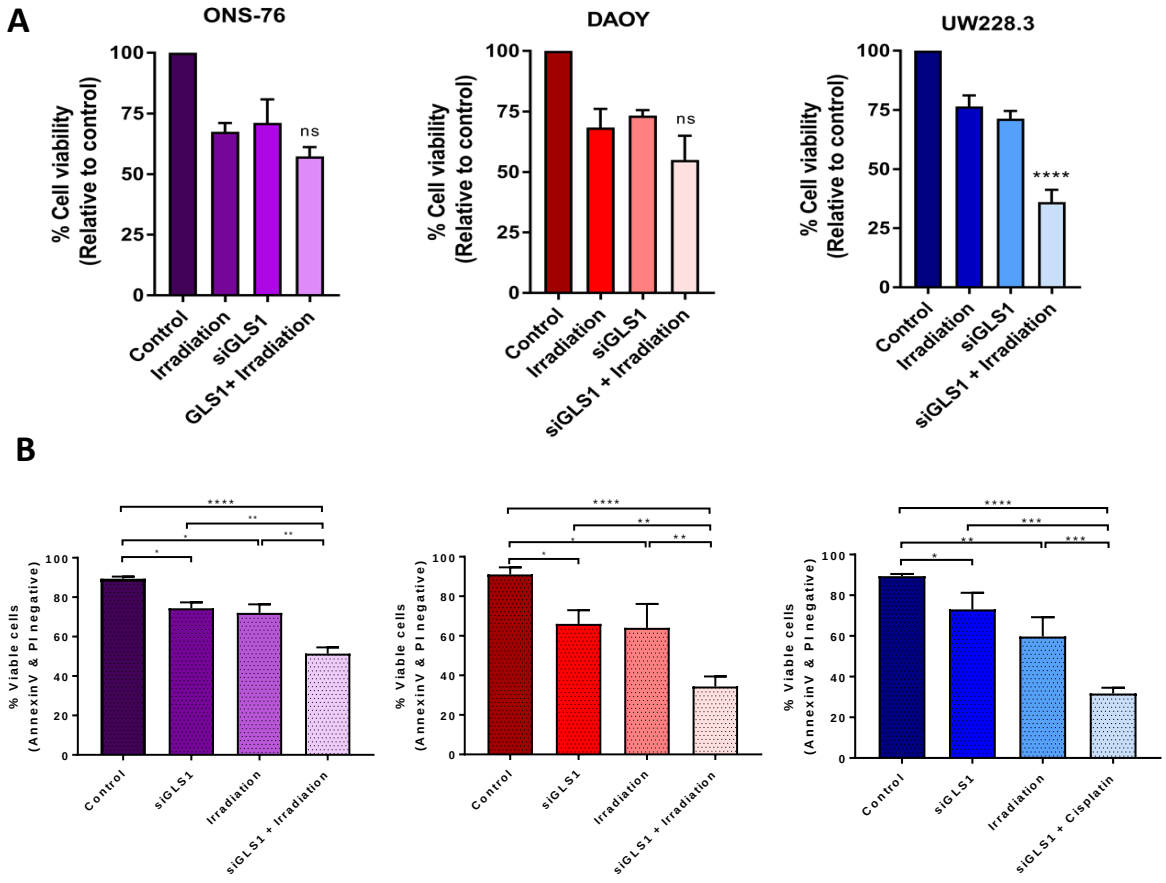

Figure 4.2.4 Knockdown of GLS1 leads to increased cytotoxicity of irradiation treatment in MB cell lines. A) An SRB viability assay was carried out to determine the effectiveness of GLS knockdown on ONS-76, DAOY and UW228.3 cell lines. Cells were treated with siNT, siNT+10Gy Irradiation, siGLS1 and siGLS1+10Gy Irradiation. Knockdown of GLS1 decreased the cell viability of all three cell lines to irradiation treatment. B) Cell death was further examined using a flow cytometry AnnexinV/PI assay. Data presented as mean ±SEM representative of three separate experiments. Significance was determined by performing a one-way ANOVA with Tukey post-hoc test in Graphpad; *p<0.05, **p<0.01, ***p<0.001, ****p<0.0001

4.2.4 GLS1 maintains redox balance through synthesis and maintenance of glutathione

Glutamate is the major precursor of glutathione synthesis, being both a substrate of the tripeptide, and a necessary component for the synthesis or import of the other two amino acids required – cysteine and glycine. Therefore, we measured isotopic label incorporation from ^{13}C-U-glutamine into both reduced glutathione (GSH) and oxidised glutathione (glutathione disulphide; GSSG) using liquid chromatography- mass spectrometry (LC-MS) in the ONS-76 cell line, in collaboration with Dr. Jurre Kamphorst (University of Glasgow, UK). The mass isotopomer distribution (MID) of GSH using labelled glutamine revealed a significant reduction of labelled GSH when GLS was knocked down, with a reduction of over 50% seen for the m+5 isotopomer (representative of the incorporation of a single glutamate molecule into GSH; Figure 4.2.5.A) and a smaller, yet significant reduction seen for the m+5 & m+10 isotopomer for GSSG (the incorporation of one [m+5] or two [m+10] glutamate molecules into GSSG). We also investigated the redox status of the ONS-76, DAOY and UW228.3 cell lines upon siNT or siGLS1, a marker of which is the GSH/GSSG ratio (Figure 4.2.5.C). A decreased ratio of reduced GSH to GSSG was observed siGLS1, confirming that GLS1 is important for maintaining the cellular protection against oxidative stress in MB cell lines (Figure 4.2.5.D).

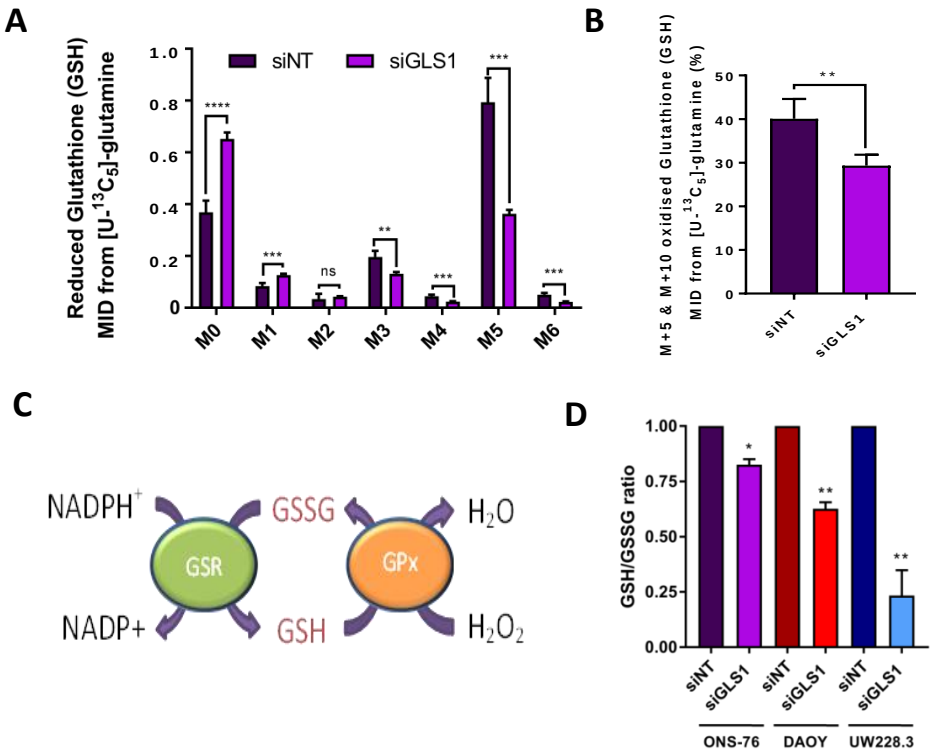

Figure 4.2.5. Knockdown of GLS1 leads to decreased glutathione synthesis and reduces the GSH/GSSG ratio in MB cell lines. A) Analysis of the mass isotopologue distribution (MID) of reduced glutathione after treatment with H_2O_2 treatment in the ONS-76 cell line only. Mass isotopomers (m+0, m+1, m+2, m+3, m+4 and m+5) correspond to ion fragments containing different ^{13}C atoms. Alterations in reduced glutathione labelling after H_2O_2 treatment are present in the DAOY and UW228.3 cell lines. B) MID analysis of oxidised glutathione shows decreased labelling with siGLS1. Diagram (C) describes the maintenance of reduced (GSH) and oxidisied (GSSG) glutathione. D) GSH:GSSG is decreased with siGLS1, as measured with a GSH/GSSG ratio detection assay kit. Data is performed in technical triplicate, mean +/- S.D. Statistical significance determined using two-tailed unpaired Student's t-test; *p<0.05, **p<0.01, ***p<0.001, ****p<0.0001

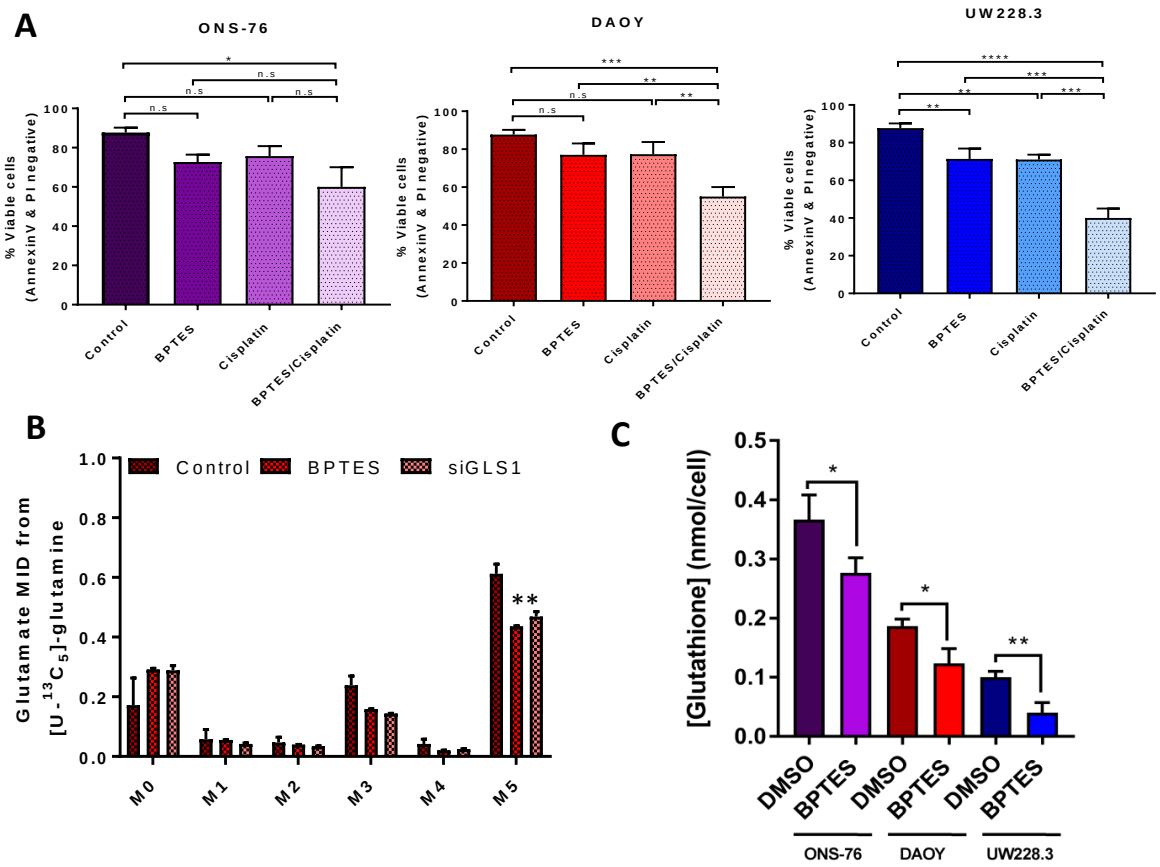

Figure 4.2.6. Pre-treatment with BPTES leads to increased cytotoxicity of Cisplatin treatment in MB cell lines. A) Cell death was examined using a flow cytometry AnnexinV/PI assay to determine the effectiveness of BPTES on ONS-76, DAOY and UW228.3 cell lines. Cells treated with DMSO, BPTES, Cisplatin or a combination of BPTES and cisplatin. BPTES pre-treatment 24 hours prior to cisplatin treatment decreased the cell viability of all three cell lines. Data presented as mean ±SEM representative of three separate experiments. Significance was determined by performing a one-way ANOVA with Tukey post-hoc test in Graphpad; *p<0.05, **p<0.01, ***p<0.001, ****p<0.0001. B) MID analysis of glutamate, comparing siGLS1 and BPTES. No differences between GLS KD and GLS inhibition was seen. C) Steady state concentrations of glutathione are decreased with BPTES treatment, as quantified by 1D 1 H-NMR spectroscopy. Data is mean +/- S.E.M and representative of at least three biological replicates. Significance determined using two-tailed unpaired student's t-test; *p<0.05, **p<0.01, ***p<0.001, ****p<0.0001

4.2.5. Pre-treatment with BPTES leads to a potentiation of treatment.

High doses of chemotherapy given to children with MB often result in adverse side effects, leading to decreased quality of life. We therefore, decided to use cisplatin in co-treatment with BPTES to see whether the GLS1 inhibitor could potentiate the effects of these cytotoxic agents, thereby providing a means of reducing cytotoxic agent dose that would be needed to treat MB. As before, an annexin/PI cell death assay was performed to determine changes in cell viability. When pre-treated for 8hr with BPTES, the DAOY and UW228.3 cell lines showed decreased viability after cisplatin treatment when compared to BPTES and cisplatin treatment alone (figure 4.2.6). However, no significant difference was observed in the ONS-76 cell line, consistent with previous data showing that siGLS1 is least effective on the cell line.

4.2.6 GLS2 protects MB cell lines against cytotoxic agents

Several studies have identified GLS2 as being important in the protection against oxidative stresses (Martín-Rufián *et al*., 2014 and Suzuki *et al*., 2010). Despite GLS2 not being highly expressed under basal conditions in our MB cell lines, we observed increased GLS2 expression after treatment with H_2O_2 (Figure 4.2.7). We sought to investigate whether this increase in GLS2 expression played a role in the defence against cytotoxic agents. To investigate this, we tested the effect of siGLS1, siGLS2 and siGLS1 and siGLS2 combined. Similarly to our previous experiments, we observed that GLS1 KD increased sensitivity to treatment in all three cell lines (Figure 4.2.4). Our results also show increased cell death in all three cell lines upon GLS2 KD, suggesting a role for this enzyme in the protection against treatment. A combination of siGLS1 and siGLS2 further potentiated H_2O_2 treatment in the ONS-76 cell line, but not in the other two lines.

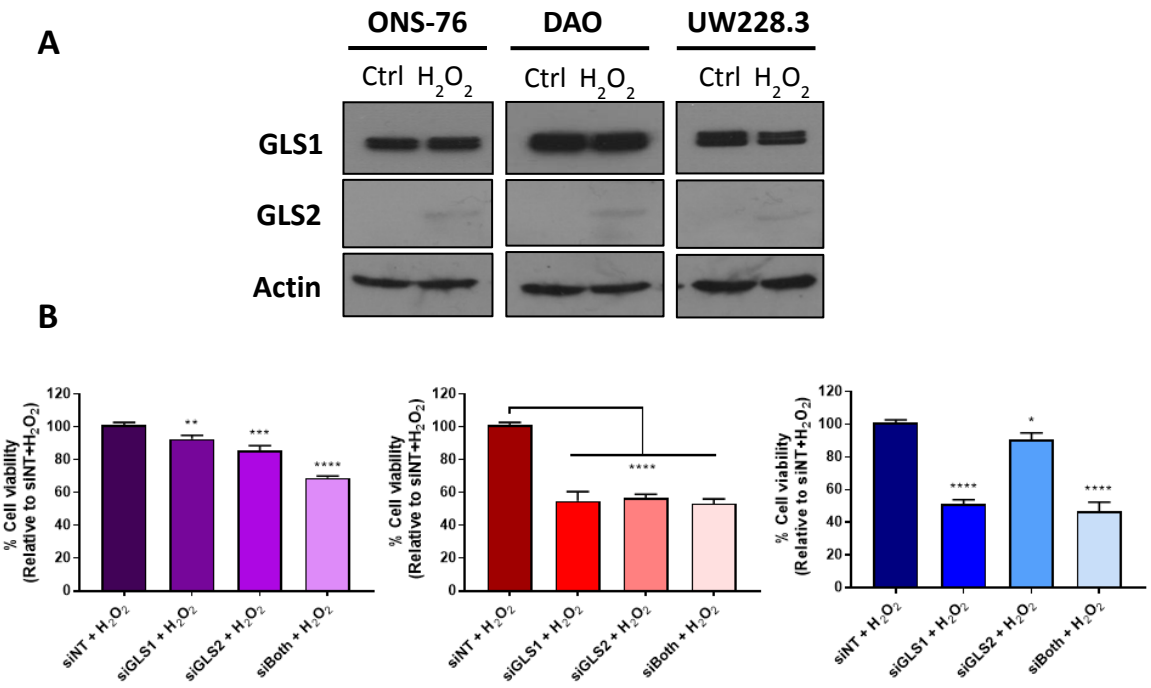

Figure 4.2.7. GLS2 expression increases with H_2O_2 treatment, leading to treatment resistance. Immunoblot analysis showing increased expression In GLS2, but not GLS1 after treatment with H_2O_2. Actin was probed as a loading control. B) Cell death was examined using a flow cytometry AnnexinV/PI assay to determine the effectiveness of siGLS1, siGLS2 or both on ONS-76, DAOY and UW228.3 cell lines. siGLS1, siGLS2 and both decreased the cell viability of all three cell lines. Data presented as mean ±SEM representative of three separate experiments. Significance was determined by performing a one-way ANOVA with Tukey post-hoc test in Graphpad; *p<0.05, **p<0.01, ***p<0.001, ****p<0.0001.

4.2.7. SLC7A11 inhibition can increase hydrogen peroxide cytotoxicity in MB cell lines.

The synthesis of glutathione from cytosolic glutamate requires two further amino acids; cysteine and glycine. A major route for the import of cysteine from the extracellular space is through its dipeptide (cystine), which is anti-ported against glutamate by the xCT (SLC7A11) transporter. Our previous data suggested that a major fate of glutamine-derived glutamate in MB cells was its excretion into the medium (Chapter 3). We investigated whether excretion of glutamate might be used to support the uptake of cystine. We therefore

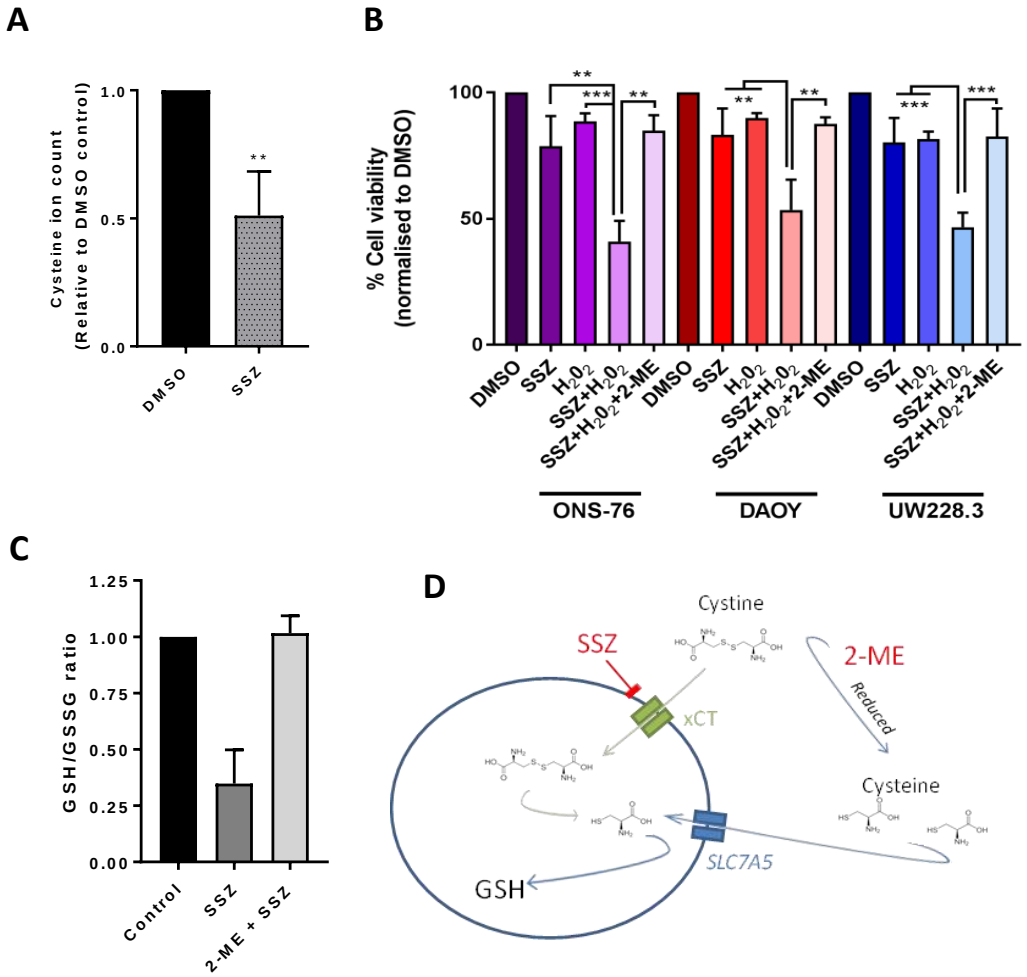

Figure 4.2.8. SLC7A11 is required for cystine uptake, and resulting maintenance of glutathione in MB. A) An SRB viability assay was carried out to determine the importance of SLC7A11 in ONS-76, DAOY and UW228.3 cell lines. Cells were treated with DMSO, SSZ, H_2O_2, SSZ and H_2O_2, or SSZ, H_2O_2 and 2-ME. A) GC-MS analysis showed a reduction of intracellular cystine upon treatment with SZZ. B) Sulfasalazine (SSZ) treatment led to a sensitisation towards hydrogen peroxide treatment, which importantly could be abolished by the addition of 2-mercaptoethanol (2-ME). C) SSZ treatment decreased the GSH:GSSG. D) Depicts the mechanistic action of SSZ and 2-ME treatment. (n=3)

treated cells with sulfasalazine, an inhibitor of the cystine/glutamate antiporter known as the xCT transporter (SLC7A11), and observed a decrease in intracellular cysteine concentrations (Figure 4.2.8A). This treatment also sensitised cells to hydrogen peroxide treatment (Figure 4.2.8C), which we show is likely due to decreased intracellular GSH:GSSG ratios (Figure 4.2.8B) caused by SZZ treatment. Importantly, this effect could be abolished by the addition of the reducing agent, 2-mercaptoethanol (2-ME) to cells, which facilitates

the uptake of cystine independently of the xCT transporter by reducing cystine to cysteine, allowing its uptake through an alternate transporter (Figure 4.2.8D)

4.2.8 Genes involved in GSH synthesis predict outcome in MB patients

We have highlighted the importance of GSH in the resistance to a wider range of treatments in our MB cell lines. We further assessed the importance of genes that control and modulate GSH in MB tumours, through two separate mRNA databases. We observed increased expression of GCLC-which encodes the rate limiting enzyme in the synthesis of GSH- in MB tumours compared to normal cerebellum. We further show GCLC expression is higher in SHH, Grp3 and Grp4 MB compared to WNT tumours, suggesting expression is coupled with a more aggressive phenotype, although, this is not quite reflected in our Newcastle survival cohort despite a strong trend. Furthermore, we detected clinical significance in GSR expression, with highly expressing patients having a poorer overall survival.

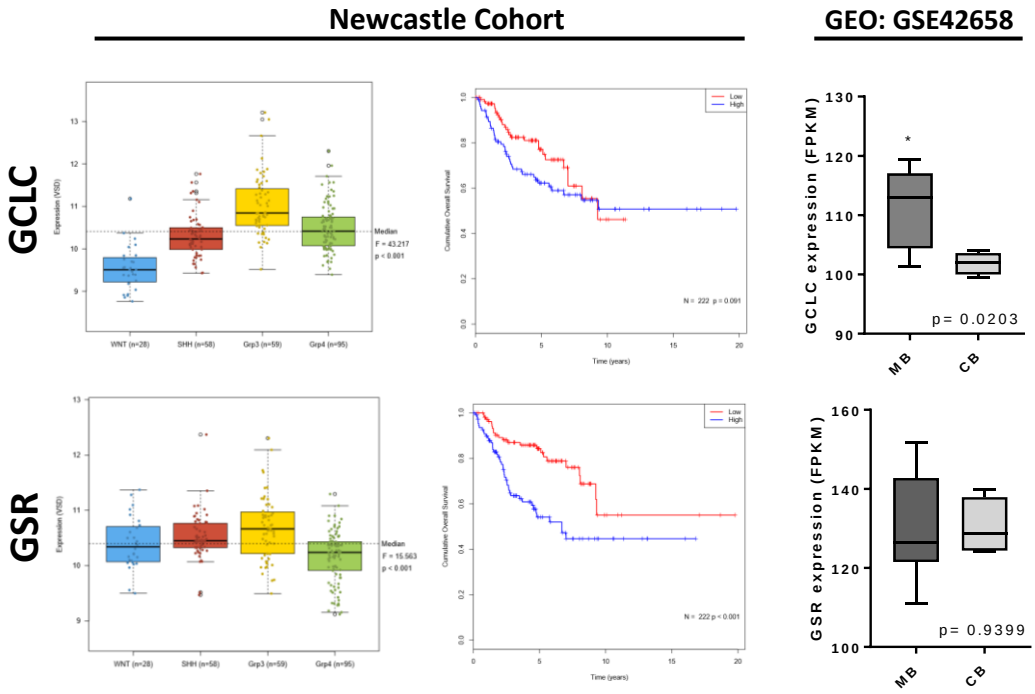

Figure 4.2.9. Expression of glutathione-related genes was associated with survival in MB tumours. A) RNA expression data compared across subgroups of MB and representative Kaplan-Meier survival curves of the MB Newcastle cohort. n=240 (WNT n=28, SHH n=58, G3 n=59 and G4 n =95). High and low expression was determined by the median expression value for each gene. Log-rank (Mantel-Cox) and Gehan-Breslow-Wilcoxon statistical tests were performed in all cases; *p<0.05, **p<0.01, ***p<0.001, ****p<0.0001.

4.2.9 Hydrogen peroxide treatment alters glutamine metabolism.

The investigations to this point have examined the sensitivity of MB cell lines to treatment after glutamine pathway manipulations, however, they have not provided any information as to the response of MB cell line metabolism to treatment. To better understand this, we measured isotopic label incorporation from ^{13}C-U-Glutamine during treatment with the oxidant, hydrogen peroxide. We found that the most sensitive cell line, UW228.3, demonstrated an increased flux of glutamine into glutamate, while a smaller increase was observed in the DAOY cell line. No significant changes were noted in the ONS-76 cell line (Figure 4.2.8).

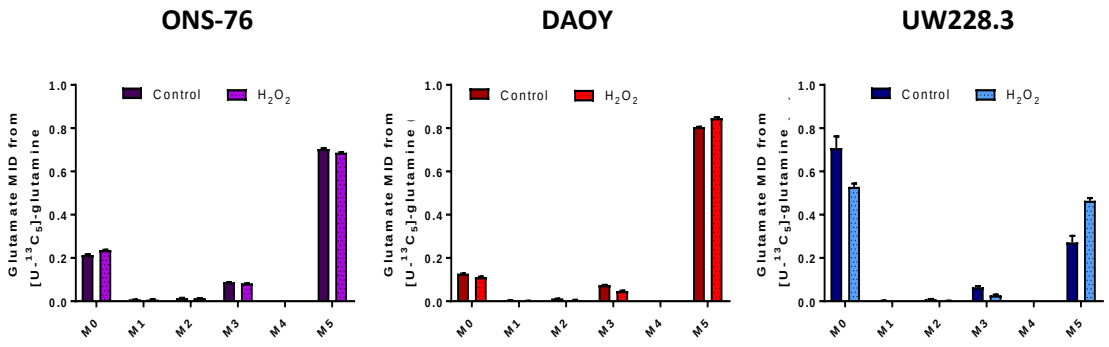

Figure 4.2.10. Hydrogen peroxide treatment alters glutamine-derived glutamate metabolism between MB cell lines. Analysis of the mass isotopologue distribution (MID) of glutamate after treatment with H_2O_2 treatment. Mass isotopologues (m+0, m+1, m+2, m+3, m+4 and m+5) correspond to ion fragments containing different ^{13}C atoms. Alterations in glutamate labelling after H_2O_2 treatment are present in the DAOY and UW228.3 cell lines. Data is performed in technical triplicate; mean +/- S.D. Statistical significance determined using two-tailed unpaired Student's t-test; *p<0.05, **p<0.01, ***p<0.001, ****p<0.0001

To further understand the alterations on metabolism upon hydrogen peroxide treatment, we investigated the changes in glutamine contribution towards several TCA cycle metabolites. Increased m+5 αKG was observed in the DAOY and UW228.3 lines after treatment, while no changes were seen in the ONS-76 cells. Hydrogen peroxide increased m+5 succinate and m+5 malate in the DAOY cell line only. Small increases in m+5 fumarate were seen in the DAOY and UW228.3 lines.

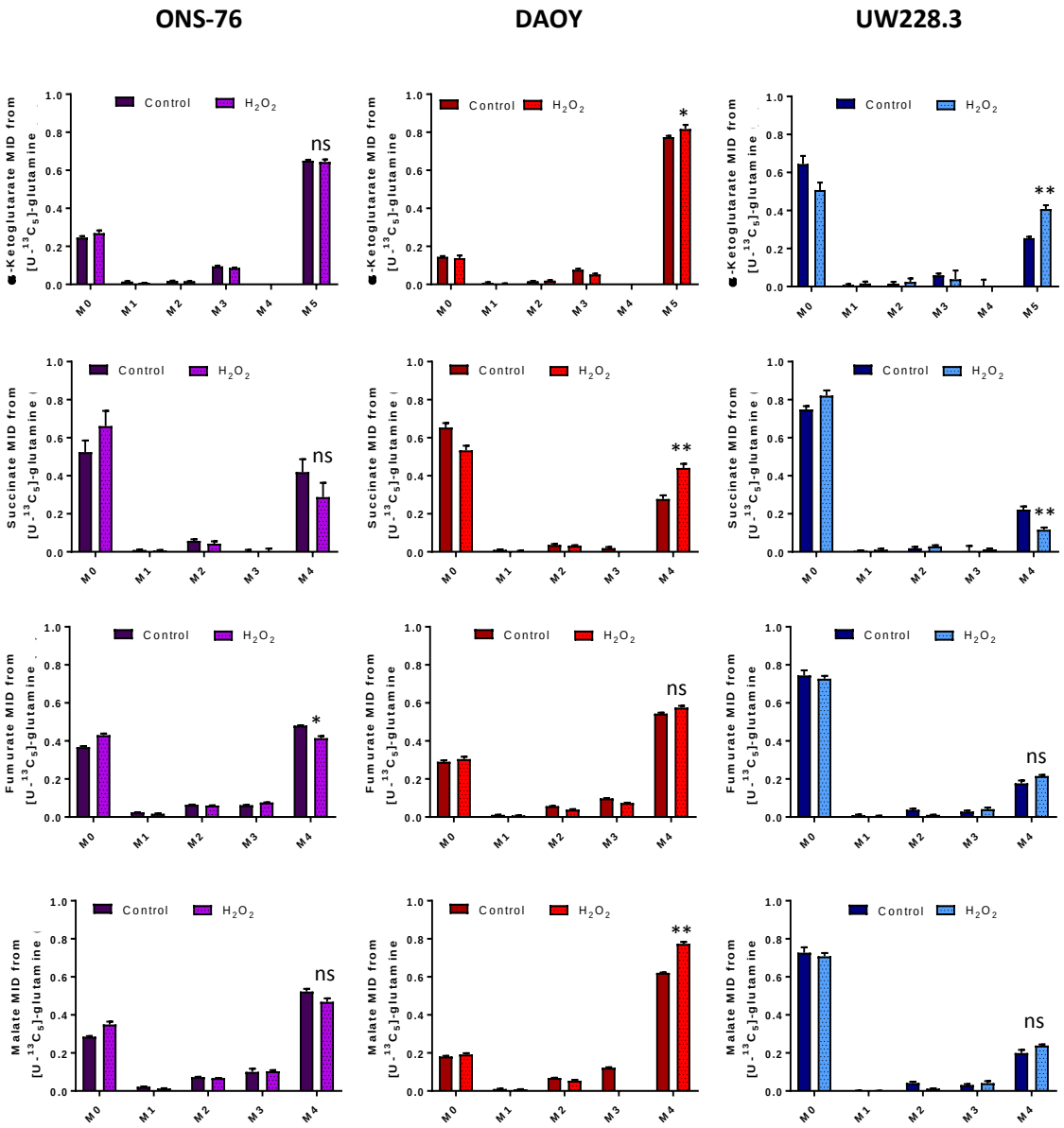

Figure 4.2.11. Hydrogen peroxide treatment elicits distinct and separate glutamine metabolism between MB cell lines. Analysis of the mass isotopologue distribution (MID) of α-ketoglutarate, succinate, fumarate and malate after treatment with H_2O_2 treatment. Mass isotopomers (m+0, m+1, m+2, m+3, m+4 and m+5) correspond to ion fragments containing different 13C atoms. Alterations in glutamate labelling after H_2O_2 treatment are present in the DAOY and UW228.3 cell lines. Data is performed in technical triplicate, mean +/- S.D. Statistical significance determined using two-tailed unpaired Student's t-test; *p<0.05, **p<0.01, ***p<0.001, ****p<0.0001

5.2.10 Hypoxia increases MB treatment resistance

Hypoxia is a regular feature of solid tumours and is frequently associated with increased treatment resistance. We performed immunohistochemical analyses of SHH-derived MB tumour tissues to determine the extent of CAIX staining (Figure 4.2.12), a commonly used marker of hypoxia. Our results highlight levels of CAIX staining within regions of the tumour tissue (Figure 4.2.12) and (Supplementary figure 4), suggesting MB tumours may harbour hypoxic niches.

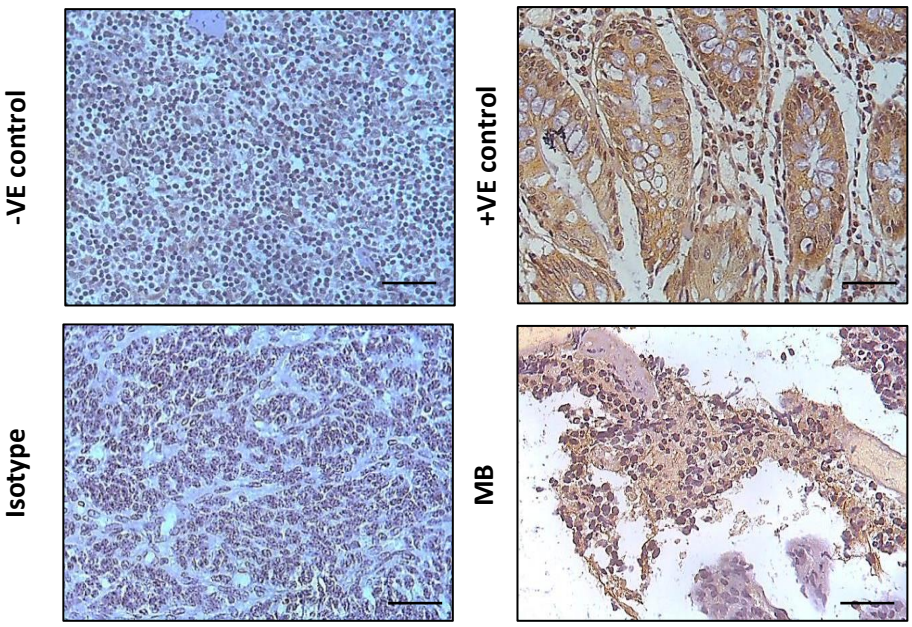

Figure 4.2.12. CAIX staining reveals hypoxic regions in MB tumours. CAIX protein expression is increased in MB tumours compared to controls. Scale bar, 50 µm.

5.2.11 MB cell lines switch to reductive metabolism in response to hypoxia

Cells typically remodel their metabolism in response to hypoxia, a major goal of which is likely to support oxygen-independent ATP production. To investigate the metabolism of glutamine in MB cell lines in hypoxia, cells were incubated for 24 hours with [U-$^{13}C_5$]-glutamine in either 21% O_2 (normoxia) or 1% O_2 (hypoxia). The incorporation of ^{13}C into citrate can be used to evaluate the relative extent of oxidative and reductive glutamine metabolism (Figure 4.2.13). The ONS-76, DAOY and UW228.3 cells displayed increased m+5 citrate, indicative of increased reductive carboxylation of glutamine-derived αKG.

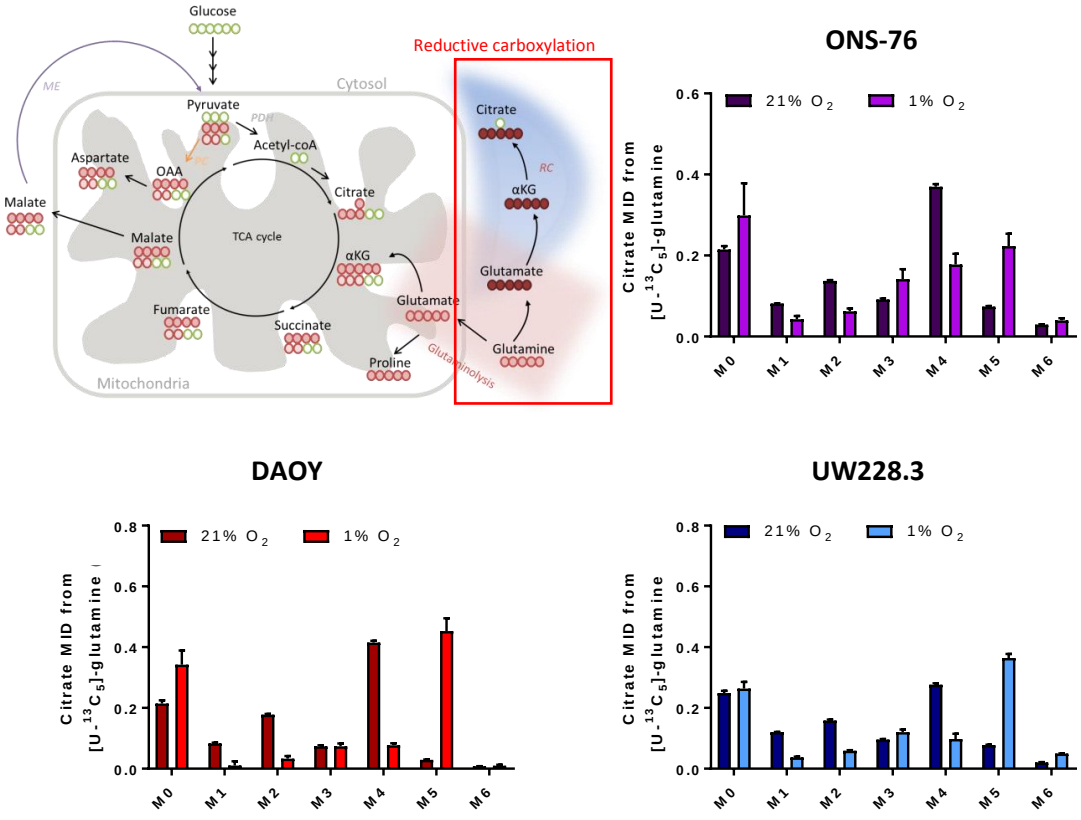

Figure 4.2.13. Hypoxia induces reductive glutamine metabolism. Comparison of the MID in citrate employing a [U-$^{13}C_5$]-glutamine tracer to assess the relative contributions of oxidative and reductive TCA activity. In normoxia, glutamine-derived αKG undergoes oxidative TCA metabolism producing M+4 citrate from M+4 TCA cycle intermediates. In hypoxia, ONS-76, DAOY and UW228.3 cells increase their reliance on reductive carboxylation of glutamine-derived αKG producing M+5 citrate. (n=3)

5.2.12 Hypoxia increase treatment resistance in MB cell lines

To investigate the role of hypoxia in treatment resistance, we incubated our cell lines in either 21% or 1% O_2 for 24h prior to H_2O_2 treatment, which is long enough to induce HIF1α expression (Figure 4.2.13 D). We observed that hypoxia has a significant protective effect in the ONS-76 and UW228.3 cell lines (Figure 4.2.13 A-B); suggesting hypoxia may play a role in treatment resistance in a subset of MB tumours. We hypothesised that as a reducing environment, hypoxia could potentially act in a similar fashion to 2-ME, therefore rendering the SLC7A11 anti-porter obsolete. To test this theory we incubated our MB cell lines in 21% O_2 and 1% O_2 and subsequently treated them with the SLC7A11 inhibitor, SSZ. Our results demonstrate that SSZ has no additional effect on treatment resistance, confirming our hypothesis (Figure 4.2.13 C).

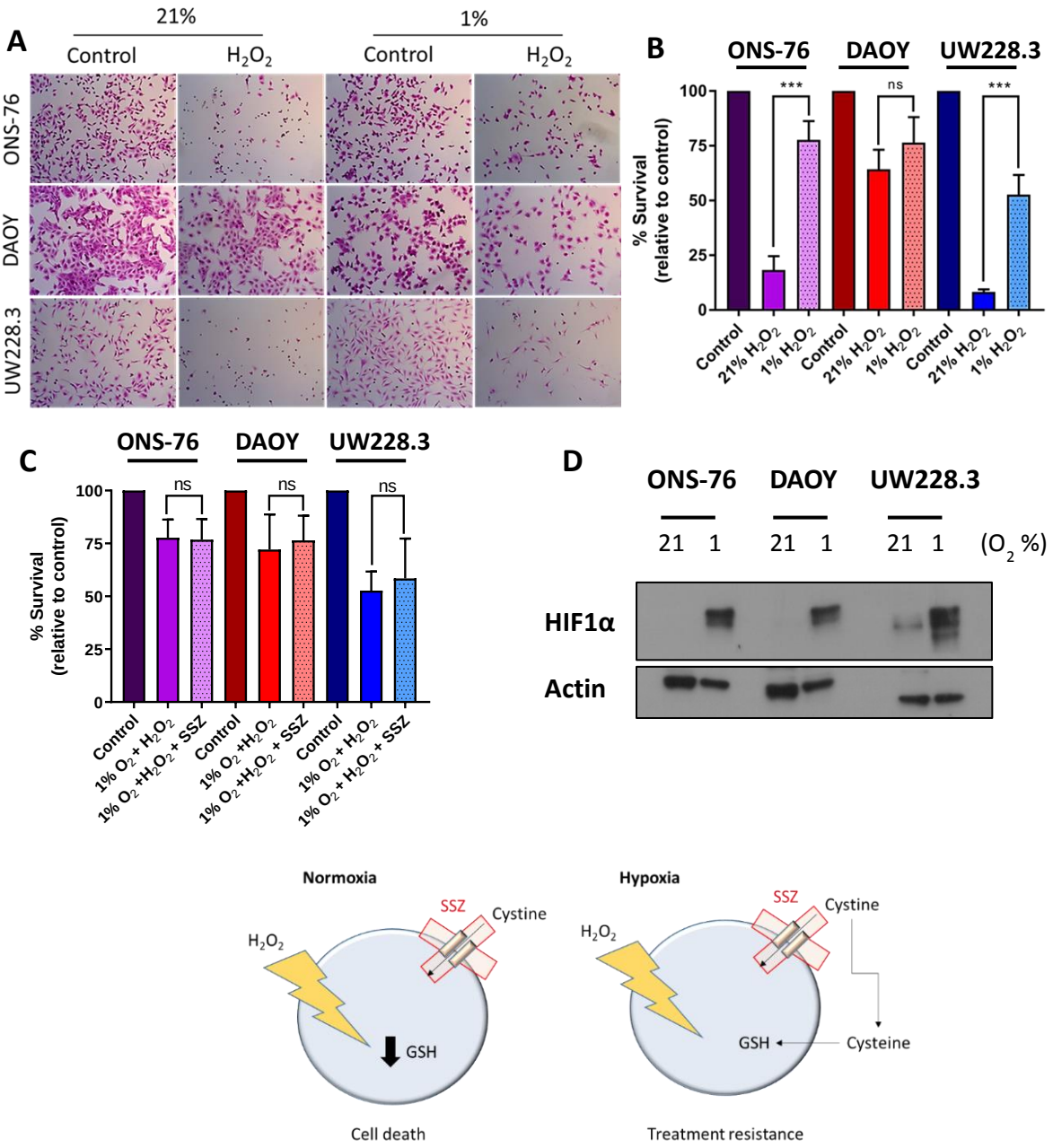

Figure 4.2.13. Hypoxia alters treatment resistance. SRB viability assays of ONS-76, DAOY and UW228.3 cells treated with H_2O_2 at 21% or 1% O2. A) Qualitative microscopic evaluation of SRB stained cells shows increased cell viability of ONS-76 and UW228.3 cells at 0.3% O_2 when compared to 21% O_2 B) Absorbance values of SRB stain confirm increased cell viability in the ONS-76 and UW228.3 lines at 0.3% O_2 when compared to 21% O_2. n=3. Data was analysed using a one way ANOVA with a Tukey post-hoc test; *p<0.05, **p<0.01, ***p<0.001, ****p<0.0001.

Discussion

4.3.1. Introduction

The important role that glutamine plays in cancer development has long been appreciated. However, approaches that interfere with glutamine metabolism to improve therapeutic outcomes have been less than ideal. Glutamine is likely to elicit a resistance phenotype through the synthesis of glutamate, where this metabolite is utilised both directly and indirectly in the synthesis of glutathione (Shelly C. Lu, 2014). More recent studies have focused on this outcome of glutamine catabolism, with particular focus on GLS. Elegant work regarding glutamine metabolism has previously been carried out in lung squamous cell carcinoma (SCC), where it was shown that the inhibition of GLS with CB-839 can effectively overcome therapeutic resistance (Momcilovic *et al.*, 2018).

Many tumour types have been dubbed 'glutamine addicted' and show sensitivity when subjected to a glutamine-starved diet (Chakrabarti *et al.*, 2015). However, the importance of glutamine in MB tumours is only just becoming established. Wilson *et al* retrospectively analysed patients with MB using 1H magnetic resonance spectroscopy (MRS) and identified that glutamate was a robust marker of survival (Wilson *et al.*, 2014). The identification of glutamate as a prognostic biomarker in this setting highlighted the importance of further studies into MB tumour metabolism, and in particular the relationship between glutamine and glutamate. Furthermore, it was recently shown that p73 status was linked to glutamine dependency in MB, where it was demonstrated that p73 expression regulated glutamine metabolism, in order to preserve cell growth and proliferation (Niklison-Chirou *et al.*, 2017). This same group were also the first to disrupt glutamine metabolism in the context of MB, strengthening our notion that glutamate is important in the context of this tumour type. However, they direct their attention towards the inhibition of p73 and GLS2, while we

establish the importance of both glutaminase isozymes, GLS1 and GLS2, and consider wider implications of glutamate metabolism.

4.3.2 Glutamine starvation sensitises MB cells to treatment.

The combination of glutamine starvation with cisplatin causes a significant cell death response in our MB cell lines (Figure 4.2.2). This response to cisplatin, in part, could be due to a mitochondria ROS response known to be prompted by cisplatin treatment (Marrache, Pathak and Dhar, 2014), where reduced glutamine and resulting glutamate may lead to a reduced mitochondrial potential and thus, potentiating the effect of cisplatin. Our results are consistent with previously published data (Niklison-Chirou *et al.*, 2017), who show a similar effect in MB cell lines. This same group also validated their results in an *in vivo* mouse model of MB, where a diet of reduced glutamine induced a substantial increase in the overall survival of these mice. However, it is important to note that these results were only observed in p73-expressing MB mice, which only represent a small subset of MB cases. Despite this, our combined work highlights the importance of glutamine in the resistance of MB tumours to treatment, and reveals a potential therapeutic option in these patients.

Starving tumours of metabolites they are 'addicted' to, or in some case dependent on is an exciting therapeutic prospect. One example of this comes from acute lymphoblastic leukaemia (ALL), which are reliant on asparagine uptake for survival. Asparaginase therapy is now a cornerstone for ALL treatment where they are consistently improving clinical outcomes in children (Pieters *et al.*, 2011). The administration of asparaginase results in rapid and complete deamination of the amino acid asparagine but also, although to a lesser extent, glutamine (Avramis, 2012). This off targeting effect on glutamine may therefore prove useful in glutamine-addicted tumours. Although, thus far its use in solid tumours has

been ineffective, as in the case of ovarian cancer (HAYS *et al.*, 2013), where serious side effects are commonly observed. However, it has recently been suggested that L-Asparaginase delivered to the tumour directly by engineered S*almonella typhimurium* could bypass these toxicities. Kim et al, demonstrated that these 'mutant' L-Asparaginases could effectively target MC38 (colon carcinoma) tumours which had been ectopically grafted into mice, with few side effects observed (Kim *et al.*, 2015). It is important to note that these treatments will be most effective in cells reliant on asparagine, which our cell lines are not (data not shown), although the extent of glutamine clearance through asparaginase treatment may be enough to elicit responses, yet low enough prevent the significant toxicities, associated with glutamine analogue usage. Interestingly, there has been emerging research exploring the role of glutamine in the protection of normal tissue to cytotoxic treatments. Savarese *et al,* suggest that reduced glutamine concentration could have a bearing on the tolerance of normal tissue to antitumor treatments. They further propose that supplementing patients with glutamine during cancer treatment has the potential to nullify treatment-related toxicity (Savarese *et al.*, 2003).

These data reveal the complicated nature associated with clearing glutamine in the tumour microenvironment. The need for more targeted therapies may therefore prove more beneficial.

4.3.3 The impact of interrupting *de novo* glutamate synthesis on the cytotoxic response to treatment, by inhibiting GLS1.

GLS1 knockdown was utilised to study the effect of glutamate on therapy resistance, as this resulted in a drastic decline in glutamate synthesis in our previous studies. We then followed up these results with compound inhibition with BPTES, which although it

introduces potential complications through off target effects, provides an opportunity for translation to the clinic.

Knockdown of GLS1 potentiated the cytotoxicity of cisplatin in our MB cell lines (Figure 4.2.3 & 4.2.4), suggesting that blocking the conversion of glutamine to glutamate may increase the efficacy of chemotherapy in MB tumours. Interestingly, the effect of GLS knockdown was more profound in the UW228.3 cell line, despite these cells being less reliant on glutamine when compared to the DAOY cells. This suggests the effect may be less dependent on cell line reliance on glutamine, but instead may be reliant on glutaminase expression - UW228.3 cells have a relatively low expression of GLS1 in comparison to the other two lines. Gaining understanding of different responses through the use of multiple cell lines is likely to lead to more successful therapies, given the heterogeneous nature of MB tumours. However, we found our results were altered between cell death assays, where killing potentiation became significant across all cell lines with the AnnexinV/PI assay, compared to variations with the SRB assay. The differences between the two techniques proved to be an issue throughout our experiments, but may be reflective of the sensitivity differences between the two assays, or what they actually measured. The AnnexinV/PI assay utilises the binding of externalised phosphatidylserine (PS) in cells undergoing apoptosis by annexin V, and cells with non-coherent plasma membranes (i.e. dead) using propidium iodide (Peixoto, de Oliveira Galvão and Batistuzzo de Medeiros, 2017). Therefore, this assay is able to identify those cells undergoing apoptosis earlier than the SRB assay and provides a more valuable tool when assessing cellular death responses. Following our results with regards to the impact of GLS1 knockdown on cisplatin cytotoxicity, we investigated whether this effect would be reproduced with gamma irradiation. We observed similar results (Figure

4.2.4), which highlighted GLS1 as a possible target with the potential to improve the efficacy of radiotherapy in MB tumours.

These are important proof of concept studies, which help identify potential therapeutic targets. However, as GLS1 inhibitors have been trialled in the clinic, we believe that it was important to test this in the MB cell line models. BPTES is an allosteric inhibitor of the dimer-to-tetramer transition of KGA GLS, which is required for its activation. BPTES pre-treatment was found to increase the effectiveness of cisplatin treatment in MB cell lines (Figure 4.2.6), strengthening the notion that GLS inhibition could be used to improve the efficacy of chemotherapeutic agents in MB tumours.

Another GLS1 inhibitor becoming more commonly used is Compound 968. However, we did not observe any additive effect on killing with pre-treatment of this agent (Supplementary figure 4). The mode of action of compound 968 is different to that of BPTES, where this inhibitor preferentially binds to the monomeric (inactive) form of GLS, and as a result prevents the dimerization required for GLS activation (Stalnecker et al., 2015). Therefore, compound 968 is unable to inhibit GLS when the enzyme is already in an active conformation. We believe our cell lines are utilising GLS1 to such a degree that the majority of the enzyme is already in its active, dimeric form, and may explain why we do not see an effect in our cell lines upon treatment.

4.3.4 GLS maintains glutathione homeostasis in order to resist cytotoxic treatments.

The effectiveness of GLS1 inhibition on treatment potentiation appears to be linked to glutathione homeostasis. We revealed a synergistic effect of reduced glutathione and improved treatment efficacy – our results showed a decrease in glutathione flux when GLS1

was knocked down in the ONS-76 cell line (Figure 4.2.5). To confirm, we then showed that knockdown of GLS decreased the GSH:GSSG in all three cell lines, suggesting the increased sensitisation of GLS1 KD cells to treatment is likely to be due to a defective GSH response.

4.3.5 The impact of interrupting *de novo* glutamate synthesis on the cytotoxic response to treatment, by inhibiting GLS2.

GLS2 has recently been characterised as a p53 target gene, able to protect against oxidative stress (Suzuki *et al.*, 2010). Since this observation, several lines of research have highlighted the importance of GLS2 in the protection against ROS (Hu *et al.*, 2010). Xiang *et al,* Knocked down GLS2 and showed a decrease in glutathione and NADH, which was able to sensitize cervical cancer to ionizing radiation (Xiang *et al.*, 2013). Furthermore, the importance of GLS2 in MB tumours was investigated by Niklison-Chirou *et al*, where they concluded that p73 regulates GLS2 to maintain glutathione levels. They show pre-treatment with compound 968 increases cell line sensitivty to cisplatin, although they claim that compound 968 acheives this by inhibiting GLS2 (Niklison-Chirou *et al.*, 2017). However, this drug has only been shown to inhibit the GLS1 splice variant, GAC (Wang *et al.*, 2010). Furthermore, our data represented here (Figure 4.2.7) only showed very low expression of GLS2 in all MB cell lines tested in basal conditions. We also demonstrated that GLS1 was the preferred isozyme under basal conditions.

We also extended the investigations to the role of GLS2 in the protection against treatment and showed, surprisingly, that GLS2 knockdown could increase the cytotoxicity of hydrogen peroxide (Figure 4.2.8), despite low basal expression in our MB cell lines. Furthermore, despite GLS2 having little role under basal conditions, our data suggested that GLS2 becomes ‘more active’ under conditions of stress, where we showed that GLS2 expression is

increased after treatment with H_2O_2. A potential explanation for siGLS2 increased sensitisation therefore, may be that knocking down GLS2 prior to treatment prevents the increase in its expression. We therefore show here the importance of GLS2 expression in MB treatment resistance, justifying further research with an aim to progress into the clinic. However, there are currently no compound inhibitors of GLS2 in clinical trials and only recently has there been the identification of a group of compounds able to inhibit GLS2 *in vitro* (Lee *et al.*, 2014). Lee and colleagues, have identified a group of Alkyl benzoquinones as novel inhibitors of GLS2, the use of which leads to mTORC1 inhibition and results in reduced tumorigenesis (Lee *et al.*, 2014). It will be interesting to see the use of these inhibitors in future studies.

4.3.6 The impact of interrupting glutamate metabolism on the cytotoxic response to treatment, inhibiting SLC7A11.

The glutamate/cystine antiporter (SLC7A11) has been associated with treatment resistance in several tumours, as it facilitates cellular uptake of cystine for the synthesis of intracellular GSH (Huang *et al.*, 2005). Polewski *et al,* Inhibited SLC7A11 with sulfasalazine (SSZ) and showed a decrease in glioma cell growth and survival. This group also co-treated with SSZ and the chemotherapeutic agent temozolomide and revealed a synergistic killing effect (Polewski *et al.*, 2016). SLC7A11 has also been highlighted as a target in triple-negative breast cancer (Timmerman *et al.*, 2013). Our data suggested that MB tumours express SLC7A11, and blocking of this anti-porter with SSZ reduced the growth of our MB cell lines. Furthermore, we found that inhibiting SLC7A11 with SSZ renders MB cell lines sensitive to hydrogen peroxide treatment. The MB cell lines used demonstrated a degree of heterogeneity with respect to glutaminase expression and inhibition sensitivity, but with respect to SCL7A11 inhibition, all three cell lines responded similarly. Unsurprisingly, we

confirmed the importance of GSH in the resistance against treatment, where SSZ significantly reduced intracellular concentrations of cystine which subsequently decreased the GSH:GSSG ratio in the MB cell lines. We demonstrated the specificity of SSZ treatment by displaying how this effect could be abolished by the addition of the reducing agent, 2-mercaptoethanol (2-ME), which facilitates the uptake of cystine independently of the xCT transporter by reducing cystine to cysteine, allowing its uptake through an alternative transporter. Our findings align strongly with studies carried out in colorectal cancer, where Ma *et al* showed SSZ was able to sensitise colorectal cancer cell lines to cisplatin through a GSH-depleting mechanism (Ma *et al.*, 2015). Our results reveal an alternate target of glutamate metabolism for MB tumours, independent of glutaminase, which could potentially be used clinically.

SSZ is an FDA approved, anti-inflammatory drug used clinically in the treatment of rheumatoid arthritis and inflammatory bowel disease, with few side-effects observed (Combe *et al.*, 2009). The use of SSZ both *in vitro* and in animal studies for the treatment of cancers is becoming more popular in recent years. However, progress into clinical trials has been limited and the two trials conducted in gliomas have produced unfavourable results. The first of these was a phase 1/2 prospective, randomised trial in 10 patients (2 anaplastic astrocytoma and 8 glioblastoma), where SSZ was unable to induce clinical responses and was subsequently discontinued due to unacceptable toxicities (Robe et al., 2009). The second trial also observed no clinical benefit when SSZ was used together with temozolomide and radiation therapy (Takeuchi *et al.*, 2014). These trials suggest the use of SSZ does not represent a potential novel means of treating glioblastoma. However, its use in the prevention of colorectal cancer in patients with heightened risk has been demonstrated.

A retrospective study of ulcerative colitis patients revealed that individuals receiving long-term SSZ were at a significantly reduced risk of developing colorectal cancer (Moody *et al.*, 1996). It has been recently observed that treatment failures using SSZ may be a direct consequence of activated resistance pathway in cancer. Kim et al, identified Nutrient-deprivation autophagy factor-1 (NAF-1) as being associated with resistance to SSZ-induced ferroptosis. These findings highlight the need of further research investigating the mechanisms governing treatment failures. This also reveals a gap in our own research as we did not explore the mechanism of cell death in our MB cell lines to SSZ treatment, despite several studies showing a significant role for ferroptosis.

Interestingly, SLC7A11 activity has been shown to amplify glutamine anaplerosis in A549 cells, thus increasing the need for glutamine. The triggering of SLC7A11 expression, through the use of NNRF2-activating agents, sensitised tumours to GLS inhibitors (Koppula *et al*, 2017). Thus, there may be a potential for this treatment to be used in conjunction with GLS inhibitors.

4.3.7 Glutathione related genes can predict survival in MB patients

Increased GSH concentrations are often observed in several tumours, correlating with increased resistance to therapy. Expression of specific genes encoding GSH biosynthetic enzymes may therefore provide information as to whether a tumour may be chemo-resistant. GSH has previously been implicated in the chemoresistance of MB, where GSH supplementation protected MB cells to campthothecin related apoptosis (Li *et al.*, 2009). Furthermore, Friedman *et al*. showed elevation in GSH and γ-glutamyl transpeptidase (which catalyses the transfer of gamma-glutamyl l groups from GSH, a key process in the gamma-glutamyl cycle) in a Cyclophosphamide (4-HC) resistant DAOY line. They confirmed

the role of increased GSH with 4-HC resistance by depleting GSH with L-buthionine-sulfoximine and showing a sensitisation to this agent (Friedman, Kaufmann and Ludeman, 1992). Through our *in vitro* cell line experiments, we have further highlighted the importance of GSH in the resistance to a wider range of treatments in MB. We also assessed whether genes involved in GSH metabolism held clinical relevance and observed increased expression of GCLC, the rate limiting enzyme in the synthesis of GSH, in MB tumours compared to normal cerebellum. We further show GCLC expression is higher in SHH, Grp3 and Grp4 MB compared to WNT tumours, suggesting expression is coupled with a more aggressive phenotype, although, this is not quite reflected in our Newcastle survival cohort despite a strong trend. Furthermore, we detected clinical significance in GSR expression, with highly expressing patients having a poorer overall survival. GRS is vital in the salvaging of GSH from GSSG but becomes less efficient during periods of oxidative stress. It is therefore not surprising that the expression of GSR is typically increased in a number of tumours and has previously been used to predict responses to cisplatin in patients with lung cancer (Ogawa *et al.*, 1993). Our data therefore suggests GSH plays an important role in MB resistance towards treatment. Furthermore, the expression of glutathione peroxidases (GPx1 and GPx4) – enzymes responsible for reducing lipid hydroperoxides – can be used to predict survival in MB patients (Supplementary figure 5).

It has also been proposed that GSH may act as a glutamate store, preventing glutamate-dependant neuronal excitotoxicity (Chen and Swanson., 2003), which would agree with our hypothesis derived from results in the previous chapter that proline synthesis acts to reduce mitochondrial glutamate concentrations.

4.3.8 Treatment alters glutamine metabolism in MB cells

Many studies have shown that treatment induces alterations in the phenotype of the tumour, as well as its environment (Barker *et al.*, 2015). Changes in metabolism after exposure to cytotoxic agents may reveal important mechanisms involved in treatment resistance, but despite this, studies focused on this are lacking in human tumours. We show for the first time in MB cell lines that glutamine flux is rapidly altered after H_2O_2 treatment. Our results demonstrate that the MB cell lines have different glutamine-related metabolisms, where the DAOY and UW228.3 lines increase their direct glutamine flux into glutamate, as seen by increased m+5 glutamate. These findings further highlight the importance of glutamate in MB resistance to treatment, and suggest these cell lines increase glutamate-derived pathways as a response to oxidative stresses, in this case towards H_2O_2 treatment. H_2O_2 is known to have a short half-life in cells, where it is quickly detoxified. This short-lived effect of H_2O_2 may not be ideal to elicit responses in ^{13}C flux and may explain the small changed observed. We therefore recommend this experiment to be repeated with both cisplatin and irradiation treatment. However, despite interesting findings, further work will be required to pull apart the precise metabolic changes associated with treatment. A recent study analysed altered metabolism in human breast cancer cell lines after BPTES treatment. Their work highlighted alterations in numerous metabolic pathways and offers vital metabolic information regarding treatment resistance mechanisms (Gowda et al., 2018). More studies like ours and those performed by Gowda *et al* are needed to reveal metabolic changes related to treatment resistances in cancer.

4.3.9 Hypoxia in MB.

Hypoxic microenvironments commonly occur in tumours. The stabilisation of HIF transcription factors (HIF-1α and HIF-2α) can enable cell survival and propagation of the tumour, through increasing; blood vessel formation, metastasis, and resistance to treatment. The presence of hypoxia in MB tumours has not been shown. However, the impact of hypoxia – particularly the role of HIF-1α – has been demonstrated (Pistollato *et al*., 2010). Our results reveal hypoxic niches within MB patient tumours, suggesting for the first time that these tumours exhibit areas of low oxygen tension. Furthermore, MB cell lines showed an increase in the proportion of m+5 citrate when incubated in 1% O_2 (hypoxia), consistent with the reductive carboxylation of glutamine-derived αKG as previously reported in hypoxic cells to support de novo lipogenesis (Metallo et al. 2011; Wise et al. 2011). We also show that hypoxia may be able to permit resistance to treatment in MB, which aligns with recent investigations, where it was revealed that Hypoxia increases chemoresistance in DAOY cells via HIF1α-mediated downregulation of the CYP2B6, CYP3A4 and CYP3A5 enzymes (Valencia-Cervantes *et al*., 2019). Although we did not find the exact mechanism in our cell line models, we suggest the reducing environment accompanying hypoxia may play a part and may also reduce the effectiveness of SSZ treatment, which we previously highlighted as a potential therapy in normoxia. The lack of efficacy observed with SSZ treatment in hypoxia suggests that applying this type of therapy in clinical practice may prove a challenge, depending on the degree of hypoxia in a given tumour. Alternatively, if normoxia is necessary for SSZ treatment efficacy, pre-treatment with vasculature normalising agents such as bevacizumab may be beneficial, where these types of therapies

have already been used extensively in the treatment of cancers (Burger *et al.*, 2011; Gilbert *et al.*, 2014).

4.3.10 Summary

In this chapter, we investigated the mechanisms in which glutamine modulates therapeutic resistance in MB cell lines. Our results show that glutamine deprivation on its own leads to cellular death, but also increases cell line sensitisation to cytotoxic agents. We further showed that these mechanisms for resistance were directed through glutamate, the inhibition of which also resulted in a potentiation of treatments. Our results are consistent with the idea that disrupting glutamine metabolism, and several of its downstream metabolites, could be used as effective strategy for MB cancer therapy.

Chapter 5

Discussion

Research presented highlights the pathways influencing glutamine, and resulting glutamate metabolism and their importance in MB biology. Through the analysis of online mRNA expression data sets and biological in vitro investigations, we now better understand these pathways in MB and have exposed possible approaches to improve current therapies.

5.1 The implication of glutamine/glutamate metabolic pathways in MB prognosis

We defined a list of genes representative of different features of glutamine and glutamate metabolism and considered their role in MB biology, as well as patient survival. Genes representing glutamine catabolism, glutamate transport and receptor activity, proline biosynthesis, glutathione biosynthesis, and GABA biosynthesis and GABAergic activity, were either increased in higher grade MB subgroups (SHH, G3 or G4 compared to WNT) or were associated with poor prognosis.

The data presented investigate the expression of metabolic genes and their clinical consequences in MB patients. We noted that in all cases, expression of the glutamate uptake transporters EAAT1 and EAAT2-4 were reduced, while the neutral amino acid transporter SLC1A5, responsible for the transport of glutamine into tumour cells, was significantly increased. Furthermore, the expression of these transporters proved to be prognostic, with low EAAT1 and high SLC1A5 being predictive of a worse overall survival in MB patients. Our data suggests that MB tumours prioritise glutamine uptake and subsequently utilise *de novo* glutamate synthesis rather than exogenous uptake.

We also investigated genes involved in glutamine catabolism (GLS1, GLS2 and GLUD1) and anabolism (GLUL) in MB tumours. GLS1 expression was highest in the SHH-MB subgroup when compared to the other three conventional groups, although when compared to normal cerebellum (CB) no expression differences were observed. Furthermore, we showed

changes in GLS1 expression between MB and CB, although no significance was observed for GLS1 expression and patient survival in the Newcastle cohort. Despite this, using another online expression database (GEO: GDS4471) we show high expressing GLS1 patients have a worse overall survival than low GLS1 expressing patients. Our proteomic data further reveal an importance of GLS1 expression in predicting survival. We show no expression changes in GLS2 in MB tumours when compared to normal cerebellum.

Our results revealed a significant alteration in GLUD1, with decreased expression found in the SHH, Grp3 and Grp MB subgroups, which are have a more aggressive phenotype than the WNT group. We also observed decreased expression in MB tumours compared to CB, which interestingly held up as a prognostic indicator in patients, with low expressing patients having a significantly poorer overall survival (OS) compared to their higher GLUD1-expressing counterparts.

5.2 Biological characterisation of glutamine/glutamate metabolic pathways in MB cell lines

After establishing that genes involved in glutamine/glutamate metabolism could play a role in the pathogenesis of MB, we investigated this further by several biological means. Similarly to our observations regarding the glutamine uptake transporter SLC1A5 in MB survival, we found that MB cell lines are glutamine 'addicted'. Not only is glutamine required for cell growth, but it is also important in cell line resistance to cytotoxic treatments, which we have shown to be largely driven through glutamate.

5.3 The role of GLS1 in MB

Many studies have focused on glutamine metabolism in cancer and although we have also explored this role, we primarily focused our attentions to the role of glutamate. Our data

highlight the importance of GLS1 in the deamination of glutamine to glutamate under basal and stressed conditions. We show through the use of GLS1 knockdown experiments that GLS1 is required for the growth of MB cell lines and that this isoform is solely responsible for glutaminolysis. We showed, for the first time, the relative expressions of the GLS1 splice variants, KGA and GAC, where GAC expression is increased compared to KGA. We also elucidate the localisation differences between the GLS1 variants and observed increased KGA localising in the cytosol, while GAC typically localises to the mitochondria. We further show, through the use of ^{13}C labelled glutamine that GAC is more responsible for label incorporation into several metabolites compared to KGA, indicative of preferential GAC-derived TCA cycle metabolism. We suggest that mitochondrial located, GAC may be more important in TCA anaplerosis, while KGA may be responsible for (but not restricted to) controlling cytosolic concentrations of glutamate and its subsequent reactions.

5.4 Clinical implications

We reveal the role of GLS1 on the resistance against cytotoxic treatments. Knockdown of GLS1 resulted in increased potentiation of hydrogen peroxide, cisplatin and irradiation, suggesting that blocking the conversion of glutamine to glutamate may increase the efficacy of chemotherapy in MB tumours. We built on this data further through GLS1 compound inhibition with BPTES, which although introduces potential complications through off target effects, provides an opportunity for translation to the clinic. Our results highlight the beneficial use of clinically available GLS1 inhibitors in the treatment of MB cell lines, which may be used to improve treatment options in MB patients.

Our results suggest that MB do not actively use GLS2 for glutaminolysis. However, we reveal a role of GLS2 in the protection against treatment, despite GLS2 having little role under

basal conditions. GLS2 expression is increased after treatment, suggesting a role of this enzyme in conditions of stress. We therefore highlighted the importance of GLS2 expression in MB treatment resistance, justifying further research with an aim to progress into the clinic.

Independently of GLS, we found that inhibiting the glutamate-cystine anti-porter (SLC7A11) with SSZ renders MB cell lines sensitive to hydrogen peroxide treatment. The MB cell lines used demonstrated a degree of heterogeneity with respect to glutaminase expression and inhibition sensitivity, but with respect to SCL7A11 inhibition, all three cell lines responded similarly. Unsurprisingly, we confirmed the importance of GSH in the resistance against treatment, where SZZ significantly reduced intracellular concentrations of cystine which subsequently decreased the GSH:GSSG ratio in the MB cell lines. We demonstrated the specificity of SZZ treatment by displaying how this effect could be abolished by the addition of the reducing agent, 2-mercaptoethanol (2-ME), which facilitates the uptake of cystine independently of the xCT transporter by reducing cystine to cysteine, which allows its uptake through an alternative transporter. Our results reveal an alternative target of glutamate metabolism for MB tumours, independent of glutaminase, which could potentially be used clinically. Importantly, our data may highlight GSH as a converging molecule in MB.

5.5 Regulation of glutamate concentrations in MB.

We observed increased expression of the biosynthetic genes (ALDH18A1, PYCR1 and PYCR2), suggestive of heightened proline biosynthesis. We also found decreased PRODH expression, which is required for the breakdown of proline, and thus strengthening the notion that MB tumours favour proline anabolism. We suggest that this amplified proline

biosynthesis from glutamate may offer a way in which to remove excess mitochondrial glutamate.

Furthermore, we show that the addition of exogenous proline decreases growth in all three cell lines in a concentration dependent manner. We demonstrated that the addition of exogenous proline reduces PYCR activity, resulting in decreased proline biosynthesis in our cell lines, which has been previously been shown to be the case in melanoma (de Ingeniis *et al.*, 2012). As a large source of proline in our cell lines, we would expect glutamate concentrations to increase as a result of reduced proline biosynthesis. We propose this might affect the finely controlled concentrations of glutamate, which we believe to be an important mechanism in MB, and may be the cause of reduced MB cell growth.

5.6. Future studies

There are several areas within this work which require addressing in future experiments. I have been successfully awarded the Midlands neuroscience teaching and research fund, which I aim to use to address these.

Although we show differential localisation of the GAC and KGA variants of GLS, we were unable to reveal the significance of this. Future studies will investigate the mitochondrial or cytosolic specific reactions that may be preferentially catalysed by one of the two variants. I will continue to utilise siRNA mediated knock down of GCA and KGA and assess by LC-MS the metabolic changes accompanied by reduced expression. Targeting GLS1 has brought with it complications due to the importance of this enzyme in normal tissue. However, the further understanding of the GLS1 variants could lead to more specific inhibitors in which to use in the clinic. I will therefore assess the importance of KGA and GAC in MB treatment resistance.

Furthermore, we have highlighted the potential importance of proline in MB, yet, did not expand upon this in our treatment chapter. I intend on inhibiting proline biosynthetic enzymes, by means of siRNA and/or compound inhibition in order to investigate the importance of these enzymes in MB biology. In particular, I would like to determine the changes in glutamate concentrations within the MB cell lines to further understand the importance of regulated glutamate concentrations.

5.7 Conclusions

Glutamine and glutamate are important metabolites, capable of impacting a diverse range of processes. Their clinical importance in MB is poorly understood, where the underlying metabolic pathways are relatively unexplored. Using gene expression, we found that glutamine/glutamate-associated pathways can predict survival. Additionally, we reveal that MB cells have heightened glutamine uptake, of which they subsequently rely of GLS1 for the biosynthesis of glutamate. We have highlighted several potential importance's of glutamate in MB, which significantly supports previous *in vivo* data showing glutamate as a prognostic marker (Wilson *et al.*, 2014). In addition to supporting these data, we show the majority of glutamate detected in MB tumours is likely to be extracellular (micro environmental), which may have important clinical consequences. Importantly, we showed that manipulation of metabolic enzymes can improve (at least *in vitro*) the current therapies for MB treatment suggesting that glutamate metabolism represent a therapeutic target to supplement existing treatment regimens. Through analysis of clinical data sets and *in vitro* investigations, we have revealed several fundamental areas of glutamate metabolism in MB and suggest that glutamate should be considered for future treatment of MB.

Supplementary figures.

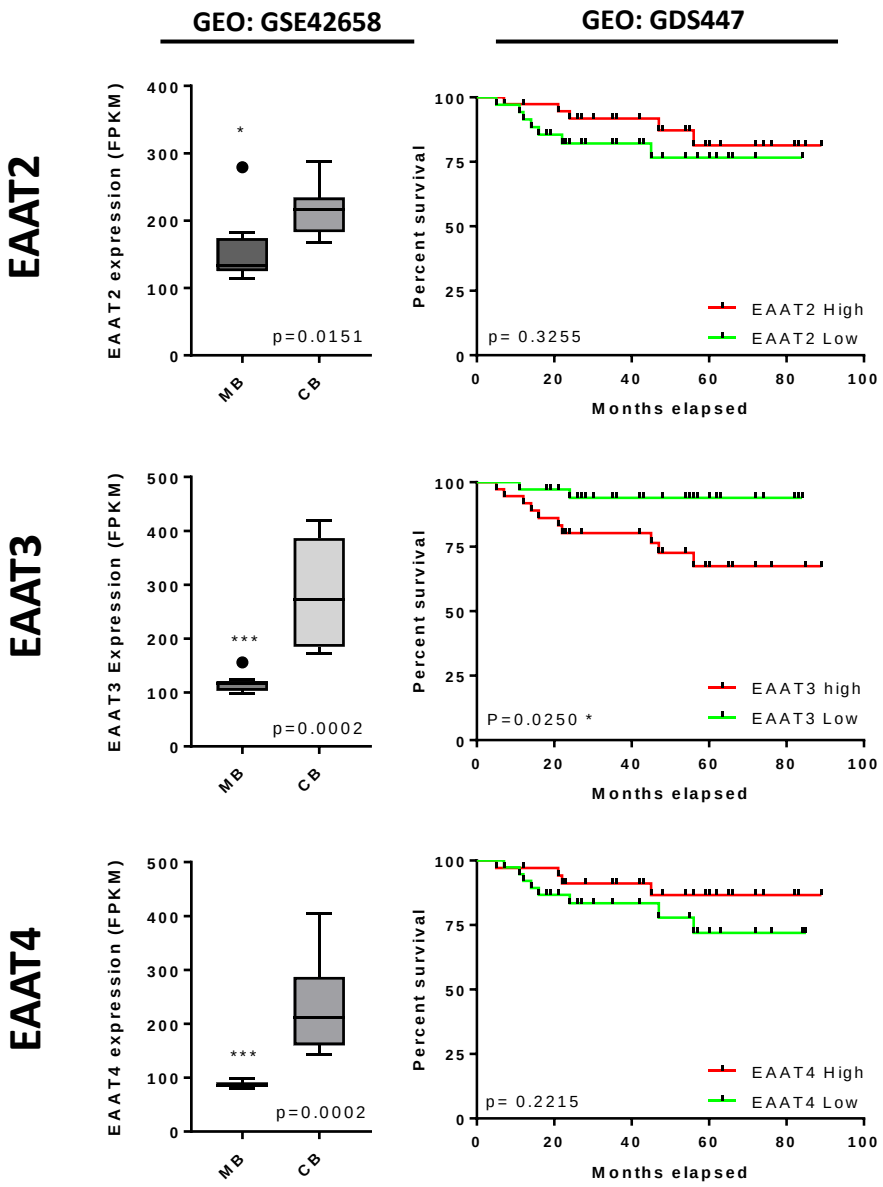

Supplementary figure 1. Expression of glutamate-related genes was associated with survival in MB tumours. A) Representative Kaplan-Meier survival curves of the online NCBI Geo repository (accession number: GDS4471). This Expression profiling array, included 76 samples, each belonging to the separate MB subgroups; WNT (n=8), SHH (n=11), G3 (n=16) and G4 (n=39). High and low expression was determined by the median expression value for each gene. Log-rank (Mantel-Cox) and Gehan-Breslow-Wilcoxon statistical tests were performed in all cases; *p<0.05, **p<0.01, ***p<0.001, ****p<0.0001.

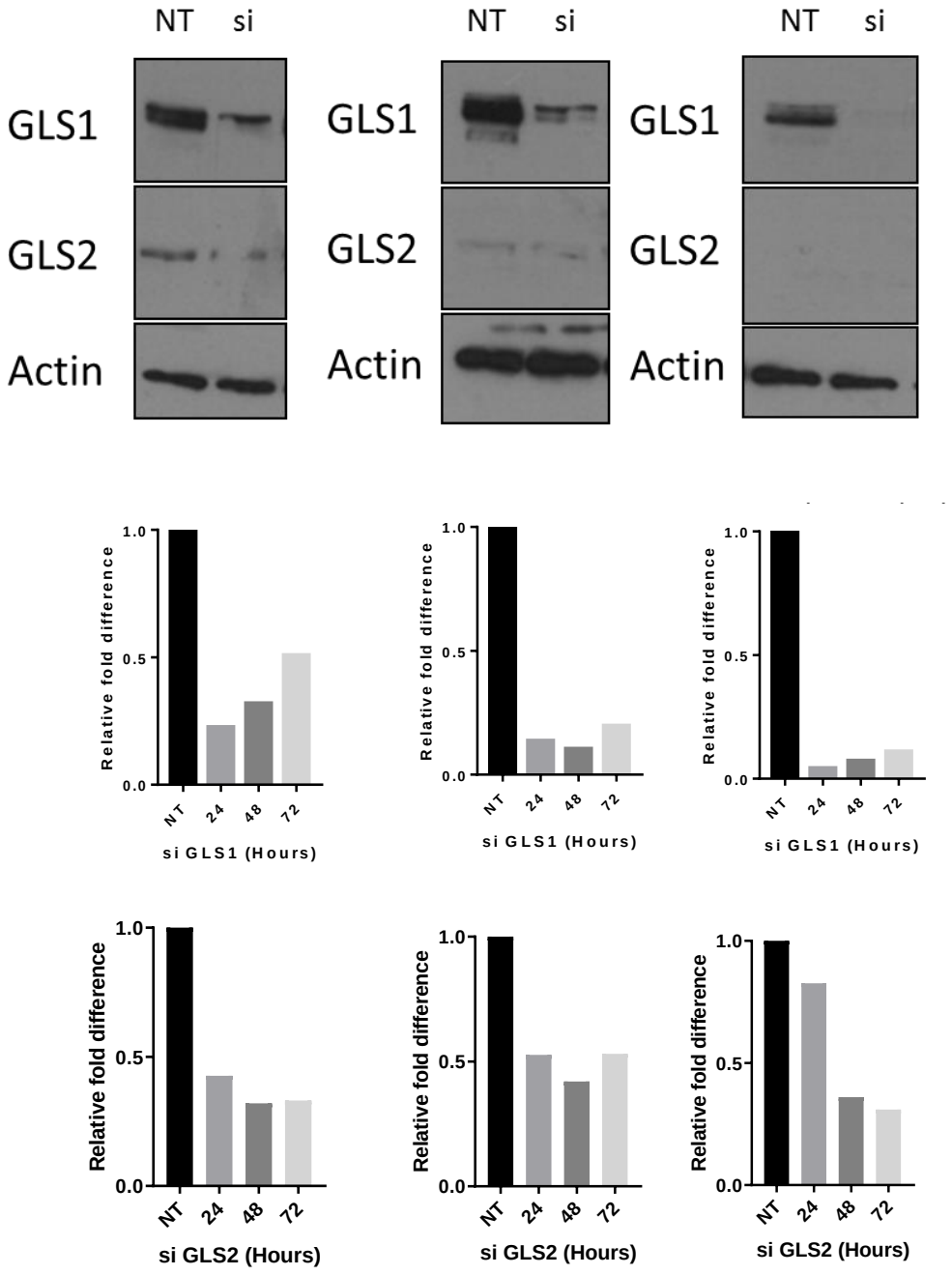

Supplementary figure 2. RNAi of GLS1 and GLS2 reduces RNA and protein levels. A) Western blot showing reduced protein upon knockdown with siGLS1 or siGLS2 after 48h. B) qPCR data showing reduced RNA levels of GLS1 or GLS2 after 24, 48 and 72 hours when normalised to siNT control.

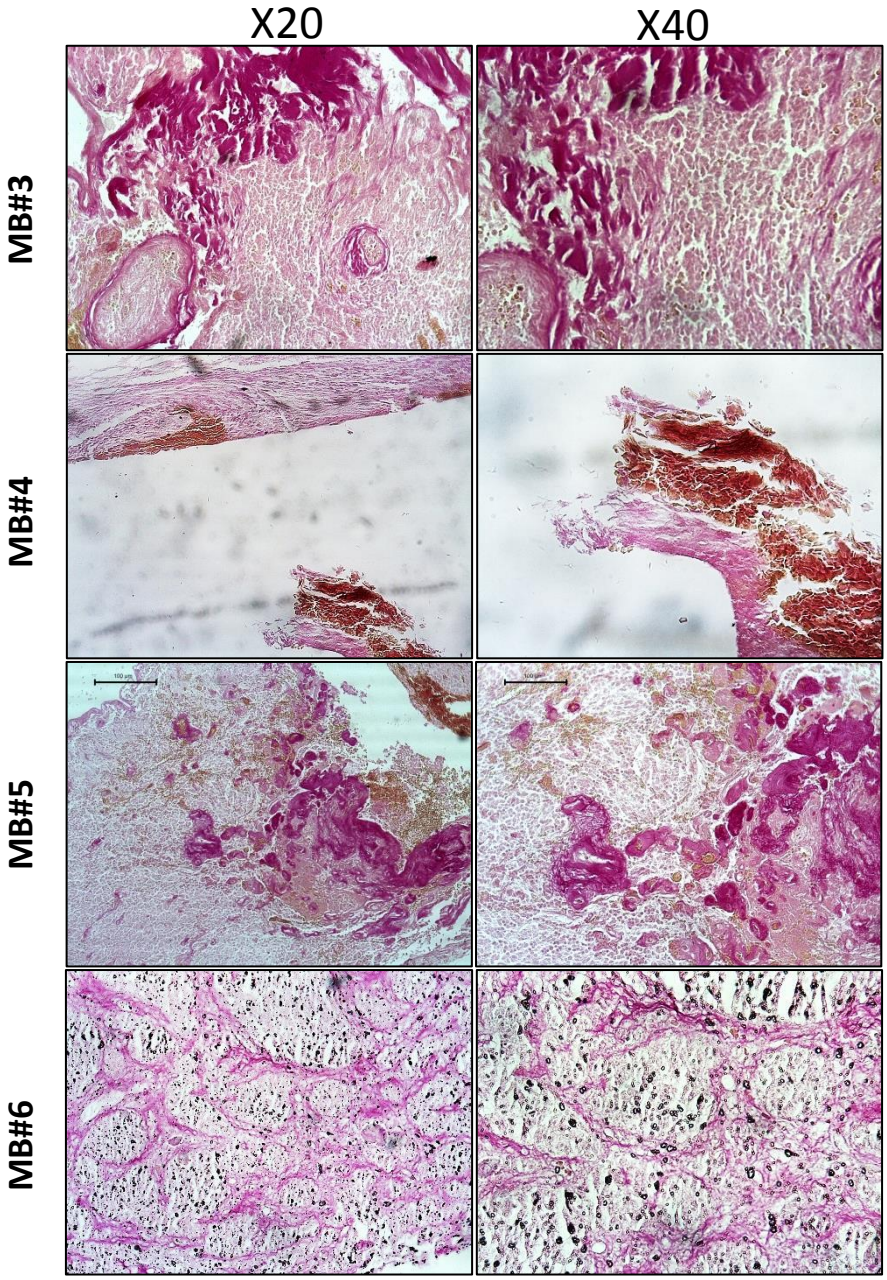

Supplementary figure 3. Histologic illustration of collagen in normal cerebellum (CB) and MB. The tumour shows increased deposits of collagen, demonstrated by the pink fibres.

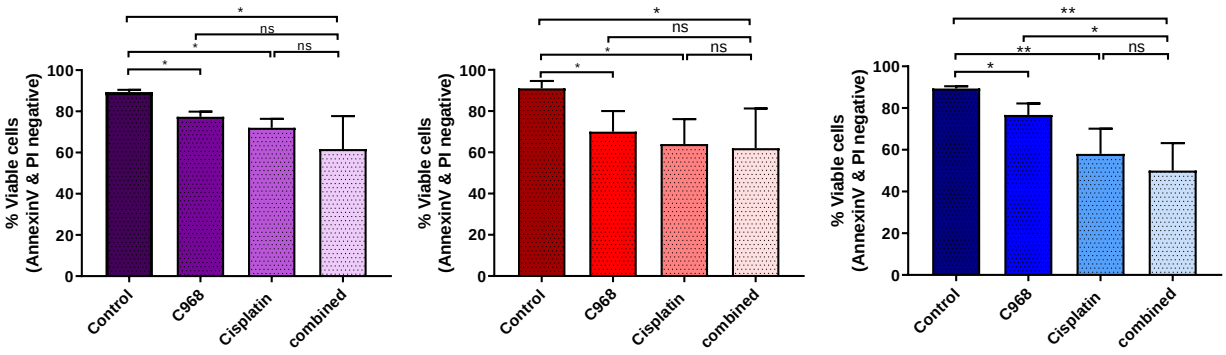

Figure 4.2.6. Pre-treatment with C968 leads to increased cytotoxicity of Cisplatin treatment in MB cell lines. A) Cell death was examined using a flow cytometry AnnexinV/PI assay to determine the effectiveness of C968 on ONS-76, DAOY and UW228.3 cell lines. Cells treated with DMSO, C968, Cisplatin or a combination of C968 and cisplatin. C968 pre-treatment 24 hours prior to cisplatin treatment does not affect cell viability. Data presented as mean ±SEM representative of three separate experiments. Significance was determined by performing a one-way ANOVA with Tukey post-hoc test in Graphpad; *p<0.05, **p<0.01, ***p<0.001, ****p<0.0001.

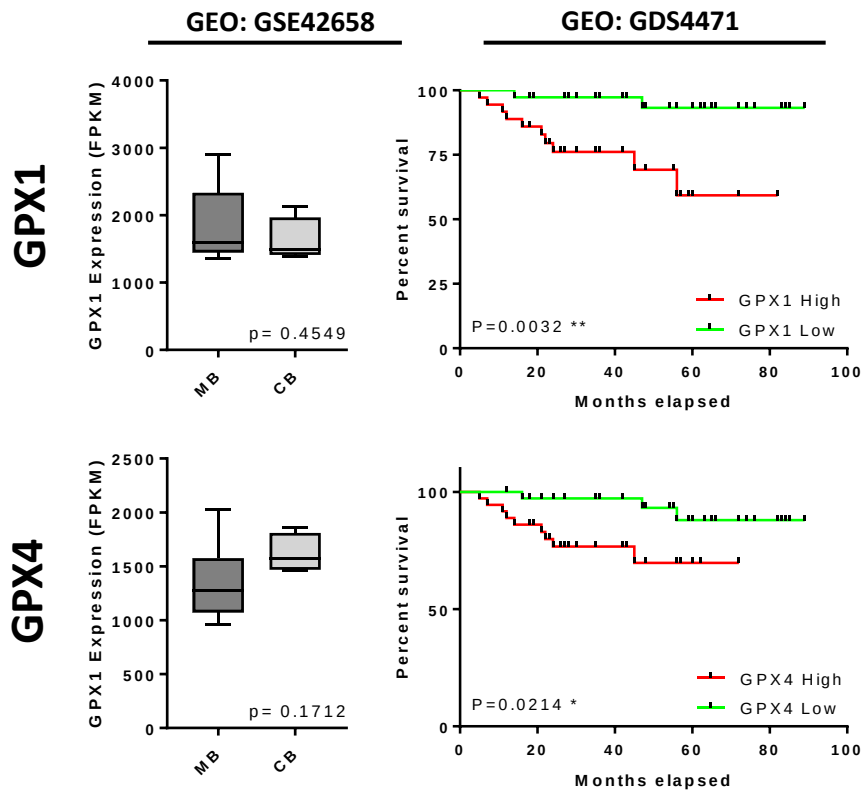

Supplementary figure 5. Expression of glutathione-related genes was associated with survival in MB tumours. A) Representative Kaplan-Meier survival curves of the online NCBI Geo repository (accession number: GDS4471). This Expression profiling array, included 76 samples, each belonging to the separate MB subgroups; WNT (n=8), SHH (n=11), G3 (n=16) and G4 (n=39). High and low expression was determined by the median expression value for each gene Log-rank (Mantel-Cox) and Gehan-Breslow-Wilcoxon statistical tests were performed in all cases; *p<0.05, **p<0.01, ***p<0.001, ****p<0.0001.

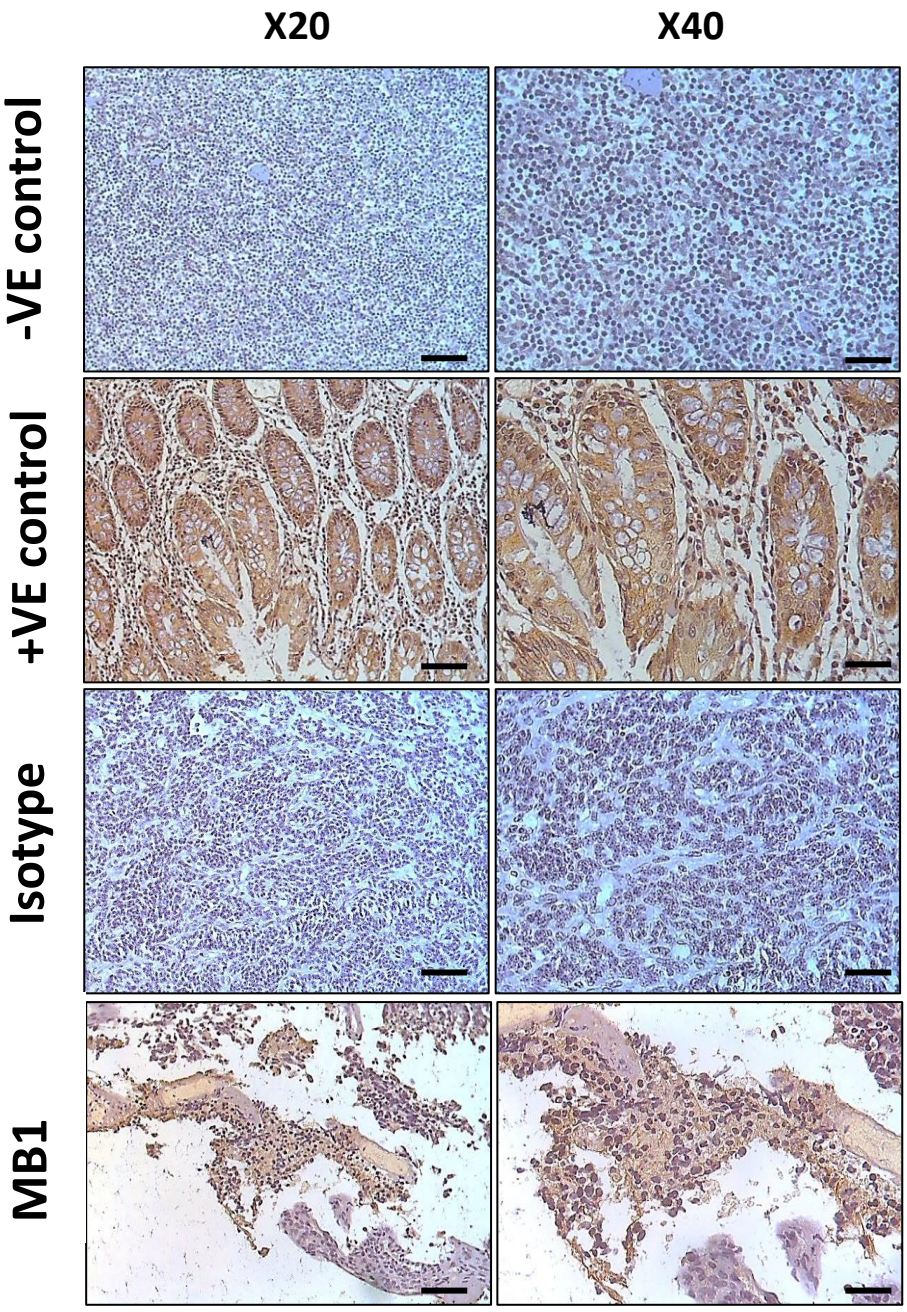

Supplementary figure 6. CAIX staining reveals hypoxic regions in MB tumours. CAIX protein expression is increased in MB tumours compared to controls. Scale bar, 50µm.

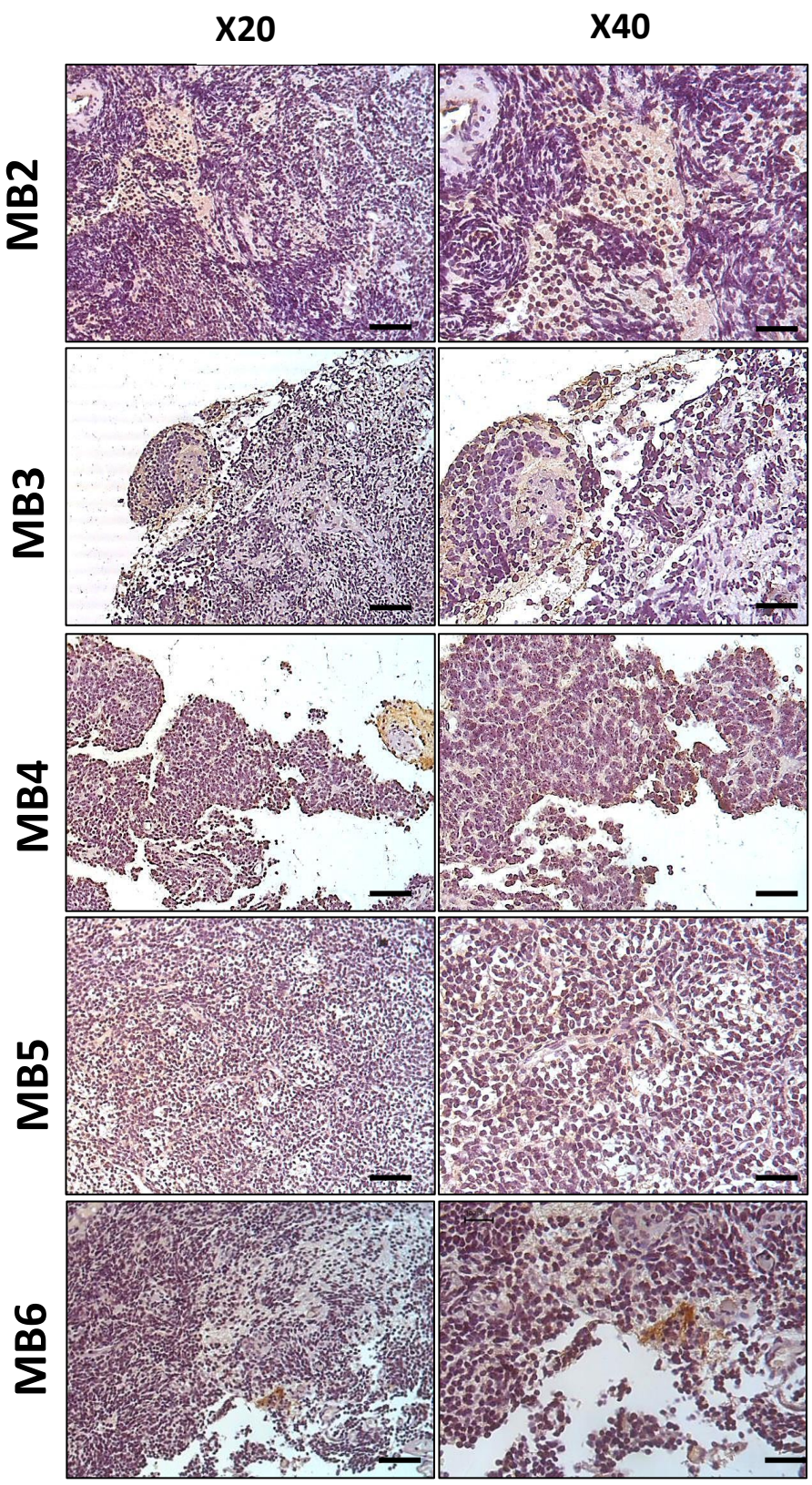

Supplementary figure 6. CAIX staining reveals hypoxic regions in MB tumours, continued. CAIX protein expression is increased in MB tumours compared to controls. Scale bar, 50µm.

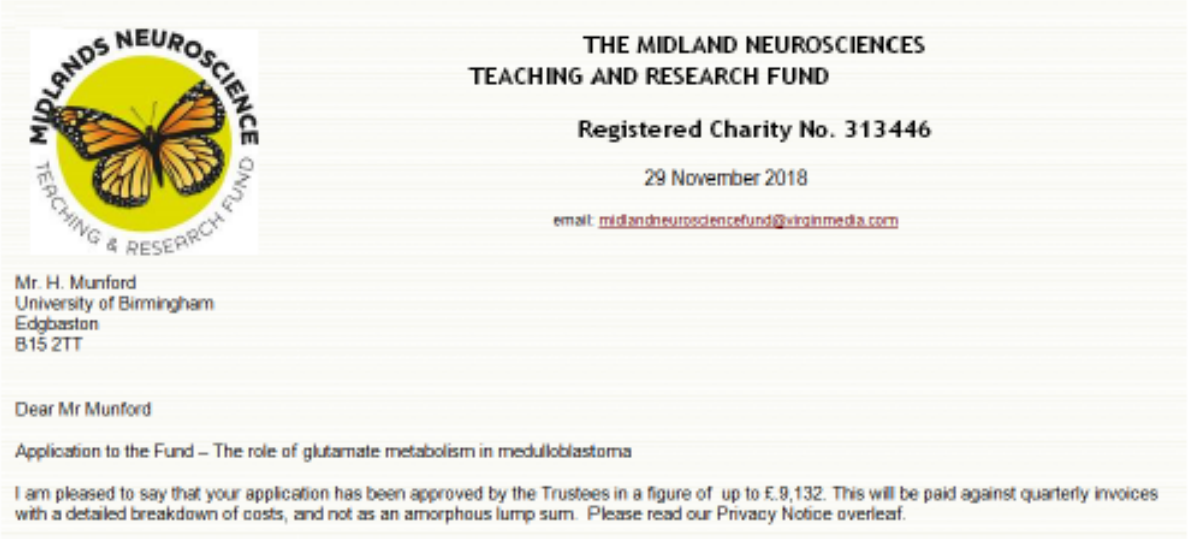

THE MIDLAND NEUROSCIENCES
TEACHING AND RESEARCH FUND

Registered Charity No. 313446

29 November 2018

email: midlandneurosciencefund@virginmedia.com

Mr. H. Munford
University of Birmingham
Edgbaston
B15 2TT

Dear Mr Munford

Application to the Fund – The role of glutamate metabolism in medulloblastoma

I am pleased to say that your application has been approved by the Trustees in a figure of up to £.9,132. This will be paid against quarterly invoices with a detailed breakdown of costs, and not as an amorphous lump sum. Please read our Privacy Notice overleaf.

Supplementary figure 7. Successful grant application

References

Aghaee, F., Islamian, J. P. and Baradaran, B. (2012) 'Enhanced radiosensitivity and chemosensitivity of breast cancer cells by 2-deoxy-D-glucose in combination therapy', *Journal of Breast Cancer*. doi: 10.4048/jbc.2012.15.2.141.

Ahluwalia, G. S. *et al.* (1990) 'Metabolism and action of amino acid analog anti-cancer agents', *Pharmacology and Therapeutics*. doi: 10.1016/0163-7258(90)90094-I.

Almuhaideb, A., Papathanasiou, N. and Bomanji, J. (2011) '18F-FDG PET/CT imaging in oncology', *Annals of Saudi Medicine*. doi: 10.4103/0256-4947.75771.

Álvarez-Buylla, A. and Ihrie, R. A. (2014) 'Sonic hedgehog signaling in the postnatal brain', *Seminars in Cell & Developmental Biology*. doi: 10.1016/j.semcdb.2014.05.008.

Antoniewicz, M. R. (2013) '13C metabolic flux analysis: Optimal design of isotopic labeling experiments', *Current Opinion in Biotechnology*. doi: 10.1016/j.copbio.2013.02.003.

Avramis, V. I. (2012) 'Asparaginases: Biochemical pharmacology and modes of drug resistance', *Anticancer Research*.

Bak, L. K., Schousboe, A. and Waagepetersen, H. S. (2006) 'The glutamate/GABA-glutamine cycle: Aspects of transport, neurotransmitter homeostasis and ammonia transfer', *Journal of Neurochemistry*. doi: 10.1111/j.1471-4159.2006.03913.x.

Barker, H. E. *et al.* (2015) 'The tumour microenvironment after radiotherapy: Mechanisms of resistance and recurrence', *Nature Reviews Cancer*. doi: 10.1038/nrc3958.

Baryawno, N. *et al.* (2010) 'Small-molecule inhibitors of phosphatidylinositol 3-kinase/Akt signaling inhibit Wnt/β-catenin pathway cross-talk and suppress medulloblastoma growth', *Cancer Research*. doi: 10.1158/0008-5472.CAN-09-0578.

Bensaad, K. *et al.* (2006) 'TIGAR, a p53-Inducible Regulator of Glycolysis and Apoptosis', *Cell*. doi: 10.1016/j.cell.2006.05.036.

Bhatia, B. *et al.* (2011) 'Mitogenic Sonic hedgehog signaling drives E2F1-dependent lipogenesis in progenitor cells and medulloblastoma', *Oncogene*. doi: 10.1038/onc.2010.454.

Bhatia, B. *et al.* (2012) 'Hedgehog-mediated regulation of PPARc controls metabolic patterns in neural precursors and shh-driven medulloblastoma', *Acta Neuropathologica*. doi: 10.1007/s00401-012-0968-6.

Biankin, A. V. *et al.* (2012) 'Pancreatic cancer genomes reveal aberrations in axon guidance pathway genes', *Nature*. doi: 10.1038/nature11547.

Brand, K. (1985) 'Glutamine and glucose metabolism during thymocyte proliferation. Pathways of glutamine and glutamate metabolism', *Biochemical Journal*. doi: 10.1042/bj2280353.

Bryant, K. L. *et al.* (2014) 'KRAS: Feeding pancreatic cancer proliferation', *Trends in*

Biochemical Sciences. doi: 10.1016/j.tibs.2013.12.004.

Bunt, J. *et al.* (2011) 'Joint binding of OTX2 and MYC in promotor regions is associated with high gene expression in medulloblastoma', *PLoS ONE*. doi: 10.1371/journal.pone.0026058.

Burger, R. A. *et al.* (2011) 'Incorporation of bevacizumab in the primary treatment of ovarian cancer.', *The New England journal of medicine*. doi: 10.1056/NEJMoa1104390.

Calvisi, D. F. *et al.* (2001) 'Activation of beta-catenin during hepatocarcinogenesis in transgenic mouse models: relationship to phenotype and tumor grade.', *Cancer research*.

Campos-Sandoval, J. A. *et al.* (2015) 'Glutaminases in brain: Multiple isoforms for many purposes', *Neurochemistry International*. doi: 10.1016/j.neuint.2015.03.006.

Carr, E. L. *et al.* (2010) 'Glutamine Uptake and Metabolism Are Coordinately Regulated by ERK/MAPK during T Lymphocyte Activation', *The Journal of Immunology*. doi: 10.4049/jimmunol.0903586.

Cassago, A. *et al.* (2012) 'Mitochondrial localization and structure-based phosphate activation mechanism of Glutaminase C with implications for cancer metabolism', *Proceedings of the National Academy of Sciences*. doi: 10.1073/pnas.1112495109.

Castegna, A. and Menga, A. (2018) 'Glutamine synthetase: Localization dictates outcome', *Genes*. doi: 10.3390/genes9020108.

Cavalli, F. M. G. *et al.* (2017) 'Intertumoral Heterogeneity within Medulloblastoma Subgroups', *Cancer Cell*. doi: 10.1016/j.ccell.2017.05.005.

Chakrabarti, G. *et al.* (2015) 'Targeting glutamine metabolism sensitizes pancreatic cancer to PARP-driven metabolic catastrophe induced by ß-lapachone', *Cancer & Metabolism*. doi: 10.1186/s40170-015-0137-1.

Chen, Y. and Swanson, R. A. (2003) 'The glutamate transporters EAAT2 and EAAT3 mediate cysteine uptake in cortical neuron cultures', *Journal of Neurochemistry*. doi: 10.1046/j.1471-4159.2003.01630.x.

Choi, J. *et al.* (2015) 'Human monocyte-derived macrophages exposed to glioblastoma cells and tumor-associated microglia/macrophages differ in glutamatergic gene expressions', *Glia*. doi: 10.1080/15384047.2015.1056406.

Christopher, F. S. (2011) 'The HPA axis and GABA-Glutamate Systems as Potential Antidepressant Targets in Prostate Cancer', *The Open Prostate Cancer Journal*. doi: 10.2174/1876822901104010001.

Coloff, J. L. *et al.* (2016) 'Differential Glutamate Metabolism in Proliferating and Quiescent Mammary Epithelial Cells', *Cell Metabolism*. doi: 10.1016/j.cmet.2016.03.016.

Combe, B. *et al.* (2009) 'Efficacy, safety and patient-reported outcomes of combination etanercept and sulfasalazine versus etanercept alone in patients with rheumatoid arthritis: A double-blind randomised 2-year study', *Annals of the Rheumatic Diseases*. doi: 10.1136/ard.2007.087106.

CRUK (2016) *Cancer Incidence Statistics*, *Cancer Research UK*.

Daye, D. and Wellen, K. E. (2012) 'Metabolic reprogramming in cancer: Unraveling the role of glutamine in tumorigenesis', *Seminars in Cell and Developmental Biology*. doi: 10.1016/j.semcdb.2012.02.002.

DeBerardinis, R. J. *et al.* (2007) 'Beyond aerobic glycolysis: Transformed cells can engage in glutamine metabolism that exceeds the requirement for protein and nucleotide synthesis', *Proceedings of the National Academy of Sciences*. doi: 10.1073/pnas.0709747104.

DeSouza, R.-M. *et al.* (2014) 'Pediatric Medulloblastoma â€" Update on Molecular Classification Driving Targeted Therapies', *Frontiers in Oncology*. doi: 10.3389/fonc.2014.00176.

Dey, P. *et al.* (2017) 'Genomic deletion of malic enzyme 2 confers collateral lethality in pancreatic cancer', *Nature*. doi: 10.1038/nature21052.

Eberlin, L. S. *et al.* (2014) 'Alteration of the lipid profile in lymphomas induced by MYC overexpression', *Proceedings of the National Academy of Sciences*. doi: 10.1073/pnas.1409778111.

Ecker, J. *et al.* (2015) 'Targeting class I histone deacetylase 2 in MYC amplified group 3 medulloblastoma', *Acta neuropathologica communications*. doi: 10.1186/s40478-015-0201-7.

Elgadi, K. M. *et al.* (1999) 'Cloning and analysis of unique human glutaminase isoforms generated by tissue-specific alternative splicing Cloning and analysis of unique human glutaminase isoforms generated by tissue-specific alternative splicing', *Physiological Genomics*. doi: 1/2/51 [pii].

Fan, X. and Eberhart, C. G. (2008) 'Medulloblastoma stem cells', *Journal of Clinical Oncology*. doi: 10.1200/JCO.2007.15.2264.

Fang, M. *et al.* (2014) 'Collagen as a double-edged sword in tumor progression', *Tumor Biology*. doi: 10.1007/s13277-013-1511-7.

Fazzari, J. *et al.* (2015) 'Inhibitors of glutamate release from breast cancer cells; New targets for cancer-induced bone-pain', *Scientific Reports*. doi: 10.1038/srep08380.

Ferrucci, V. *et al.* (2018) 'Metastatic group 3 medulloblastoma is driven by PRUNE1 targeting NME1-TGF-β-OTX2-SNAIL via PTEN inhibition', *Brain*. doi: 10.1093/brain/awy039.

Fossati, P., Ricardi, U. and Orecchia, R. (2009) 'Pediatric medulloblastoma: Toxicity of current treatment and potential role of protontherapy', *Cancer Treatment Reviews*. doi: 10.1016/j.ctrv.2008.09.002.

Friedman, H. S., Kaufmann, S. H. and Ludeman, S. M. (1992) 'Cyclophosphamide Resistance in Medulloblastoma', *Cancer Research*.

Fuchs, B. C. and Bode, B. P. (2005) 'Amino acid transporters ASCT2 and LAT1 in cancer: Partners in crime?', *Seminars in Cancer Biology*. doi: 10.1016/j.semcancer.2005.04.005.

Gerber, N. U. *et al.* (2012) 'A long duration of the prediagnostic symptomatic interval is not associated with an unfavourable prognosis in childhood medulloblastoma', *European Journal of Cancer*. doi: 10.1016/j.ejca.2011.11.012.

Gerber, N. U. *et al.* (2014) 'Recent developments and current concepts in Medulloblastoma', *Cancer Treatment Reviews*. doi: 10.1016/j.ctrv.2013.11.010.

Gibson, P. *et al.* (2010) 'Subtypes of medulloblastoma have distinct developmental origins', *Nature*. doi: 10.1038/nature09587.

Gilbert, M. R. *et al.* (2014) 'A randomized trial of bevacizumab for newly diagnosed glioblastoma.', *The New England journal of medicine*. doi: 10.1056/NEJMoa1308573.

Gillies, R. J., Robey, I. and Gatenby, R. A. (2008) 'Causes and Consequences of Increased Glucose Metabolism of Cancers', *Journal of Nuclear Medicine*. doi: 10.2967/jnumed.107.047258.

de Groot, J. and Sontheimer, H. (2011) 'Glutamate and the biology of gliomas', *GLIA*. doi: 10.1002/glia.21113.

de Groot, J. F. *et al.* (2005) 'The excitatory amino acid transporter-2 induces apoptosis and decreases glioma growth in vitro and in vivo.', *Cancer Research*. doi: 10.1158/0008-5472.CAN-04-3626.

Gross, M. I. *et al.* (2014) 'Antitumor Activity of the Glutaminase Inhibitor CB-839 in Triple-Negative Breast Cancer', *Molecular Cancer Therapeutics*. doi: 10.1158/1535-7163.MCT-13-0870.

Hanahan, D. and Weinberg, R. A. (2011) 'Hallmarks of cancer: The next generation', *Cell*. doi: 10.1016/j.cell.2011.02.013.

Hao, Y. *et al.* (2016) 'Oncogenic PIK3CA mutations reprogram glutamine metabolism in colorectal cancer', *Nature Communications*. doi: 10.1038/ncomms11971.

Harris, I. S. *et al.* (2015) 'Glutathione and Thioredoxin Antioxidant Pathways Synergize to Drive Cancer Initiation and Progression', *Cancer Cell*. doi: 10.1016/j.ccell.2014.11.019.

Hassanein, M. *et al.* (2015) 'Targeting SLC1a5-mediated glutamine dependence in non-small cell lung cancer', *International Journal of Cancer*. doi: 10.1002/ijc.29535.

Hawkins, R. A. (2009) 'The blood-brain barrier and glutamate', in *American Journal of Clinical Nutrition*. doi: 10.3945/ajcn.2009.27462BB.

Hay, N. (2016) 'Reprogramming glucose metabolism in cancer: Can it be exploited for cancer therapy?', *Nature Reviews Cancer*. doi: 10.1038/nrc.2016.77.

HAYS, J. L. *et al.* (2013) 'A phase II clinical trial of polyethylene glycol-conjugated L-asparaginase in patients with advanced ovarian cancer: Early closure for safety', *Molecular and Clinical Oncology*. doi: 10.3892/mco.2013.99.

Hedeskov, C. J. (1968) 'Early Effects of Phytohaemagglutinin on Glucose Metabolism of Normal Human Lymphocytes', *The Biochemical journal*. doi: 10.1042/bj1100373.

Heiden, M. G. Vander, Cantley, L. C. and Thompson, C. B. (2009) 'Understanding the warburg effect: The metabolic requirements of cell proliferation', *Science*. doi: 10.1126/science.1160809.

Hemmati, H. D. *et al.* (2003) 'Cancerous stem cells can arise from pediatric brain tumors',

Proceedings of the National Academy of Sciences. doi: 10.1073/pnas.2036535100.

Hiller, K. *et al.* (2009) 'MetaboliteDetector: Comprehensive Analysis Tool for Targeted and Nontargeted GC/MS Based Metabolome Analysis', *Analytical Chemistry*, 81(9), pp. 3429–3439. doi: 10.1021/ac802689c.

Hu, W. *et al.* (2010) 'Glutaminase 2, a novel p53 target gene regulating energy metabolism and antioxidant function', *Proceedings of the National Academy of Sciences*. doi: 10.1073/pnas.1001006107.

Huang, F., Zhang, Q., *et al.* (2014) 'Expression of glutaminase is upregulated in colorectal cancer and of clinical significance', *International Journal of Clinical and Experimental Pathology*.

Huang, F., Zhao, Y., *et al.* (2014) 'Upregulated SLC1A5 promotes cell growth and survival in colorectal cancer', *Int J Clin Exp Pathol*.

Huang, G. H. *et al.* (2016) 'Medulloblastoma stem cells: Promising targets in medulloblastoma therapy', *Cancer Science*. doi: 10.1111/cas.12925.

Huang, Y. *et al.* (2005) 'Cystine-glutamate transporter SLC7A11 in cancer chemosensitivity and chemoresistance', *Cancer Research*. doi: 10.1158/0008-5472.CAN-04-4267.

Ignarro, R. S. *et al.* (2016) 'Sulfasalazine intensifies temozolomide cytotoxicity in human glioblastoma cells', *Molecular and Cellular Biochemistry*. doi: 10.1007/s11010-016-2742-x.

de Ingeniis, J. *et al.* (2012) 'Functional Specialization in Proline Biosynthesis of Melanoma', *PLoS ONE*. doi: 10.1371/journal.pone.0045190.

Ito, K. and Suda, T. (2014) 'Metabolic requirements for the maintenance of self-renewing stem cells', *Nature Reviews Molecular Cell Biology*. doi: 10.1038/nrm3772.

Januchowski, R. *et al.* (2016) 'Increased expression of several collagen genes is associated with drug resistance in ovarian cancer cell lines', *Journal of Cancer*. doi: 10.7150/jca.15371.

Kamisawa, T. *et al.* (2016) 'Pancreatic cancer', *Lancet (London, England)*. doi: 10.1016/S0140-6736(16)00141-0.

Katt, W. P. and Cerione, R. A. (2014) 'Glutaminase regulation in cancer cells: A druggable chain of events', *Drug Discovery Today*. doi: 10.1016/j.drudis.2013.10.008.

Kieran, M. W. (2014) 'Targeted treatment for sonic hedgehog-dependent medulloblastoma', *Neuro-Oncology*. doi: 10.1093/neuonc/nou109.

Kim, K. *et al.* (2015) 'L-Asparaginase delivered by Salmonella typhimurium suppresses solid tumors', *Molecular Therapy - Oncolytics*. doi: 10.1038/mto.2015.7.

Kim, S. *et al.* (2013) 'Expression of glutamine metabolism-related proteins according to molecular subtype of breast cancer', *Endocrine-Related Cancer*. doi: 10.1530/ERC-12-0398.

Ko, Y. H. *et al.* (2011) 'Glutamine fuels a vicious cycle of autophagy in the tumor stroma and oxidative mitochondrial metabolism in epithelial cancer cells: Implications for preventing chemotherapy resistance', *Cancer Biology and Therapy*. doi: 10.4161/cbt.12.12.18671.

Kool, M. *et al.* (2008) 'Integrated genomics identifies five medulloblastoma subtypes with

distinct genetic profiles, pathway signatures and clinicopathological features', *PLoS ONE*. doi: 10.1371/journal.pone.0003088.

Kool, M. *et al.* (2014) 'Genome sequencing of SHH medulloblastoma predicts genotype-related response to smoothened inhibition', *Cancer Cell*. doi: 10.1016/j.ccr.2014.02.004.

Koppula P, Zhang Y, Shi J, Li W, Gan B. The glutamate/cystine antiporter SLC7A11/xCT enhances cancer cell dependency on glucose by exporting glutamate. J Biol Chem. 2017;292(34):14240–14249. doi:10.1074/jbc.M117.798405

Lacroix, M. *et al.* (2001) 'A multivariate analysis of 416 patients with glioblastoma multiforme: prognosis, extent of resection, and survival', *Journal of Neurosurgery*. doi: 10.3171/jns.2001.95.2.0190.

Landau, B. R. *et al.* (1958) 'Certain metabolic and pharmacologic effects in cancer patients given infusions of 2-deoxy-d-glucose', *Journal of the National Cancer Institute*. doi: 10.1093/jnci/21.3.485.

Le, A. *et al.* (2010) 'Inhibition of lactate dehydrogenase A induces oxidative stress and inhibits tumor progression', *Proceedings of the National Academy of Sciences of the United States of America*. doi: 10.1073/pnas.0914433107.

Le, A. *et al.* (2012) 'Glucose-independent glutamine metabolism via TCA cycling for proliferation and survival in b cells', *Cell Metabolism*. doi: 10.1016/j.cmet.2011.12.009.

Lee, Y.-Z. *et al.* (2014) 'Discovery of selective inhibitors of Glutaminase-2, which inhibit mTORC1, activate autophagy and inhibit proliferation in cancer cells.', *Oncotarget*. doi: 10.18632/oncotarget.2173.

Li, J., Mahajan, A. and Tsai, M. D. (2006) 'Ankyrin repeat: A unique motif mediating protein-protein interactions', *Biochemistry*. doi: 10.1021/bi062188q.

Li, X. *et al.* (2007) 'Gli1 acts through Snail and E-cadherin to promote nuclear signaling by β-catenin', *Oncogene*. doi: 10.1038/sj.onc.1210241.

Li, Y. *et al.* (2009) 'Camptothecin and Fas receptor agonists synergistically induce medulloblastoma cell death: ROS-dependent mechanisms', *Anti-Cancer Drugs*. doi: 10.1097/CAD.0b013e32832fe472.

Liang, Y. *et al.* (2008) 'Type I collagen is overexpressed in medulloblastoma as a component of tumor microenvironment', *Journal of Neuro-Oncology*. doi: 10.1007/s11060-007-9457-5.

Lin, Z. *et al.* (2016) 'Suppression of GLI sensitizes medulloblastoma cells to mitochondria-mediated apoptosis', *Journal of Cancer Research and Clinical Oncology*. doi: 10.1007/s00432-016-2241-1.

Liu, W. *et al.* (2012) 'Reprogramming of proline and glutamine metabolism contributes to the proliferative and metabolic responses regulated by oncogenic transcription factor c-MYC', *Proceedings of the National Academy of Sciences*. doi: 10.1073/pnas.1203244109.

Liu, W. *et al.* (2015) 'Proline biosynthesis augments tumor cell growth and aerobic glycolysis: Involvement of pyridine nucleotides', *Scientific Reports*. doi: 10.1038/srep17206.

Liu, Y. *et al.* (2009) 'Gammaaminobutyric acid A receptor alpha 3 subunit is overexpressed in

lung cancer.', *Pathology oncology research : POR*. doi: 10.1007/s12253-008-9128-7.

Liu, Y. *et al.* (2012) 'A Small-Molecule Inhibitor of Glucose Transporter 1 Downregulates Glycolysis, Induces Cell-Cycle Arrest, and Inhibits Cancer Cell Growth In Vitro and In Vivo', *Molecular Cancer Therapeutics*. doi: 10.1158/1535-7163.MCT-12-0131.

Locasale, J. W. and Cantley, L. C. (2011) 'Metabolic flux and the regulation of mammalian cell growth', *Cell Metabolism*. doi: 10.1016/j.cmet.2011.07.014.

Louis, D. N. *et al.* (2016) 'The 2016 World Health Organization Classification of Tumors of the Central Nervous System: a summary', *Acta Neuropathologica*. doi: 10.1007/s00401-016-1545-1.

Ma, M. Z. *et al.* (2015) 'Xc^- inhibitor sulfasalazine sensitizes colorectal cancer to cisplatin by a GSH-dependent mechanism', *Cancer Letters*. doi: 10.1016/j.canlet.2015.07.031.

Mabbott, D. J. (2006) 'Diffusion tensor imaging of white matter after cranial radiation in children for medulloblastoma: Correlation with IQ', *Neuro-Oncology*. doi: 10.1215/15228517-2006-002.

Mann, K. M. *et al.* (2016) 'KRAS-related proteins in pancreatic cancer', *Pharmacology and Therapeutics*. doi: 10.1016/j.pharmthera.2016.09.003.

Marrache, S., Pathak, R. K. and Dhar, S. (2014) 'Detouring of cisplatin to access mitochondrial genome for overcoming resistance', *Proceedings of the National Academy of Sciences*. doi: 10.1073/pnas.1405244111.

Martín-Rufián, M. *et al.* (2014) 'Both GLS silencing and GLS2 overexpression synergize with oxidative stress against proliferation of glioma cells', *Journal of Molecular Medicine*. doi: 10.1007/s00109-013-1105-2.

Matés, J. M. *et al.* (2002) 'Glutamine and its relationship with intracellular redox status, oxidative stress and cell proliferation/death', *International Journal of Biochemistry and Cell Biology*. doi: 10.1016/S1357-2725(01)00143-1.

Matoba, S. *et al.* (2006) 'P53 Regulates Mitochondrial Respiration.', *Science (New York, N.Y.)*. doi: 10.1126/science.1126863.

Matuszek, M., Jesipowicz, M. and Kleinrok, Z. (2001) 'GABA content and GAD activity in gastric cancer.', *Medical science monitor : international medical journal of experimental and clinical research*.

McBrayer, S. K. *et al.* (2012) 'Multiple myeloma exhibits novel dependence on GLUT4, GLUT8, and GLUT11: Implications for glucose transporter-directed therapy', *Blood*. doi: 10.1182/blood-2011-09-377846.

Metallo, C. M. *et al.* (2012) 'Reductive glutamine metabolism by IDH1 mediates lipogenesis under hypoxia', *Nature*. doi: 10.1038/nature10602.

Metzler, B., Gfeller, P. and Guinet, E. (2016) 'Restricting Glutamine or Glutamine-Dependent Purine and Pyrimidine Syntheses Promotes Human T Cells with High FOXP3 Expression and Regulatory Properties', *The Journal of Immunology*. doi: 10.4049/jimmunol.1501756.

Miao, Y. *et al.* (2010) 'GABA-receptor agonist, propofol inhibits invasion of colon carcinoma

cells', *Biomedicine and Pharmacotherapy*. doi: 10.1016/j.biopha.2010.03.006.

Miladinovic, T., Nashed, M. G. and Singh, G. (2015) 'Overview of glutamatergic dysregulation in central pathologies', *Biomolecules*. doi: 10.3390/biom5043112.

Momcilovic, M. *et al.* (2018) 'The GSK3 Signaling Axis Regulates Adaptive Glutamine Metabolism in Lung Squamous Cell Carcinoma', *Cancer Cell*. doi: 10.1016/j.ccell.2018.04.002.

Moody, G. A. *et al.* (1996) 'Long-term therapy with sulphasalazine protects against colorectal cancer in ulcerative colitis: A retrospective study of colorectal cancer risk and compliance with treatment in Leicestershire', *European Journal of Gastroenterology and Hepatology*. doi: 10.1097/00042737-199612000-00009.

Morrish, F. *et al.* (2010) 'Myc-dependent mitochondrial generation of acetyl-CoA contributes to fatty acid biosynthesis and histone acetylation during cell cycle entry', *Journal of Biological Chemistry*. doi: 10.1074/jbc.M110.141606.

Murai, S. *et al.* (2017) 'Inhibition of malic enzyme 1 disrupts cellular metabolism and leads to vulnerability in cancer cells in glucose-restricted conditions', *Oncogenesis*. doi: 10.1038/oncsis.2017.34.

Newsholme, P. *et al.* (2003) 'Glutamine and glutamate - Their central role in cell metabolism and function', *Cell Biochemistry and Function*. doi: 10.1002/cbf.1003.

Niehrs, C. (2012) 'The complex world of WNT receptor signalling', *Nature Reviews Molecular Cell Biology*. doi: 10.1038/nrm3470.

Niehrs, C. and Acebron, S. P. (2012) 'Mitotic and mitogenic Wnt signalling', *EMBO Journal*. doi: 10.1038/emboj.2012.124.

Niklison-Chirou, M. V. *et al.* (2017) 'TAp73 is a marker of glutamine addiction in medulloblastoma', *Genes and Development*. doi: 10.1101/gad.302349.117.

Northcott, P. A. *et al.* (2014) 'Enhancer hijacking activates GFI1 family oncogenes in medulloblastoma', *Nature*. doi: 10.1038/nature13379.

Ogawa, J. -I *et al.* (1993) 'Immunohistochemical study of glutathione-related enzymes and proliferative antigens in lung cancer. Relation to cisplatin sensitivity', *Cancer*. doi: 10.1002/1097-0142(19930401)71:7<2204::AID-CNCR2820710707>3.0.CO;2-O.

Oikari, S. *et al.* (2016) 'Hexosamine biosynthesis in keratinocytes: Roles of GFAT and GNPDA enzymes in the maintenance of UDP-GlcNAc content and hyaluronan synthesis', *Glycobiology*. doi: 10.1093/glycob/cww019.

Olalla, L. *et al.* (2002) 'Nuclear localization of L-type glutaminase in mammalian brain', *Journal of Biological Chemistry*. doi: 10.1074/jbc.C200373200.

Packer, R. J. and Vezina, G. (2008) 'Management of and prognosis with medulloblastoma: Therapy at a crossroads', *Archives of Neurology*. doi: 10.1001/archneur.65.11.1419.

Pallud, J. *et al.* (2014) 'Cortical GABAergic excitation contributes to epileptic activities around human glioma', *Science Translational Medicine*. doi: 10.1126/scitranslmed.3008065.

Pan, T. *et al.* (2015) 'Elevated expression of glutaminase confers glucose utilization via glutaminolysis in prostate cancer', *Biochemical and Biophysical Research Communications*. doi: 10.1016/j.bbrc.2014.11.105.

Paszek, M. J. *et al.* (2005) 'Tensional homeostasis and the malignant phenotype', *Cancer Cell*. doi: 10.1016/j.ccr.2005.08.010.

Pavlova, N. N. and Thompson, C. B. (2016) 'The Emerging Hallmarks of Cancer Metabolism', *Cell Metabolism*. doi: 10.1016/j.cmet.2015.12.006.

Pei, Y. *et al.* (2012) 'An Animal Model of MYC-Driven Medulloblastoma', *Cancer Cell*. doi: 10.1016/j.ccr.2011.12.021.

Peixoto, M. S., de Oliveira Galvão, M. F. and Batistuzzo de Medeiros, S. R. (2017) 'Cell death pathways of particulate matter toxicity', *Chemosphere*. doi: 10.1016/j.chemosphere.2017.08.076.

Pelicano, H. *et al.* (2006) 'Glycolysis inhibition for anticancer treatment', *Oncogene*. doi: 10.1038/sj.onc.1209597.

Phang, J. M. *et al.* (2015) 'Proline metabolism and cancer: Emerging links to glutamine and collagen', *Current Opinion in Clinical Nutrition and Metabolic Care*. doi: 10.1097/MCO.0000000000000121.

Piao, Y., Lu, L. and de Groot, J. (2009) 'AMPA receptors promote perivascular glioma invasion via 1 integrin-dependent adhesion to the extracellular matrix', *Neuro-Oncology*. doi: 10.1215/15228517-2008-094.

Pieters, R. *et al.* (2011) 'L-asparaginase treatment in acute lymphoblastic leukemia', *Cancer*. doi: 10.1002/cncr.25489.

Polakis, P. (2012) 'Drugging Wnt signalling in cancer', *EMBO Journal*. doi: 10.1038/emboj.2012.126.

Polet, F. *et al.* (2016) 'Inhibition of glucose metabolism prevents glycosylation of the glutamine transporter ASCT2 and promotes compensatory LAT1 upregulation in leukemia cells.', *Oncotarget*. doi: 10.18632/oncotarget.10131.

Polewski, M. D. *et al.* (2016) 'Increased Expression of System xc- in Glioblastoma Confers an Altered Metabolic State and Temozolomide Resistance', *Molecular Cancer Research*. doi: 10.1158/1541-7786.MCR-16-0028.

Ramaswamy, V. *et al.* (2016) 'Medulloblastoma subgroup-specific outcomes in irradiated children: Who are the true high-risk patients?', *Neuro-Oncology*. doi: 10.1093/neuonc/nou357.

Ramsbottom, S. and Pownall, M. (2016) 'Regulation of Hedgehog Signalling Inside and Outside the Cell', *Journal of Developmental Biology*. doi: 10.3390/jdb4030023.

Rathkopf, D. E. *et al.* (2013) 'A phase 2 study of intravenous panobinostat in patients with castration-resistant prostate cancer', *Cancer Chemotherapy and Pharmacology*. doi: 10.1007/s00280-013-2224-8.

Renault, M. A. *et al.* (2010) 'Sonic hedgehog induces angiogenesis via Rho kinase-dependent

signaling in endothelial cells', *Journal of Molecular and Cellular Cardiology*. doi: 10.1016/j.yjmcc.2010.05.003.

Robert, S. M. and Sontheimer, H. (2014) 'Glutamate transporters in the biology of malignant gliomas', *Cellular and Molecular Life Sciences*. doi: 10.1007/s00018-013-1521-z.

Robinson, G. *et al.* (2012) 'Novel mutations target distinct subgroups of medulloblastoma', *Nature*. doi: 10.1038/nature11213.

Roussel, M. F. and Robinson, G. W. (2013) 'Role of MYC in medulloblastoma', *Cold Spring Harbor Perspectives in Medicine*. doi: 10.1101/cshperspect.a014308.

S., H. *et al.* (2016) 'Novel SMO-independent hedgehog inhibitor 4SC-208 for treatment of SHH medulloblastoma', *Oncology Research and Treatment*.

Savarese, D. M. F. *et al.* (2003) 'Prevention of chemotheraphy and radiation toxicity with glutamine', *Cancer Treatment Reviews*. doi: 10.1016/S0305-7372(03)00133-6.

Schüller, U. *et al.* (2008) 'Acquisition of Granule Neuron Precursor Identity Is a Critical Determinant of Progenitor Cell Competence to Form Shh-Induced Medulloblastoma', *Cancer Cell*. doi: 10.1016/j.ccr.2008.07.005.

Schwalbe, E. C. *et al.* (2017) 'Novel molecular subgroups for clinical classification and outcome prediction in childhood medulloblastoma: a cohort study', *The Lancet Oncology*. doi: 10.1016/S1470-2045(17)30243-7.

Seidlitz, E. P. *et al.* (2009) 'Cancer cell lines release glutamate into the extracellular environment', *Clinical and Experimental Metastasis*. doi: 10.1007/s10585-009-9277-4.

Shankar, G. M. and Brastianos, P. K. (2014) 'Human breast cancer metastases to the brain display GABAergic properties in the neural niche', *Breast Diseases*. doi: 10.1016/j.breastdis.2014.07.037.

Sharma, M. K., Seidlitz, E. P. and Singh, G. (2010) 'Cancer cells release glutamate via the cystine/glutamate antiporter', *Biochemical and Biophysical Research Communications*. doi: 10.1016/j.bbrc.2009.10.168.

Shelly C. Lu, M. D. (2014) 'Glutathione Synthesis', *Biochim Biophys Acta*. doi: 10.1016/j.bbagen.2012.09.008.GLUTATHIONE.

Shroff, E. H. *et al.* (2015) 'MYC oncogene overexpression drives renal cell carcinoma in a mouse model through glutamine metabolism', *Proceedings of the National Academy of Sciences*. doi: 10.1073/pnas.1507228112.

Shukla, K. *et al.* (2012) 'Design, synthesis, and pharmacological evaluation of bis-2-(5-phenylacetamido-1,2,4-thiadiazol-2-yl)ethyl sulfide 3 (BPTES) analogs as glutaminase inhibitors', *Journal of Medicinal Chemistry*. doi: 10.1021/jm301191p.

Smith, M. J. *et al.* (2015) 'Germline mutations in SUFU cause Gorlin syndrome-associated childhood medulloblastoma and redefine the risk associated with PTCH1 mutations', *Journal of Clinical Oncology*. doi: 10.1200/JCO.2014.58.2569.

Smith, Q. R. (2000) 'Transport of Glutamate and Other Amino Acids at the Blood-Brain Barrier', *The Journal of Nutrition*. doi: 10.1093/jn/130.4.1016S.

Smits, A. *et al.* (2012) 'GABA-a channel subunit expression in human glioma correlates with tumor histology and clinical outcome', *PLoS ONE*. doi: 10.1371/journal.pone.0037041.

Son, J. *et al.* (2013) 'Glutamine supports pancreatic cancer growth through a KRAS-regulated metabolic pathway', *Nature*. doi: 10.1038/nature12040.

Song, Z. *et al.* (2017) 'Glutaminase sustains cell survival via the regulation of glycolysis and glutaminolysis in colorectal cancer', *Oncology Letters*. doi: 10.3892/ol.2017.6538.

Sontheimer, H. (2008) 'A role for glutamate in growth and invasion of primary brain tumors', *Journal of Neurochemistry*. doi: 10.1111/j.1471-4159.2008.05301.x.

Stalnecker, C. A. *et al.* (2015) 'Mechanism by which a recently discovered allosteric inhibitor blocks glutamine metabolism in transformed cells', *Proceedings of the National Academy of Sciences*. doi: 10.1073/pnas.1414056112.

Stumvoll, M. *et al.* (1999) 'Role of glutamine in human carbohydrate metabolism in kidney and other tissues', *Kidney International*. doi: 10.1046/j.1523-1755.1999.055003778.x.

Suzuki, S. *et al.* (2010) 'Phosphate-activated glutaminase (GLS2), a p53-inducible regulator of glutamine metabolism and reactive oxygen species', *Proceedings of the National Academy of Sciences*. doi: 10.1073/pnas.1002459107.

Szeliga, M. *et al.* (2008) 'Relative expression of mRNAS coding for glutaminase isoforms in CNS tissues and CNS tumors', *Neurochemical Research*. doi: 10.1007/s11064-007-9507-6.

Szeliga, M. *et al.* (2014) 'Silencing of GLS and overexpression of GLS2 genes cooperate in decreasing the proliferation and viability of glioblastoma cells', *Tumor Biology*. doi: 10.1007/s13277-013-1247-4.

Szeliga, M. and Obara-Michlewska, M. (2009) 'Glutamine in neoplastic cells: Focus on the expression and roles of glutaminases', *Neurochemistry International*. doi: 10.1016/j.neuint.2009.01.008.

Takano, T. *et al.* (2001) 'Glutamate release promotes growth of malignant gliomas', *Nat Med*. doi: 10.1038/nm0901-1010.

Takehara, A. *et al.* (2007) 'Gamma-aminobutyric acid (GABA) stimulates pancreatic cancer growth through overexpressing GABAA receptor pi subunit.', *Cancer research*. doi: 10.1158/0008-5472.CAN-07-2099.

Takeuchi, S. *et al.* (2014) 'Sulfasalazine and temozolomide with radiation therapy for newly diagnosed glioblastoma', *Neurology India*. doi: 10.4103/0028-3886.128280.

Tanaka, K. *et al.* (2015) 'Compensatory glutamine metabolism promotes glioblastoma resistance to mTOR inhibitor treatment', *Journal of Clinical Investigation*. doi: 10.1172/JCI78239.

Tardito, S. *et al.* (2015) 'Glutamine synthetase activity fuels nucleotide biosynthesis and supports growth of glutamine-restricted glioblastoma', *Nature Cell Biology*. doi: 10.1038/ncb3272.

Taylor, M. D. *et al.* (2012) 'Molecular subgroups of medulloblastoma: The current consensus', *Acta Neuropathologica*. doi: 10.1007/s00401-011-0922-z.

Thangavelu, K. *et al.* (2012) 'Structural basis for the allosteric inhibitory mechanism of human kidney-type glutaminase (KGA) and its regulation by Raf-Mek-Erk signaling in cancer cell metabolism', *Proceedings of the National Academy of Sciences*. doi: 10.1073/pnas.1116573109.

Thompson, E. M. *et al.* (2016) 'Prognostic value of medulloblastoma extent of resection after accounting for molecular subgroup: a retrospective integrated clinical and molecular analysis', *The Lancet Oncology*. doi: 10.1016/S1470-2045(15)00581-1.

Thornburg, J. M. *et al.* (2008) 'Targeting aspartate aminotransferase in breast cancer', *Breast Cancer Research*. doi: 10.1186/bcr2154.

Timmerman, L. A. *et al.* (2013) 'Glutamine Sensitivity Analysis Identifies the xCT Antiporter as a Common Triple-Negative Breast Tumor Therapeutic Target', *Cancer Cell*. doi: 10.1016/j.ccr.2013.08.020.

Turner, A. and McGivan, J. D. (2003) 'Glutaminase isoform expression in cell lines derived from human colorectal adenomas and carcinomas.', *The Biochemical journal*. doi: 10.1042/BJ20021360.

Ulanet, D. B. *et al.* (2014) 'Mesenchymal phenotype predisposes lung cancer cells to impaired proliferation and redox stress in response to glutaminase inhibition', *PLoS ONE*. doi: 10.1371/journal.pone.0115144.

Valcourt, J. R. *et al.* (2012) 'Staying alive: Metabolic adaptations to quiescence', *Cell Cycle*. doi: 10.4161/cc.19879.

Vansteenkiste, J. *et al.* (2008) 'Early phase II trial of oral vorinostat in relapsed or refractory breast, colorectal, or non-small cell lung cancer', *Investigational New Drugs*. doi: 10.1007/s10637-008-9131-6.

Vardon, A. *et al.* (2017) 'Arginine auxotrophic gene signature in paediatric sarcomas and brain tumours provides a viable target for arginine depletion therapies', *Oncotarget*. doi: 10.18632/oncotarget.18843.

Vastrad, C. and Vastrad, B. (2018) 'Bioinformatics analysis of gene expression profiles to diagnose crucial and novel genes in glioblastoma multiform', *Pathology Research and Practice*. doi: 10.1016/j.prp.2018.07.015.

Wang, J. Bin *et al.* (2010) 'Targeting mitochondrial glutaminase activity inhibits oncogenic transformation', *Cancer Cell*. doi: 10.1007/s12540-013-3026-6.

Wang, T., Marquardt, C. and Foker, J. (1976) 'Aerobic glycolysis during lymphocyte proliferation.', *Nature*. doi: 10.1038/261702a0.

Warburg, O. (1925) 'The Metabolism of Carcinoma Cells', *The Journal of Cancer Research*. doi: 10.1158/jcr.1925.148.

Ward, P. S. and Thompson, C. B. (2012) 'Metabolic Reprogramming: A Cancer Hallmark Even Warburg Did Not Anticipate', *Cancer Cell*. doi: 10.1016/j.ccr.2012.02.014.

Weinberg, F. *et al.* (2010) 'Mitochondrial metabolism and ROS generation are essential for Kras-mediated tumorigenicity', *Proceedings of the National Academy of Sciences*. doi:

10.1073/pnas.1003428107.

Wilson, M. *et al.* (2014) 'Noninvasive detection of glutamate predicts survival in pediatric medulloblastoma', *Clinical cancer research : an official journal of the American Association for Cancer Research*. doi: 10.1158/1078-0432.CCR-13-2320.

Wise, D. R. *et al.* (2008) 'Myc regulates a transcriptional program that stimulates mitochondrial glutaminolysis and leads to glutamine addiction', *Proceedings of the National Academy of Sciences*. doi: 10.1073/pnas.0810199105.

Wise, D. R. and Thompson, C. B. (2010) 'Glutamine addiction: a new therapeutic target in cancer', *Trends in Biochemical Sciences*. doi: 10.1016/j.tibs.2010.05.003.

Wu, G. *et al.* (2011) 'Proline and hydroxyproline metabolism: Implications for animal and human nutrition', *Amino Acids*. doi: 10.1007/s00726-010-0715-z.

Wu, M. ???C, Arimura, G. K. and Yunis, A. A. (1978) 'Mechanism of sensitivity of cultured pancreatic carcinoma to asparaginase', *International Journal of Cancer*. doi: 10.1002/ijc.2910220615.

Xiang, L. *et al.* (2013) 'Knock-down of glutaminase 2 expression decreases glutathione, NADH, and sensitizes cervical cancer to ionizing radiation', *Biochimica et Biophysica Acta - Molecular Cell Research*. doi: 10.1016/j.bbamcr.2013.08.003.

Xiang, Y. *et al.* (2015) 'Targeted inhibition of tumor-specific glutaminase diminishes cell-autonomous tumorigenesis', *Journal of Clinical Investigation*. doi: 10.1172/JCI75836.

Yang, C. *et al.* (2018) 'Glutamine-utilizing transaminases are a metabolic vulnerability of TAZ/YAP-activated cancer cells', *EMBO reports*. doi: 10.15252/embr.201643577.

Yang, L. *et al.* (2014) 'Metabolic shifts toward glutamine regulate tumor growth, invasion and bioenergetics in ovarian cancer', *Molecular Systems Biology*. doi: 10.1002/msb.20134892.

Yang, Z. J. *et al.* (2008) 'Medulloblastoma Can Be Initiated by Deletion of Patched in Lineage-Restricted Progenitors or Stem Cells', *Cancer Cell*. doi: 10.1016/j.ccr.2008.07.003.

Yauch, R. L. *et al.* (2009) 'Smoothened mutation confers resistance to a hedgehog pathway inhibitor in medulloblastoma', *Science*. doi: 10.1126/science.1179386.

Ye, Z. C. and Sontheimer, H. (1999) 'Glioma cells release excitotoxic concentrations of glutamate', *Cancer Research*. doi: 10.1016/0896-6273(88)90162-6.

Yin, Y. *et al.* (2013) 'Glutamine synthetase functions as a negative growth regulator in glioma', *Journal of Neuro-Oncology*. doi: 10.1007/s11060-013-1168-5.

Yoo, H. *et al.* (2008) 'Quantifying reductive carboxylation flux of glutamine to lipid in a brown adipocyte cell line', *Journal of Biological Chemistry*. doi: 10.1074/jbc.M706494200.

Young, S. Z. and Bordey, A. (2009) 'GABA's control of stem and cancer cell proliferation in adult neural and peripheral niches.', *Physiology (Bethesda, Md.)*. doi: 10.1152/physiol.00002.2009.

Yun, J. *et al.* (2009) 'Glucose deprivation contributes to the development of KRAS pathway

mutations in tumor cells', *Science*. doi: 10.1126/science.1174229.

Zhang, C. *et al.* (2016) 'Glutaminase 2 is a novel negative regulator of small GTPase Rac1 and mediates p53 function in suppressing metastasis', *eLife*. doi: 10.7554/eLife.10727.

Zhang, J. *et al.* (2013) 'Epigenetic silencing of glutaminase 2 in human liver and colon cancers', *BMC Cancer*. doi: 10.1186/1471-2407-13-601.

Zhang, X. *et al.* (2013) 'Expression of gamma-aminobutyric acid receptors on neoplastic growth and prediction of prognosis in non-small cell lung cancer', *Journal of Translational Medicine*. doi: 10.1186/1479-5876-11-102.

Zhao, F. *et al.* (2016) 'Molecular subgroups of adult medulloblastoma: A long-term single-institution study', *Neuro-Oncology*. doi: 10.1093/neuonc/now050.